PRECONSOLIDATION PRESSURE
OF
SOFT, HIGH-PLASTIC CLAYS

by

Göran Sällfors

Göteborg 1975

CONTENTS

PREFACE

The present thesis deals with the preconsolidation pressure of soft, high-plastic clays, and includes numerous laboratory tests as well as four full-scale loading tests.

This project was supported by grants from the Swedish Council for Building Research.

The work was carried out at Chalmers University of Technology, Geotechnical Department, under the supervision of Professor Sven Hansbo, Head of the Department.

The experimental investigation was in part carried out under my supervision by J-O. Nilsson, S. Öberg, K.Jonasson, O. Sjöberg, T. Wiberg, E. Sellgren, E. Ottosson, T. Olsson, B. Ekengren, and C. Bontell. Their useful help is greatly appreciated.

Furthermore, I wish to express my sincere thanks to all my colleagues for invaluable assistance and encouragement.

Göran Sällfors
Göteborg, October 1975.

SUMMARY

In the early days only the ground that was best from a geotechnical point of view was used for foundations, but now, owing to the growth of cities and to the rising prices of land, softer and more compressible soils, less suitable for foundations, are also often used.

The choice of foundation method is both economically and technically an important matter, and thorough testing of the soil is often needed to determine its geotechnical properties, and thus, to furnish necessary information.

The most important parameter in a discussion of foundation methods on clay is the preconsolidation pressure, which is usually determined from the results of oedometer tests.

For the last 30 years, the loading procedure suggested by Terzaghi has been used, where the sample is loaded in increments of 24-hour duration each. The Casagrande construction is then used for determining the preconsolidation pressure. Lately other methods have been suggested by Leonards (1962) and Bjerrum (1973), where reduced increments of shorter duration are used so as to give a better defined pressure/compression curve.

The introduction of routines where the sample is continuously loaded made it possible to carry out more detailed studies of the stress/strain characteristics of clays in the laboratory.

Carefully performed full-scale tests are then needed to enable a comparison of the stress/strain behaviour in situ with that found in the laboratory.

Scope of thesis

The present thesis consists of the following parts:

- Investigation and comparison of results of incremental and continuous oedometer tests.
- Study of the development of shear stresses in the sample during oedometer tests.
- Comparison of results of carefully performed full-scale tests on three different types of clays with results of oedometer tests.

Oedometer tests

Several incremental loading routines were used to study the effect of load increment and duration. Numerous oedometer tests were also made, where the sample was deformed at a constant rate of strain (CRS). Typical results are given in FIG. I. In addition to a completely defined pressure/compression curve on arithmetic, i.e. uniformly graduated, scales along x and y axes, this graph also shows the variation in the pore pressure at the undrained bottom. The pore pressure increases at the beginning of the test and then remains fairly constant. As the preconsolidation pressure is reached, the pore pressure increases again, and this indicates a breakdown in the structure of the clay.

The effect of the rate of strain is illustrated in FIG. II, which also represents a comparison with results of incremental loading tests. A CRS test giving approximately the same results as a standard test can be completed in 24 hours.

Tests were also made where the sample was continuously loaded in such a manner that the pore pressure at the undrained bottom was kept constant (Constant Gradient Test).

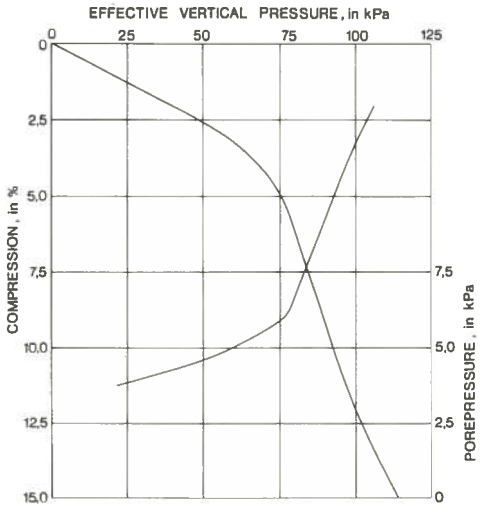

FIG. I Pressure/compression curve obtained from a CRS test at a rate of strain of 0,0024 mm/min. Variation in pore pressure is also shown.

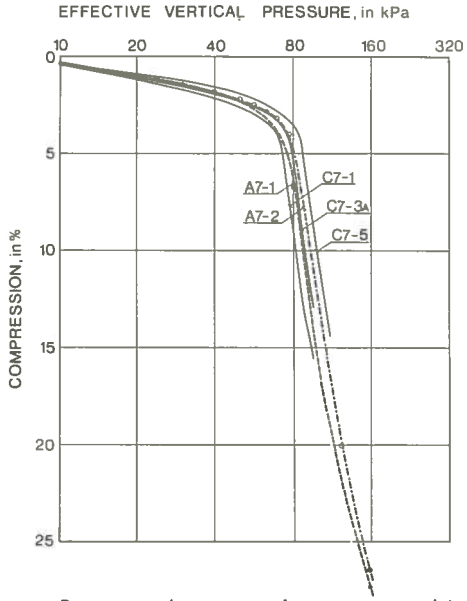

Legend

Test	Loading routine	Rate of def. mm/min
A7-1	STD	--
A7-2	NGI	--
C7-1	CRS	0,0006
C7-3A	CRS	0,0024
C7-5	CRS	0,0090

FIG. II Pressure/compression curves obtained from CRS tests and incremental loading tests. Bäckebol, 7 m.

Shear stresses in oedometer tests

A detailed study of the development of shear stresses during a constant rate of strain test was made. Typical results are given in FIG. III. The shear stress is seen to increase rather rapidly in the early stage of the test until it reaches a certain definite value, a critical shear stress. From there on, large deformations are necessary before the material can sustain any futher shear stresses. The critical shear stress was found to coincide with the preconsolidation pressure.

Different stress paths were investigated, and the critical shear stress was found to decrease with increasing isotropic consolidation pressure. A comparison in some respects was made with the concepts of the Critical State Soil Mechanics.

This section ends with a discussion of clay microstructure.

The generally accepted model, where the clay structure is believed to consist of aggregates (dense clusters of particles) connected by links or bridges, is found capable of explaining most of the observed phenomenon.

Full-scale tests

Three sites were chosen where full-scale tests were made *in situ*. At two of the sites a tank was used as a loading device, and the tests were made at a constant rate of loading. The build-up of pore pressures in piezometers at two different depths is shown in FIG. IV. At a depth of 2 m the effective vertical stress increases to about 19 kPa and then no more, in spite of the increasing total pressure. This is interpreted as an indication that the preconsolidation pressure is reached. The 5-m curve illustrates the behaviour of a normally consolidated clay.

At the third site the clay was varved, and a test embankment was constructed in five steps. The preconsolidation pressures were found from the load/settlement curves.

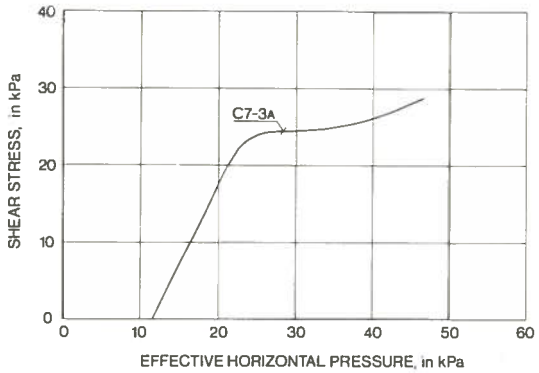

FIG. III Development of shear stresses during a CRS test performed at a rate of deformation of 0,0024 mm/min.

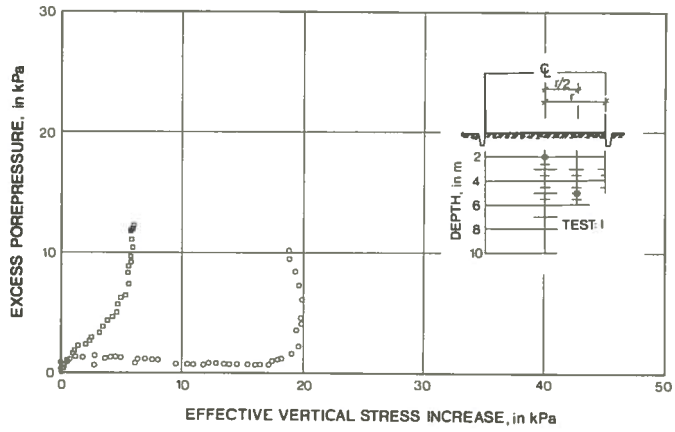

FIG. IV Variation in pore pressure and effective vertical stress increase at Välen. Piezometers at depths of 2 and 5 m.

Determination of the preconsolidation pressure

The question how to evaluate the preconsolidation pressure from the pressure/compression curve obtained from a CRS test is discussed, and the following method is suggested, see FIG. V. The pressure/compression curve is plotted on arithmetic scales and its linear parts are extended to intersect each other at B. An isosceles triangle is inscribed and the point B' is taken as representing the preconsolidation pressure.

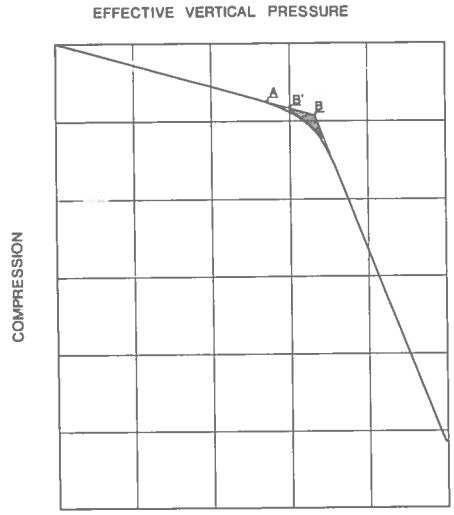

FIG. V Principle of suggested method for determination of the preconsolidation pressure from a CRS test.

This method was used, and FIG. VI illustrates the generally found extremely good agreement between the values of the preconsolidation pressure determined from laboratory and field tests.

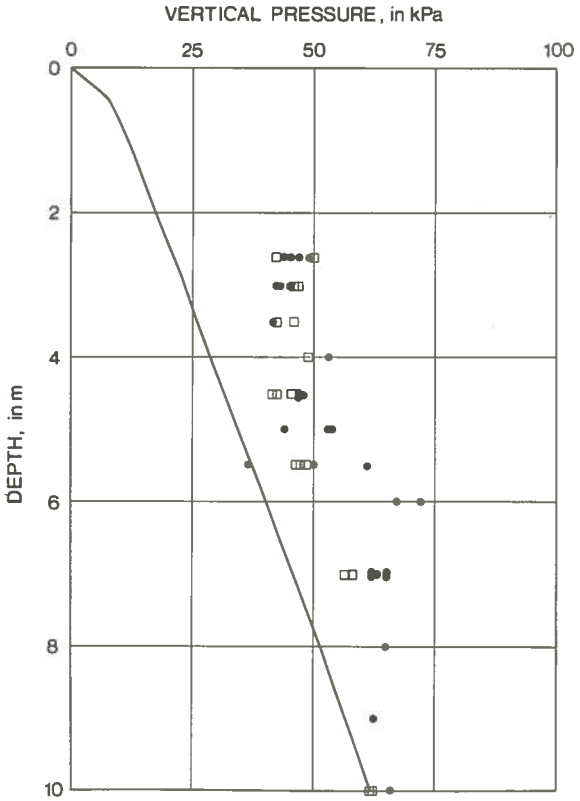

FIG. VI Preconsolidation pressures determined from field and laboratory tests, see FIG.85 and FIG.106.
• σ'_c determined from CRS tests
□ σ'_c determined from full-scale tests

NOTATIONS AND SYMBOLS

Roman letters

a	radius, FIG. 104
a_v	coefficient of compressibility
A7-3	etc., see Special symbols for oedometer tests
A-5	etc., see Special symbols for oedometer tests
B5-2	etc., see Special symbols for oedometer tests
c_v	coefficient of consolidation
CGT test	oedometer test, constant pore pressure gradient
CRS test	oedometer test, constant rate of strain
C7-1	etc., see Special symbols for oedometer tests
DTU	data transfer unit
e	void ratio
e_o	initial void ratio
$F(\frac{z}{H},T_v)$	function defined in Eq.(13)
$F_3(T_v)$	function defined in Eq.(15)
H	height of sample
I_p	plasticity index
k	permeability
k_1,k_2,k_3	constants
K_0	coefficient of earth pressure at rest
K'_o	incremental coefficient of earth pressure, $\sigma'_v>\sigma'_c$
K''_o	incremental coefficient of earth pressure, $\sigma'_v<\sigma'_c$
K^o_{rb}	coefficient of earth pressure during unloading
LIN test	oedometer test, daily and equal increments
LVDT	linear variable displacement transducer
L3-2	etc., see Special symbols for oedometer tests
M	oedometer modulus
m_v	modulus of compressibility
NGI test	etc., see Special symbols for oedometer tests
K3-1	etc., see Special symbols for oedometer tests
R	ratio defined in Eq.(18)
p	mean normal stress
P	vertical load
P'	vertical load
q	deviator stress
r	average rate of deformation

S_t	sensitivity
t, t_1, t_2	time
t_{50}	time for 50 % consolidation
T_v	time factor
Δt	time increment
STD test	etc., see Special symbols for oedometer tests
u	pore pressure
$\bar{U}$	degree of consolidation
u_b	pore pressure at undrained bottom in the oedometer
$u(z,t)$	function describing variation of pore pressure with depth and time
v	vertical displacement of a horizontal layer
w_n	natural water content
w_F	cone liquid limit
w_L	percussion liquid limit
w_p	plasticity limit
V4,5-3	etc., see Special symbols for oedometer tests
z	depth

Greek letters

α_1, α_2	angle, FIG. 72
ε	relative compression
$\varepsilon(z,t)$	function defined in Eq.(13)
$\Delta\varepsilon$	incremental compression
ν	Poisson's ratio
ρ	radius, FIG. 104
ρ	density
ρ_w	density of water
σ	total vertical pressure
σ'	effective vertical pressure
$\sigma(z,t)$	function describing variation of σ with depth and time
σ'_c	preconsolidation pressure
σ_h	total horizontal stress
σ'_h	effective horizontal stress
σ'_{ho}	*in situ* effective horizontal stress
σ'_o	effective overburden pressure
σ_v	total vertical pressure
σ'_v	effective vertical pressure
σ'_{vo}	*in situ* effective vertical pressure

$\sigma_1, \sigma_2, \sigma_3$	principal stresses
$\Delta\sigma$	incremental stress
$\Delta\sigma'_h$	horizontal stress increase
$\Delta\sigma'_v$	vertical stress increase
$\Delta\sigma'_k$	effective vertical stress increase necessary for σ'_c *in situ* to be reached
τ	shear stress
$\Delta\tau_{\rho z}$	additional shear stress, FIG. 105
τ_{fu}	undrained shear strength
ϕ'	effective angle of internal friction

SPECIAL SYMBOLS FOR OEDOMETER TESTS

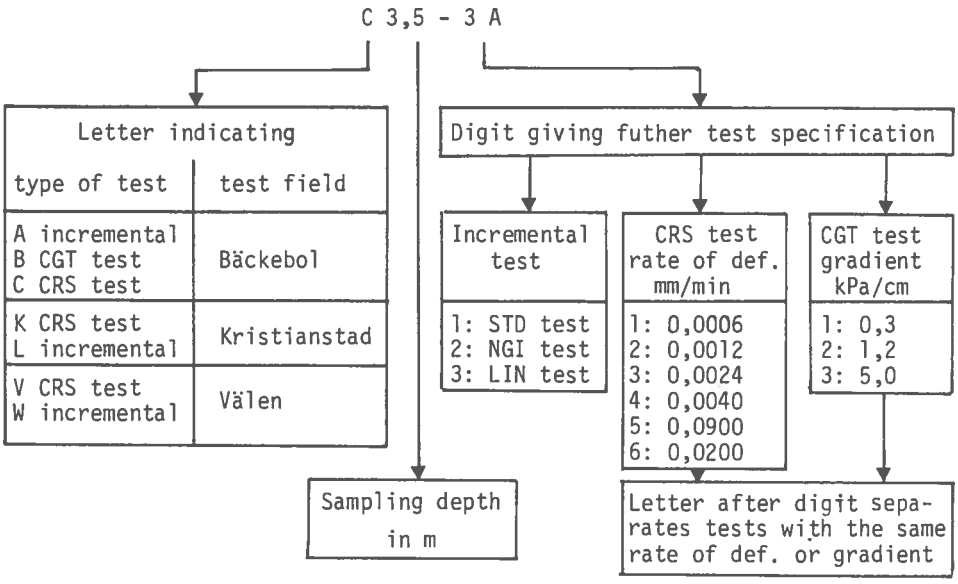

A - 7

Indicate CRS tests on artificially sedimented clay

1 INTRODUCTION

1.1 Introductory remarks

In the early days only the ground that was best from a geotechnical point of view was used for foundations, but now, owing to the growth of cities and to the rising prices of land,softer and more compressible soils, less suitable for foundations, are also often used.

The choice of foundation method is both economically and technically an important matter, and thorough testing of the soil is often needed to determine its geotechnical properties, and thus, to furnish necessary information.

In soft clays piling has been the most common foundation method. Recently it has been recognized that many clays, earlier considered as normally consolidated deposits, are lightly overconsolidated. This means that the clay can carry some additional load without undergoing significant settlements. This overconsolidation effect is sometimes so large that piling can be avoided and a raft foundation can be used instead. Moreover, ground settlements due to a lowering of the ground water table caused by building construction are reduced if the clay is slightly overconsolidated.

The most important parameter in a discussion of foundation methods on clay is the vertical preconsolidation pressure, which is usually determined from the results of oedometer tests.

1.2 Present methods for determining the preconsolidation pressure

The stress/strain characteristics of a clay are usually determined in the laboratory by using the test procedure suggested by Terzaghi, where the load is applied in increments (duration 24 hours), each increment being equal to the previous consolidation load. This gives 7 to 9 points of the pressure/compression curve, which are plotted in a semi-logarithmic graph where the assumed pressure/compression curve can be drawn. Various methods are then used to obtain the preconsolidation pressure as a single value.

The most common method is the Casagrande construction, but the methods suggested by Schmertmann and Burmister are also used.

In the past fifteen years other loading routines using smaller load increments have been proposed by Leonards (1962) and Bjerrum (1973), in order to get a better defined pressure/compression curve.

Other methods where the sample is continuously deformed have been examined lately, but are not yet widely used in practice.

In some cases test fills were built to investigate the soil properties *in situ*.

Conventional oedometer tests are widely used by soil engineers, but the uncertainty in the preconsolidation pressure determined from these tests is large, and a potential overconsolidation effect is perhaps not taken into account.

The procedure using smaller increments gives indeed a better defined pressure/compression curve, but time effects may influence the result in a way which is perhaps not yet fully understood.

The methods where the sample is continuously deformed are not yet used, probably because most laboratories do not have the necessary equipment, but here again too little is known about the applicability of the results to *in situ* conditions.

From the number of articles published on this subject every year, or closely related to the subject, the conclusion can be drawn that there is a need for a better understanding of the fundamentals involved. Most urgent is probably to study the soil behaviour *in situ* and to relate that to the results obtained in laboratory tests. A correct determination of the preconsolidation pressure is extremely important in soft high-plastic clays since a load, even slightly above the preconsolidation pressure, usually leads to large settlements.

1.3 Scope of study

The scope of this study has been to investigate the results of oedometer tests, mainly concerning the preconsolidation pressure, and to compare them with the *in situ* behaviour.

First, a comparison is made between the results of oedometer tests using different loading routines. The influence of time is thoroughly investigated.

The constant rate of strain (CRS) test, where the sample is deformed at a constant rate, is chosen for the detailed studies of the three-dimensional stress/strain behaviour of the clay. The concept of critical shear stress is introduced.

Full-scale loading tests were made and interpretations of the *in situ* preconsolidation pressures are presented for three different test fields.

Finally a comparison is made between the results of laboratory and field tests.

2 SURVEY OF LITERATURE

2.1 Introduction

The following survey of the literature presents a summary and an analysis of the literature relevant to this research project. The literature on the subject of deformation characteristics of soft clays is enormous, and this survey has mainly been restricted to papers dealing with the preconsolidation pressure, except for a few papers that deal with the stress path concept. The coefficient of consolidation is also treated.

The survey is divided into the following five groups of subjects:

- Oedometer tests, incremental loading
- Oedometer tests, continuous loading
- Empirical methods for determination of the peconsolidation pressure
- Stress paths in oedometer tests
- Field tests for determination of *in situ* preconsolidation pressure

Special emphasis is put on time effects on the preconsolidation pressure and also on the study of stress paths and its applicability to field conditions. Rate of consolidation and secondary compression are only briefly dealt with.

2.2 Determination of the preconsolidation pressure by oedometer test, incremental loading

The oedometer (οἴδος, from Greek = swelling), which usually contains the soil sample in a confined ring, has been used over a long period of time to determine the compression characteristics of soils. In Sweden the oedometer shown in FIG. 1 was constructed (Statens Järnvägar, 1922), and in 1918 Virgin already explained the consolidation phenomena (Virgin, 1918). The fundamentals of the consolidation process were explained by Terzaghi in 1925, and since then the testing procedure proposed by Terzaghi has been widely used.

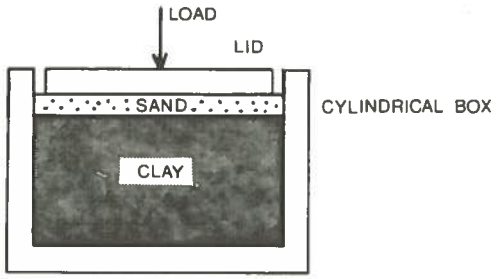

FIG. 1 Oedometer constructed by the Geotechnical Commision of Swedish State Railways.

Terzaghi's well-known equation of the consolidation process is

$$\frac{\partial u}{\partial t} = c_v \frac{\partial^2 u}{\partial z^2} \qquad (1)$$

where c_v is the coefficient of consolidation.

Terzaghi proposed that the sample should be loaded in increments (duration of 24 hours), each increment being equal to the previous consolidation load. The strain for each increment is then plotted against the effective vertical stress so as to give a typical curve shown in FIG. 2.

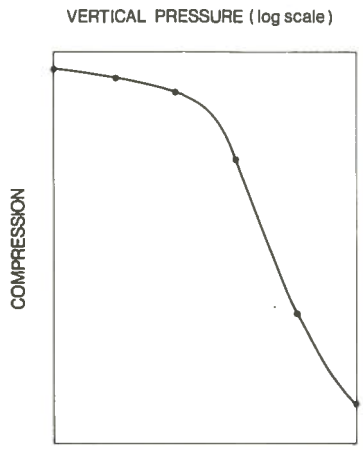

FIG. 2 Log pressure/compression curve. Typical results of an oedometer test.

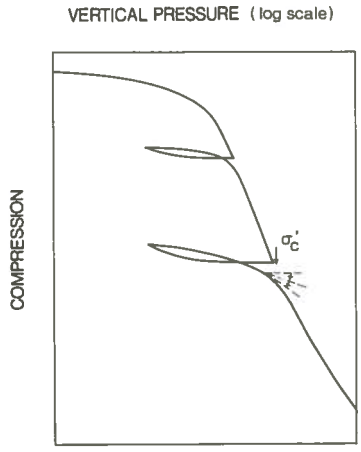

FIG. 3 Log pressure/compression curve and the principle of the Casagrande construction. (Casagrande, 1936)

For determining the preconsolidation pressure, the Casagrande method illustrated in FIG. 3 has been widely used. (Casagrande, 1936). This method involves the selection of the point corresponding to the minimum radius of curvature of the reloading curve. Through that point a horizontal line and a tangent to the pressure/compression curve are drawn. The angle between this line and the tangent is bisected. The straight portion of the virgin curve is extended and the intersection with the bisectrix is interpreted as the preconsolidation pressure. This procedure can be applied to the first loading curve if the sample disturbance and the time effects are neglected.

Other methods have been proposed by Burmister (1951) and Schmertmann (1953) and the various constructions are illustrated in FIGs. 4a and 4b. Burmister suggests that when the straight portion of the virgin curve is approached, the sample should be unloaded and then reloaded. The triangle formed between the unloading and reloading curves is reconstructed on the first loading curve. In this construction the vertical leg is more important than the horizontal.

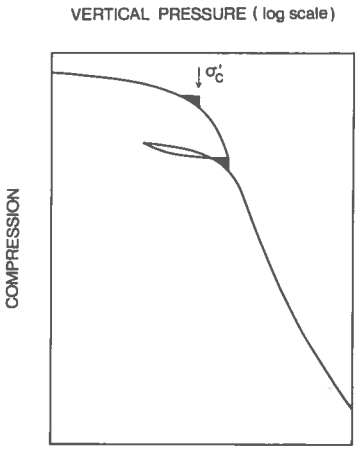

FIG. 4a Burmister construction of preconsolidation pressure. (Burmister, 1951).

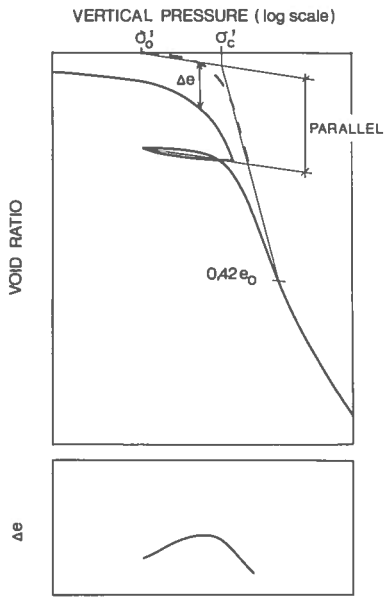

FIG. 4b Schmertmann construction of preconsolidation pressure. (Schmertmann, 1953).

The Schmertmann construction also involves unloading of the sample to the *in situ* stresses as the straight portion of the virgin curve is approached. From the point corresponding to e_o, σ'_o (*in situ* conditions) a line is drawn parallel to the mean slope of the rebound curve. From an assumed value of σ'_c a line is drawn to the virgin curve corresponding to a void ratio of 0,42 e_o. The dash-line curve in FIG. 4b represents the assumed virgin curve. The difference between the assumed virgin curve and the laboratory curve is plotted versus the logarithm of the pressure (σ'). This procedure is repeated several times, and the curve giving the most symmetrical Δe-distribution, at the bottom of the figure, is assumed to represent the *in situ* compression curve, thus also giving the best estimate of σ'_c.

So far no definite answer has been given to the question which method results in the best estimate of the *in situ* preconsolidation pressure.

It is, however, also important to bear in mind that the value of the preconsolidation pressure determined in this way can be affected by sampling disturbances and also by time effects.

Janbu (1969) abandons the traditional log pressure/compression curve and states: "... to enable a rational determination of the preconsolidation load arithmetic plots are absolutely necessary".

Depending on type of material, Janbu suggests that either the pressure/compression curve or the oedometer modulus/pressure curve should be used.

The preconsolidation pressure is an extremely important factor in a settlement analysis, and this problem has been treated by many investigators since it had been recognized. An important step was taken when different loading procedures were investigated, e.g. Leonards and Ramiah (1959); Hamilton and Crawford (1959); Leonards and Girault (1961); Crawford (1964). These investigations clearly showed that the position of the oedometer curve was

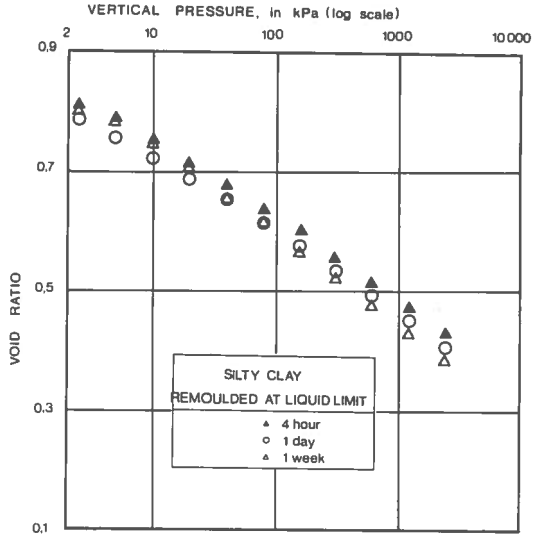

FIG. 5 Effect of load duration on a silty clay. (Leonards and Ramiah, 1959).

dependent on the rate of loading as illustrated in FIG. 5. Longer duration of each increment means that the ε-log σ' curve is lowered and displaced to the left in the diagram. Thus, the lower would the σ'_c-value be, evaluated with any standard procedure. This time effect was an important discovery, which initiated studies concerning the nature of the preconsolidation pressure.

It was known that a clay could be lightly overconsolidated even though the deposit in the past had not carried any load greater than the existing overburden pressure. It was known that an overconsolidation effect could be caused by weathering, cementation, etc.

Leonards and Altschaeffl (1964) found that when a clay sample was subjected to a sustained constant effective vertical stress, the secondary compression would result in what they called a quasi-preconsolidation pressure as illustrated in FIG. 6.

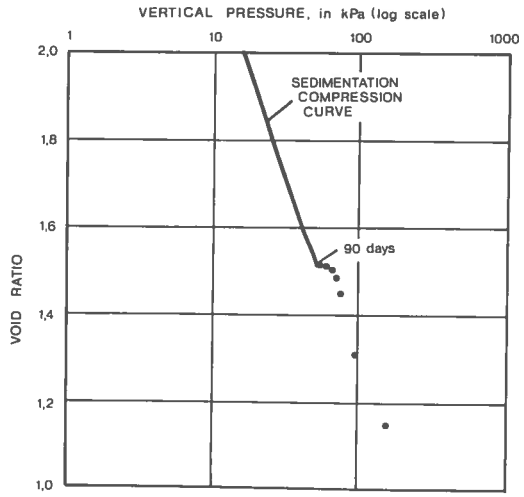

FIG. 6 Increased preconsolidation pressure developed during 90 days. (Leonards and Altschaeffl, 1964).

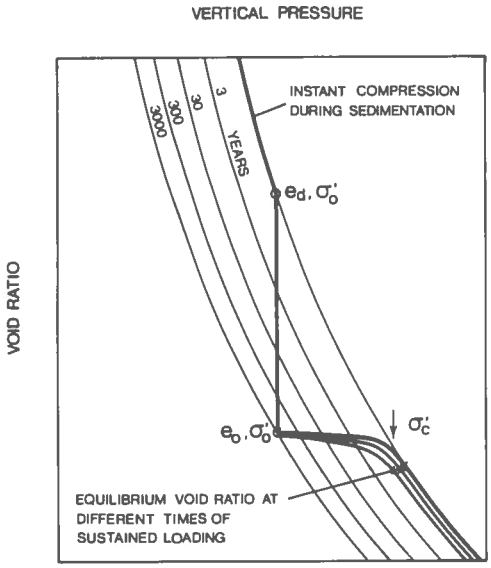

FIG. 7 Effects of secondary compression on void ratio and preconsolidation pressure. (Bjerrum, 1967, 1972)

Later, Bjerrum (1967) in his Seventh Rankine Lecture said that the secondary compression characteristics of a clay that had undergone delayed compression could be explained by a system of curves such as shown in FIG. 7. If a clay with a void ratio e_d and effective stress σ'_o is allowed to compress under constant effective stresses, it will undergo a delayed compression (e_o, σ'_o). When a consolidation test is performed on such a sample it will exhibit an increased preconsolidation pressure equal to σ'_c. The preconsolidation pressure (σ'_c) itself, however, is time-dependent. If the increments in an oedometer test are allowed to continue for several days, more secondary compression will take place, and this in turn will result in a lower preconsolidation pressure. Bjerrum (1972) stated that this increased preconsolidation pressure could be explained with the help of the same system of curves, see FIG. 7. According to Bjerrum's explanation, the increased preconsolidation pressure would vanish if the test were made slowly enough. Leonards (1972) presented contradictory data.

The doubling of the load in the oedometer test was questioned at the same time. Experiments were made with different load increments and the time-dependency of the oedometer curve was found to be the same as when the duration of each increment in the standard test was varied.

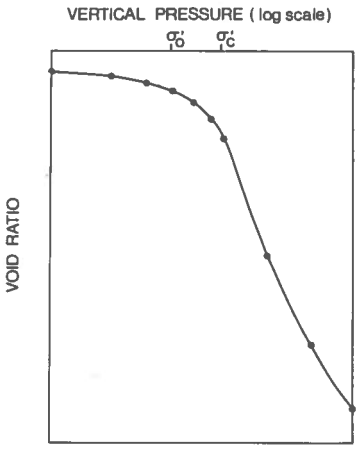

FIG. 8 Log pressure/compression curve illustrating the loading procedure suggested by Bjerrum. (Bjerrum, 1973)

Leonards (1962) suggests that reduced increments should be used in in an oedometer test until the straight portion of the ε-log σ' curve is reached, followed by rebounding (to σ'_o) and loading in conventional loading increments. Then the Burmister construction should be used.

Bjerrum (1973) suggests a similar procedure where the sample is loaded up to the *in situ* vertical stress (σ'_o) in three steps, the increment being $\sigma'_o/3$. After that the σ'_c is estimated and the loading is continued above the σ'_c-value in increments of $(\sigma'^{est.}_c - \sigma'_o)/3$. The duration of each increment is governed by the fact that only primary consolidation is allowed to take place.

For vertical pressures higher than the preconsolidation pressure, the increment is equal to half the previous consolidation load, and its duration is 24 hours, see FIG. 8. This procedure gives a well-defined oedometer curve but a comparatively high value of the preconsolidation pressure, as this test is rather rapid.

Furthermore, Leonards (1975) states that the σ'_c-value could be dependent on the load increment used in the test and that the governing factor may very well be a critical strain instead of a critical stress.

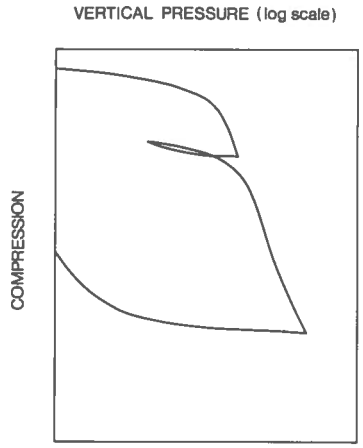

FIG. 9 Swelling of a sample unloaded to zero vertical stress.

As was pointed out by Larsson (1975*a*), much greater strains are required to reach the preconsolidation pressure on the first loading curve than on the second loading curve. The reason is illustrated in FIG. 9, where most of the swelling is found to take place at vertical loads lower than the *in situ* vertical stress.

An important contribution to the understanding of the stress/strain characteristics in the oedometer was made by Hansbo (1960) and Kallstenius (1963) in their investigations of the friction between the oedometer ring and the clay sample. The frictional loss was found to be dependent on the material of the oedometer ring and also to a great degree on the surface smoothness, FIG. 10. The ring friction also seemed to increase with time, FIG. 11, and this has to be taken into account when the increase in preconsolidation pressure is investigated in the laboratory, as the increase of friction contributes to the evaluated preconsolidation pressure.

Although it is not within the scope of this thesis to study the time rate of consolidation, a very brief summary will be made of different procedures for determining the coefficient of consolidation (c_v).

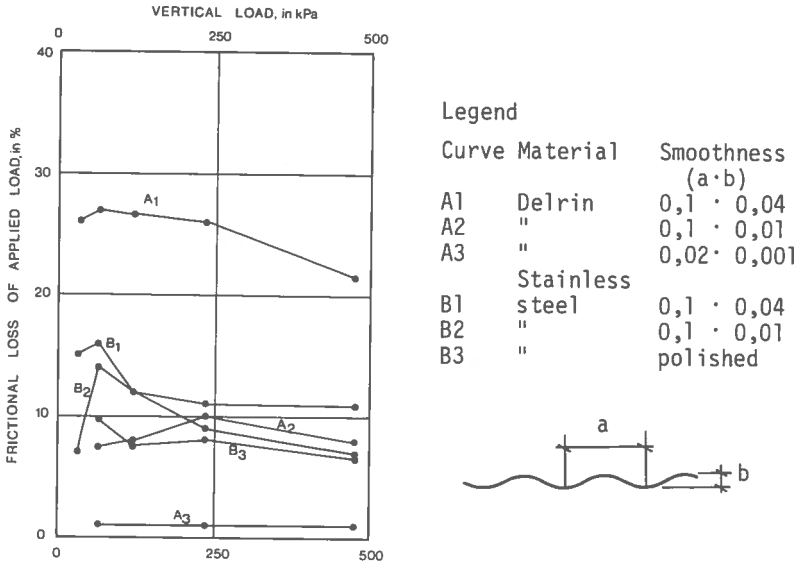

FIG. 10 Effects of ring material and smoothness on friction in oedometer. (Kallstenius, 1963).

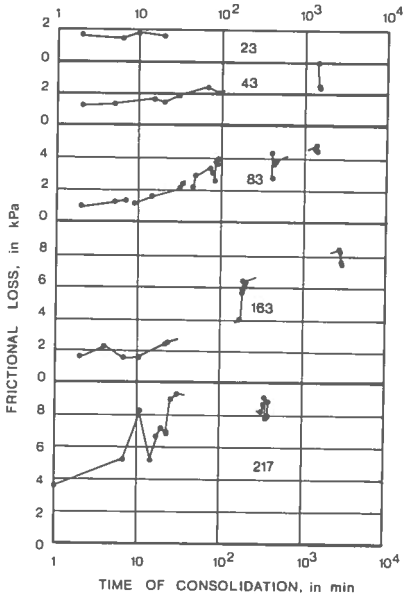

FIG. 11 Frictional loss observed in an oedometer test. (Hansbo, 1960). Figures in graph indicate total vertical loads.

The Casagrande method involves plotting the deformation versus the logarithm of time (FIG. 12). This figure shows the construction of $\bar{U}$ = 100 %. The c_v-value is then calculated from Eq. (2).

$$c_v = T_{50} \frac{h^2_{50}}{t_{50}} \qquad (2)$$

where T_{50} = time factor for 50 % consolidation

h_{50} = height of sample at 50 % consolidation divided by 2

t_{50} = time, in seconds, at 50 % consolidation

This c_v-value represents a pressure equal to the previous consolidation load plus half the increment.

The other commonly used method was proposed by Taylor (1942). The deformation of the sample is plotted versus the square root of time. FIG. 13 shows the construction for $\bar{U}$ = 90 % and 100 %. The c_v-value is calculated from the expression

$$c_v = T_{90} \frac{H^2}{t_{90}} \qquad (3)$$

and consequently represents a pressure equal to the previous consolidation load plus 0,9 times the increment.

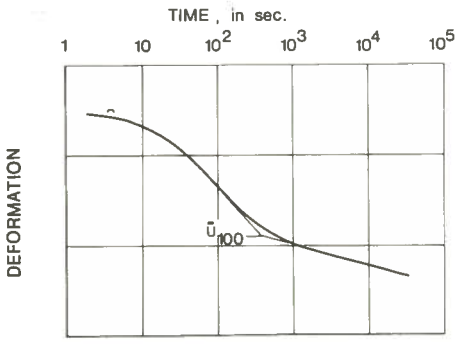

FIG. 12 The logarithm of time fitting method for determination of 100 % primary consolidation.

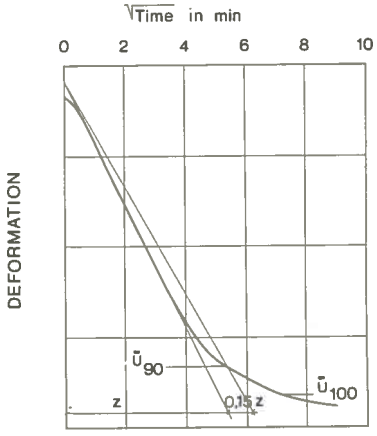

FIG. 13 The square root of time fitting method for determining 100 % primary consolidation. (Taylor, 1942).

2.3 Determination of the preconsolidation pressure by oedometer test, continuous loading

A serious drawback of the results of an oedometer test where the sample is loaded in increments is that the stress/strain curve is not completely defined, only some points are obtained. The final stress/strain curve is to a certain degree a matter of drawing technique, and the determined preconsolidation pressure can vary, within certain limits, depending on the evaluator. This problem can be avoided if the sample is continuously loaded under controlled conditions. If readings of vertical pressure, deformation, and pore pressure are taken at short intervals, the stress/strain curve will be uniquely defined.

Crawford (1964, 1965) reports consolidation tests where the sample was deformed at a constant rate of strain. In FIG. 14 the time effect is clearly illustrated. The advantages of this test procedure are pointed out by several authors, and it is concluded that a more accurate determination of the preconsolidation pressure should be possible in a much shorter time than in the conventional oedometer test. However, the coefficient of consolidation could not at that time be determined for a constant rate of strain test.

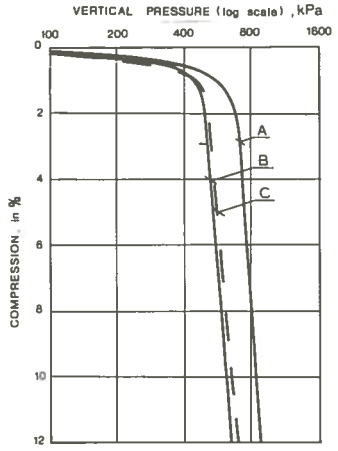

Legend

Test	Loading pattern
A	CRS: 2%/hour
B	CRS: 0,16%/hour
C	Incremental

FIG. 14 Pressure/compression curves for a specimen loaded at different rates of strain. (Crawford, 1965)

At that time Crawford stated that: "An important question requiring further study is the maximum laboratory rate of compression that can be used to compute the correct field settlement".

Four years later Smith and Wahls (1969) reported a thorough investigation concerning the Constant Rate of Strain test (CRS test). Their paper includes a theoretical study of the CRS test where they make the following assumptions:

1. The soil is both homogeneous and saturated
2. Both the water and the solids are incompressible in comparison with the soil skeleton
3. Darcy's law is valid for flow through the soil
4. The soil is laterally confined and drainage occurs only in the vertical direction
5. Stress differentials occur only between different horizontal planes

Assuming the permeability (k) to be independent of the depth (z), the coefficient of consolidation can be calculated at any time from Eq. (4).

$$c_v = \frac{r\,H^2}{a_v \cdot u_b}\left(\frac{1}{2} - \frac{b}{r} \cdot \frac{1}{12}\right) \qquad (4)$$

where $r = \frac{de}{dt}$

H = height of sample

a_v = coefficient of compressibility

u_b = pore pressure at the undrained bottom

$\frac{b}{r}$ = dimensionless ratio expressing the variation in void ratio with depth $\left(0 < \frac{b}{r} < 2\right)$

Correspondingly the average effective stress in the sample can be calculated from Eq. (5).

$$\sigma' = \sigma - \alpha \cdot u_b \qquad (5)$$

where u_b = pore pressure at the undrained bottom

α = coefficient dependent on $\frac{b}{r}$ $(0{,}667 < \alpha < 0{,}75)$

Hence, if α is assumed to be constant and equal to 2/3, the following simple equations are obtained

$$\sigma' = \sigma - \frac{2}{3} u_b \qquad (6)$$

$$c_v = \frac{d\sigma'}{dt} \cdot \frac{H^2}{2\, u_b} \qquad (7)$$

if we substitute $a_v = \frac{de}{d\sigma'}$ and $r = \frac{de}{dt}$.

A thorough mathematical analysis was made by Wissa and Heiberg (1969). They used the consolidation equation derived by Janbu (1965).

$$\frac{\partial \varepsilon}{\partial t} = c_v \frac{\partial^2 \varepsilon}{\partial z^2} \qquad (8)$$

They treated two cases separately. First a linear material was analyzed on the assumption that M is constant and they arrived at an equation for c_v which is identical with Eq. (7). Then the material was assumed to have an oedometer modulus which increased linearly with increasing effective stress from a zero value at zero effective stress. Then they deduced the following expression for the coefficient of consolidation:

$$c_v = -\frac{H^2}{2\Delta t} \cdot \frac{\log \{\frac{\sigma t_2}{\sigma t_1}\}}{\log\{1 - \frac{u_b}{\sigma_v}\}} \qquad (9)$$

where $\Delta t = t_2 - t_1$

The permeability was then calculated from

$$k = c_v \cdot \frac{1}{M} \cdot g\rho_w \qquad (10)$$

where M = oedometer modulus

Wissa and Heiberg also made a comparison between these two expressions for the coefficient of consolidation, c_v, and found that the difference between them increased with increasing excess pore pressure, and was zero when the excess pore pressure was zero, see FIG. 15.

From FIG. 15 it is found that as long as the pore pressure is not higher than 15 % of the total vertical stress, the error in the c_v-value is less than 10 %, if the simple Eq. (7) is used.

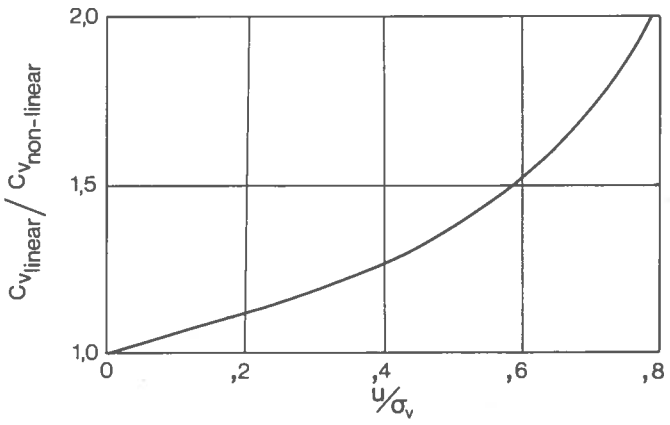

FIG. 15 Comparison of coefficients of consolidation determined from linear and non-linear theories and represented as functions of the ratio of the excess pore pressure to the applied total stress. (Heiberg and Wissa, 1969).

Typical consolidation curves from CRS tests are given in FIG. 16a. The variation in the c_v-value for these tests is shown in FIG.16b.

In the same year Lowe (1969) presented the Constant Gradient Consolidation Test (CGT). In this test the loading is governed by a servo-system in such a way that the pore pressure at the undrained bottom is kept constant.

If the pore pressure distribution in the sample is assumed to be parabolic, the average effective stress can be calculated as

$$\sigma' = \sigma - \frac{2}{3} u_b$$

On the same basic assumptions as Smith, Lowe arrived at the same expression for the coefficient of consolidation. Typical test results are given in FIG. 17.

Later Lowe(1974) presented a modified theory, where the variation in m_v, k and H is taken into account. Futhermore the preconsolidation pressure is found to be dependent of strain rate.

If a material has a linear pressure/compression curve, the two tests, CRS test and CGT test, are identical. Thus, the sample will deform at a constant rate of strain generating a constant

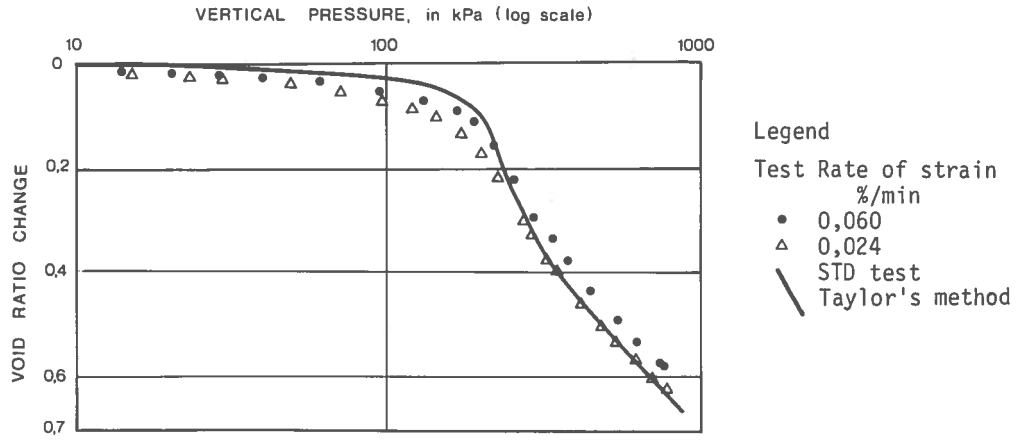

FIG. 16a Pressure/compression curves from CRS tests at different rates of strain. (Smith and Wahls, 1969).

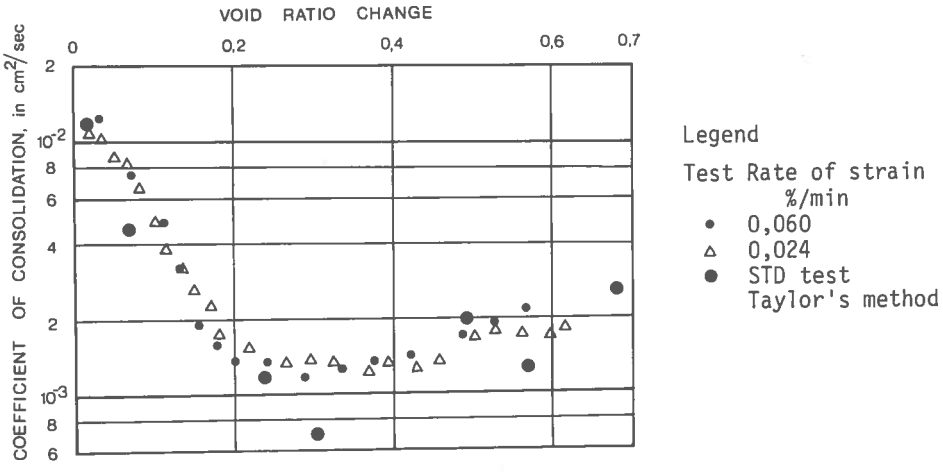

FIG. 16b Variation in coefficient of consolidation in the tests shown in FIG. 15. (Smith and Wahls, 1969).

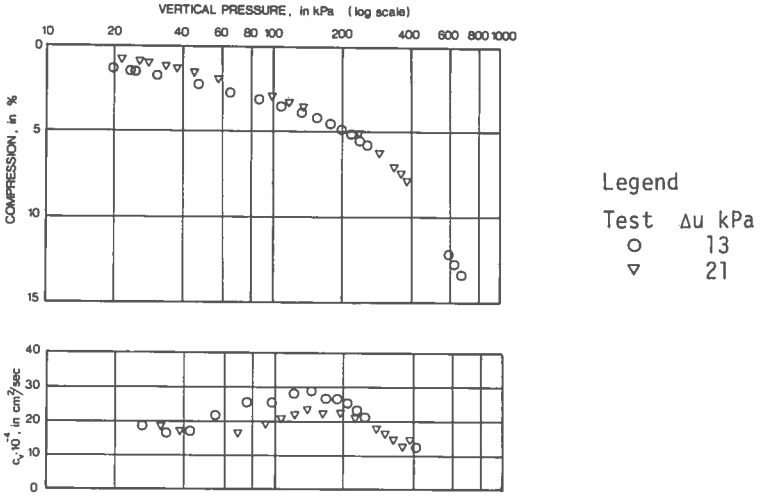

FIG. 17 Controlled gradient test on overconsolidated clay. Top: Strain versus log effective stress. Bottom: coefficient of consolidation versus log effective stress. (Lowe, 1969).

pore pressure throughout the test. In addition, the vertical load will increase linearly with time. But when the material deviates from the above assumptions, the two types of tests will differ significantly.

Consequently a third way of performing an oedometer test under continuous loading is to load the sample at a constant rate. This type of test will not be treated here.

The question how to evaluate the preconsolidation pressure from a CRS or a CGT test has been treated by Lowe (1969), Jamiolkowski and Marchetti (1969), and Wissa (1969) and others. Lowe suggests that the preconsolidation pressure should be evaluated from the c_v/log σ' curve, while Jamiolkowski prefers to evaluate it from the modulus/log pressure curve. In both cases it is the oedometer modulus that is studied as c_v reflects the change in modulus.

Unfortunately most of the experimental results treated in the literature concern soils with much lower clay content and compressibility than the soils dealt with in this thesis. A thorough analysis is therefore of little interest.

2.4 Empirical methods for determination of the preconsolidation pressure

An oedometer test is time-consuming and requires advanced laboratory equipment. Empirical methods for determination of the preconsolidation pressure have therefore been suggested as a complement to the oedometer test.

Skempton (1954) reports good correlation of the ratio of shear strength to effective overburden pressure and the plasticity index.

$$\frac{\tau_{fu}}{\sigma'_o} = 0{,}11 + 0{,}0037\ I_p \qquad (11)$$

Three years later Hansbo (1957) suggested that the same ratio should be expressed in terms of the cone-liquid limit.

$$\frac{\tau_{fu}}{\sigma'_o} = 0{,}45\ w_F \qquad (12)$$

Subsequently these formulae have been used for estimating the preconsolidation pressure, letting σ'_o represent the preconsolidation pressure instead.

The reliability of the above formulae was investigated by Karlsson and Viberg (1967). The scatter was found to be rather large. Still, especially the formula given by Hansbo (1957) is widely used in practice in Sweden.

2.5 Stress paths in oedometer tests

It is well recognized that the oedometer test is a three-dimensional problem so far as stresses are concerned, although the strains take place in a single direction and only the vertical stress is measured during the test. The progress of laboratory technique has made it possible to measure also side friction, and moreover to a certain extent the horizontal stress during the consolidation process. Lately use has been made of the K_0-test, in the triaxial cell, where the diameter of the sample is kept constant by adjusting the cell pressure.

If the horizontal stress is also known, the shear stress in the sample can be determined, and can be studied together with vertical stress and strain. This gives a more complete picture of the stress/strain characteristics of a material.

The general behaviour of an idealized clay is thoroughly treated in the theory of Critical State Soil Mechanics developed at Cambridge University by Roscoe and Schofield (1963), and Schofield and Wroth (1968). In this theory stresses and strains are treated simultaneously, and the behaviour of the material is clearly visualized in the three-dimensional plot in FIG. 18 where the mean stress $(\sigma_1'+\sigma_2'+\sigma_3'/3)$ and the deviator stress $(\sigma_1-\sigma_3)$ are plotted versus the void ratio.

The theory in question will not be treated rigorously in what follows, only a few remarks will be made in connection with FIG. 18.

The three-dimensional graph shown in FIG. 18 represents different stress/strain conditions to which the sample can be subjected. The curved surface, CC" D" E" ED, is called the state boundary surface. The soil can be in equilibrium for a combination of stresses representing points below the state boundary surface. If a soil is

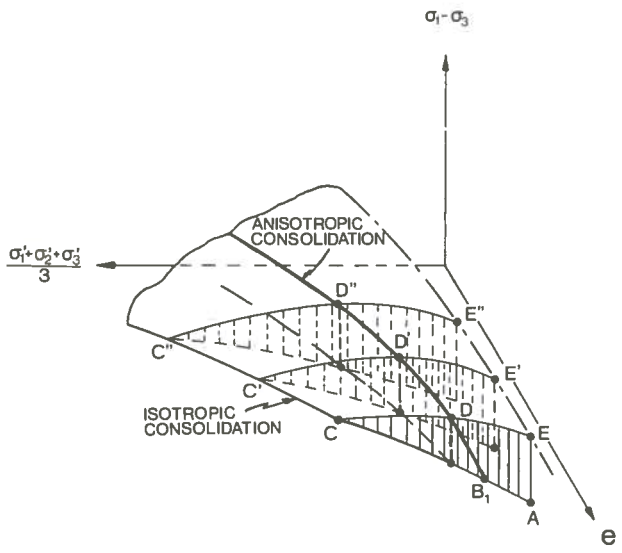

FIG. 18 State boundary surface. (Roscoe and Schofield, 1963).

in equilibrium for a certain definite combination of stresses, say at point B_1 in FIG. 18, and the stresses in the sample are increased, then the soil will yield when the stress path hits the state boundary surface. The point where it hits the state boundary surface is dependent on the type of test. An isotropic consolidation would lead to a stress path like B_1 C C' C", with yield at C, while the sample in an oedometer test would probably follow a stress path like B_1 D D' D", with yielding first at D.

The principle illustrated in FIG. 18 gives a very clear picture of the close connection between stresses and strains in a clay. The critical state theory also involves a mathematical theory of a model clay, but this theory cannot be expected to agree completely with real soils, and will therefore not be treated any further here.

The critical state theory shows that yield occurs when the stress path hits the state boundary surface. Hansbo (1960), Bjerrum (1967, 1973) and Berre (1972), suggest that the preconsolidation pressure can be of the same nature as an internal shear failure or reaching a critical shear stress, as illustrated in FIG. 19 (Berre, 1972).

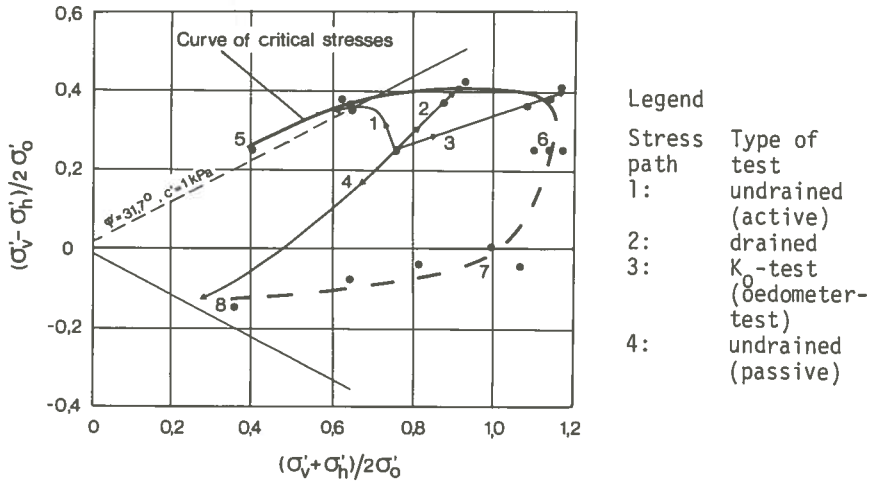

FIG. 19 Critical stress curve shown in a Mohr-Coulomb diagram. Plastic clay from Drammen. (Berre, 1972).

To investigate the variation in horizontal stresses during an oedometer test, several authors have constructed oedometer rings where the horizontal stresses can be measured. The most common method is the use of a semi-stiff ring with strain gauges applied on the outside.

The tests described by Brooker and Ireland (1965) and Som (1970) were all made as incremental tests. They found the relation between vertical and horizontal stresses to be a function of the stress history as well as of the stress level.

FIG. 20a shows a typical stress path in an oedometer test, including unloading. FIG. 20b gives the variation in the incremental coefficient ($\Delta\sigma_h'/\Delta\sigma_v'$), which is low at the beginning of the test (0,28) but higher (0,64) at larger stresses.

Most investigators have used remoulded clay for the oedometer test but those who have used undisturbed samples have obtained slightly lower values of the incremental coefficient. It has therefore been questioned whether it is possible to measure the true horizontal stresses in the overconsolidated region as the edge of the sample is slightly disturbed, and an active pressure is mobilized at very small horizontal deformations, Larsson (1975*b*).

Results similar to those reported by Brooker and Ireland (1965) were obtained when tests with no lateral strain were run in the triaxial cell, Simon and Som (1969).

Results of so-called K_0-tests are often presented in the literature. Unfortunately this expression is used by many investigators for tests where a stress path is chosen so that $\Delta\sigma_h'/\Delta\sigma_v'$ is kept constant throughout the test and the lateral strain is not controlled. Such tests usually have little resemblance to an oedometer test. It is the Author's opinion that a K_0-test should be strain-controlled so that the diameter of the sample is kept constant.

Generally the ratio of horizontal to vertical effective stress is referred to as the coefficient of earth pressure at rest K_0. This is a unique value for the soil *in situ*, while the ratio of horizontal to vertical effective stress in the oedometer is dependent

A thorough analysis would demand a detailed calculation of the stress distribution for the soil profile. This has not been done.

Friman-Clausen (1970) reports results similar to those obtained by Höeg, *et al.*, (1969), but the available data are not sufficient to enable a detailed comparison.

Tavenas, *et al.*, (1974) report results relating to three test fills on Champlain clay. The development of pore pressures during construction is shown in FIG. 22a. The piezometers were all situated 2,6 m under the centres of the fills. Tavenas, *et al.*, (1974) attribute the change in behaviour in the case where the surface load is 25 kPa to a change in weather conditions. However, the increase in effective vertical pressure at 2,6 m, when the pore pressure curves bend off, corresponds very well with the difference between the preconsolidation pressure and the effective overburden pressure, see FIG. 22b. The breaks in the pore pressure curves probably reflect the change in modulus of the clay at the time when the preconsolidation pressure is reached.

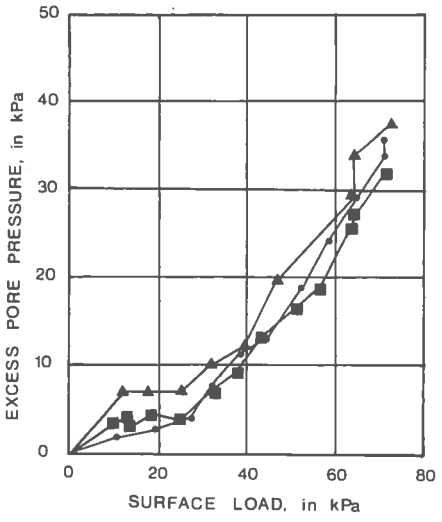

FIG.22a Pore pressures observed by means of three different piezometers 2,6 m under centre lines of test fills on Champlain clay. (Tavenas, *et al.*, 1974).

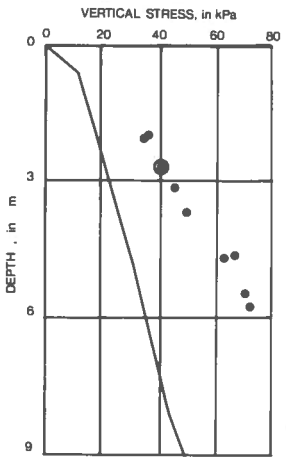

FIG.22b Effective overburden pressure and preconsolidation pressures for Champlin clay. (Tavenas, *et al.*, 1974)
• σ' from oedometer tests
● σ_c' determined from FIG. 22a by the Author.

This indicates that when a clay is loaded *in situ* the increase in measured pore pressures will be larger once the preconsolidation pressure is reached. In what follows, five test embankments are considered.

When the surface load in a field test on a clay with low permeability is applied in a relatively short period of time, the test will be performed under what is called undrained conditions. If the soil is saturated the induced pore pressures will be of the same order as the octahedral stress, as was found, for example, for the test fill at Åsrum, (Höeg, *et al.*, 1969). The increase in pore pressures indicated by the piezometers at a depth of 3 m is shown in FIG. 21a. The bend-off in the curve was assumed to be caused by a local yield because the undrained shear strength of the soil was exceeded, and elaborate calculations showed good correlation. On the other hand, the increase in vertical effective stress at that time corresponded fairly well to the preconsolidation pressure, see FIG. 21b.

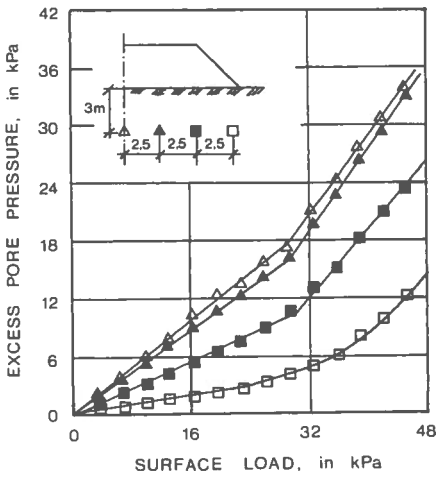

FIG.21a Observed excess pore pressures in load test I at Åsrum, depth 3 m. (Höeg, *et al.*, 1969).

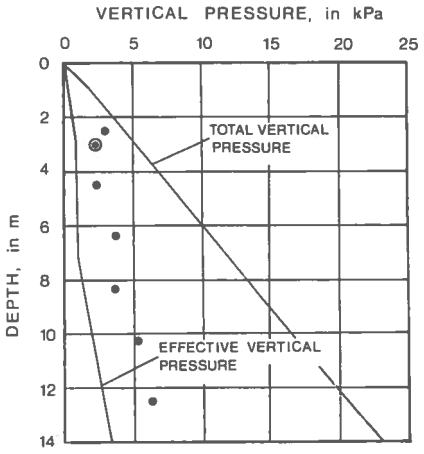

FIG.21b Effective overburden pressure and preconsolidation pressure at Åsrum.(Hoëg, *et al.*, 1969).
• σ'_c from oedometer tests
● σ'_c determined from FIG.21a by the Author.

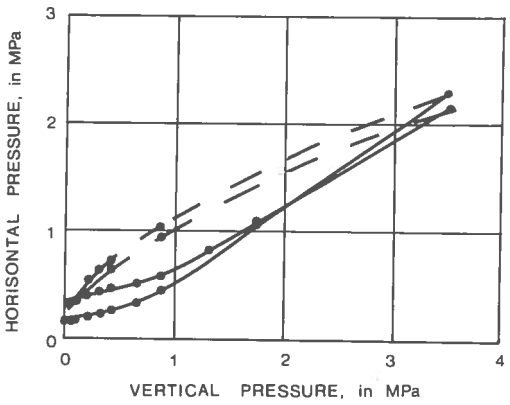

FIG. 20a Stress paths for one-dimensional consolidation of undisturbed London clay. (Som, 1970).

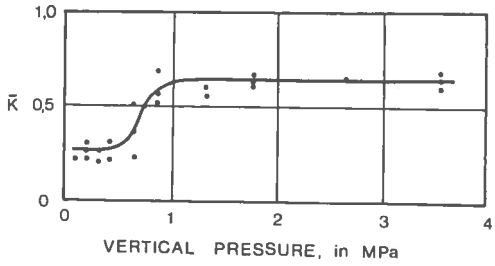

FIG. 20b Incremental coefficiant ($\bar{K}$) versus effective vertical stress for the tests treated in FIG. 21a. (Som, 1970)

on stress history and stress level (test procedure). Therefore it is necessary to differentiate between four values of the coefficient of earth pressure.

a. K_0 = ratio of existing horizontal and vertical effective stresses *in situ*. (Unique value).

b. K_0 = ratio of horizontal and vertical effective stresses in the oedometer. (Depends on testing procedure).

c. K_o' = ratio of the effective stress increments $(\Delta\sigma_h'/\Delta\sigma_v')$ in the oedometer for values of $\sigma_v' > \sigma_c'$.

d. K_o'' = ratio of the effective stress increments $(\Delta\sigma_h'/\Delta\sigma_v')$ in the oedometer for values of $\sigma_v' < \sigma_c'$.

2.6 Determination of the preconsolidation pressure *in situ*

The reliability of the results of laboratory tests has often been questioned, and many attempts have been made to avoid sampling and to determine the soil properties *in situ* instead. Many tests embankments have been built on soft ground, and in 1972 a conference was held at Purdue, where results obtained from 21 test embankments were reported. The general report (Bjerrum, 1972) states that the interest centred in the factor of safety, and that many test fills have been loaded to failure.

However, quite a few embankments were reported where the study of the settlements was the main purpose. Calculated settlements have been compared with those measured, and the vertical pressures were usually much higher than the preconsolidation pressure. It is often difficult to check the preconsolidation pressure determined in the laboratory against the field values from the results presented. Few fills are known where the only object has been to study the preconsolidation pressure *in situ*. However, on the basis of the results obtained from the test fills reported, the following general statement was made by Bjerrum (1972). "For small additional loads – within the range of the σ_c'-effect – the settlements will be small, the excess pore pressures will be small, and they will dissipate rather rapidly. For additional loads leading to the σ_c'-values being exceeded the settlements will be large, the excess pore pressures will be high and dissipate slowly".

The three test embankments discussed so far were rather rapidly loaded to full height, 10 to 20 days, and are generally considered to be undrained. Still it is interesting to note that the change in behaviour of the soil, so far as the pore pressure is concerned, coincides fairly well with the preconsolidation pressure.

d'Appolonia, *et al.*, (1971) report results obtained from a test fill on Boston blue clay, where it took about 4 months to reach full height of the fill. Some of the pore pressure curves are given in FIG. 23a. For piezometer P6, a surface load of 120 kPa is required to create any significant excess pore pressures. However, for piezometers P7 to P9 the pore pressure increases markedly already from the beginning. The increase in effective vertical pressure at the bend-off for piezometer P6 is plotted in FIG. 23b, and it is found to correspond extremely well with the values of the preconsolidation pressure determined from laboratory tests.

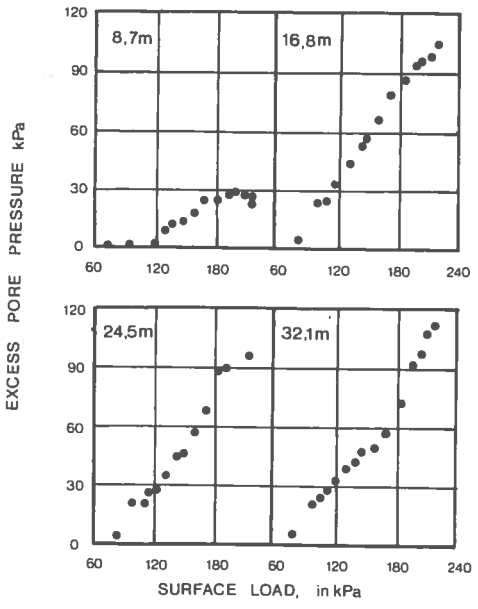

FIG.23a Excess pore pressures observed by means of four piezometers under a test fill on Boston blue clay. Figures in graphs indicate depths below ground surface. (d'Appolonia, *et al.*, 1971).

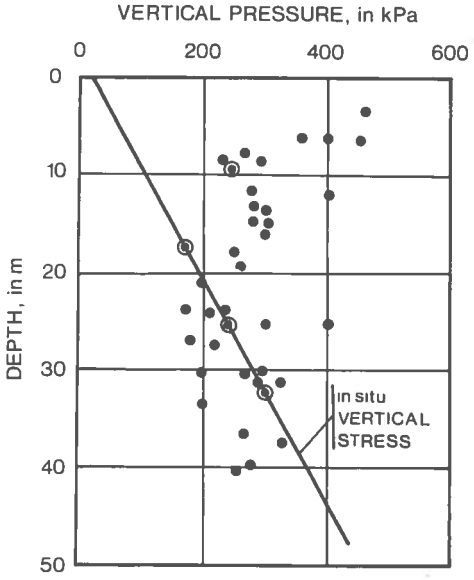

FIG.23b Effective overburden pressure and preconsolidation pressures for Boston blue clay. (d'Appolonia, *et al.*, 1971).
• σ' from oedometer tests
● σ'_c determined from FIG. 23a by the Author.

This holds good also for piezometers P7 to P9, where the increase in effective vertical stress is small, and the clay at this depth can be assumed to be normally consolidated, as indicated in the figure.

Similar results were obtained by Dascal, *et al.*, (1975), and typical pore pressure curves are presented in FIG. 24a. The pre-consolidation pressures determined as the sum of the effective overburden pressure and the effective stress increase, when the development of pore pressure drastically changes, is given in FIG. 24b, together with the preconsolidation pressures evaluated from oedometer tests.

All investigators agree that local yield at the piezometer is the cause of the change in behaviour, and all conclusions concern the undrained shear strength. But, as Bjerrum (1973) said in his state of the art report: "Under drained conditions the stress-strain behaviour is very nearly identical to that observed under undrained conditions". Most of the pore pressure curves discussed were taken from piezometers under the centre of the fills and fairly close to the surface, and consequently have boundary conditions reminding of those in the oedometer. The local yield is therefore believed to be closely connected with the preconsolidation pressure, or a critical shear stress.

An analysis of results obtained from piezometers at larger depths or closer to the edge of the fill would require a further study of stress distribution.

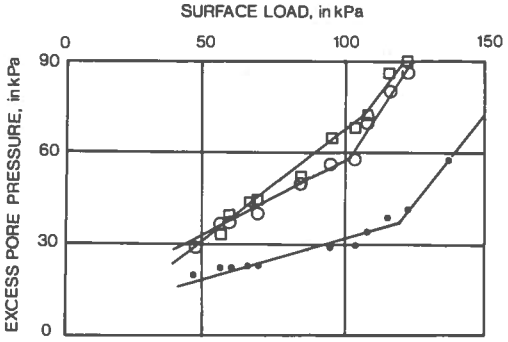

FIG. 24a Excess pore pressures observed during construction of MIT test fill. Figures in graph indicate piezometer depths below ground surface. (Dascal, *et al.*,1975).

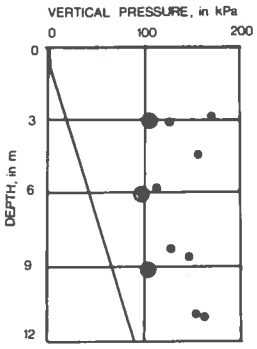

Fig 24b Variation in preconsolidation pressure with depth under MIT test fill. (Dascal, *et al.*, 1975).
- • σ'_c from oedometer tests
- ● σ'_c determined from FIG. 24a by the Author

3 OEDOMETER TESTS

3.1 Introduction

In the survey of the literature several loading routines for oedometer tests were described. It was pointed out that the loading routine, i.e. the magnitude of the load increment and the load duration, can greatly affect the stress/strain behaviour of a clay. As the main purpose of this work is to study the pre-consolidation pressure, a thorough investigation has been carried out in order to make a comparison of the results obtained by using different loading routines.

Although the coefficient of consolidation is only briefly dealt with, typical results are in some cases presented in connection with the pressure/compression curves.

Five different loading routines were used, viz., three where the sample was loaded in increments and two where the sample was continuously deformed.

All tests discussed in this section were performed, if not stated otherwise, on a soft, high-plastic, and lightly overconsolidated clay from Bäckebol, Göteborg. Samples were taken with the Swedish piston sampler St I, at depths of 5 m and 7 m. The geotechnical properties are listed in Table 1.

Table 1. Geotechnical properties of tested material

	ρ(t/m^3)	w(%)	w_L(%)	w_p(%)	τ_{fu}(kPa)	S_t
5 m	1,58	80	85	32	15	15
7 m	1,47	102	99	34	13	25

The clay content is about 55 % at a depth of 5 m and slightly above 70 % at 7 m.

3.1.1 Oedometer test, incremental loading

Test apparatus

The apparatus used for incremental loading tests is shown in FIG. 25.

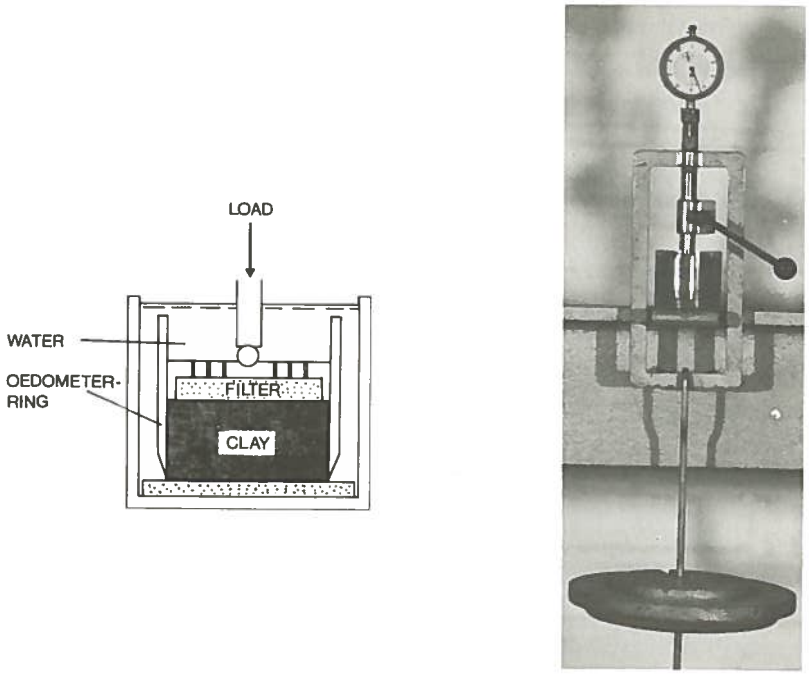

FIG. 25 Apparatus used for incremental oedometer tests.

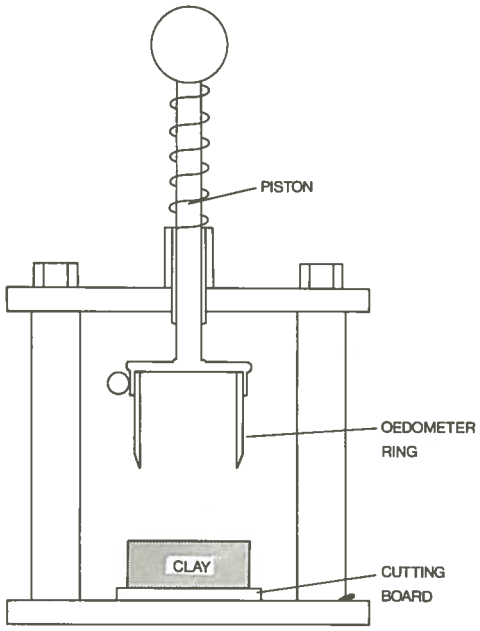

FIG. 26 Cutting device used for mounting clay samples.

The oedometer ring is 40 mm in diameter, and is provided with a cutting edge at the bottom. When mounting a sample, a 20 mm thick sample is extruded from the 50-mm diameter sampling tube and placed on a cutting board, see FIG. 26. The oedometer ring is fastened vertically in the holder, and the sample is trimmed into the ring by slowly pushing the piston downwards. By this procedure a very close fit is achieved between the clay and the oedometer ring. The ring was previously lubricated with molybdenum sulphide, to reduce friction between the clay and the oedometer ring.

The oedometer is then placed in the loading frame, see FIG. 25, where the load is applied by weights. When a new increment is to be applied, the piston in FIG. 25 can be locked, thus protecting the sample from improper shocking.

The deformation is measured with a dial gauge, where readings can be taken with the accuracy of 2/1000 of a millimetre.

Loading routines

Three different procedures were used for incremental loading:

A. Standard procedure: daily load increments, each increment being equal to the previous consolidation load; in what follows called STD test.

B. Loading procedure suggested by Leonards (1962) and Bjerrum (1973), where a new increment is applied at the end of primary consolidation. The increments are chosen so that the existing *in situ* overburden pressure is reached in three equivalent increments, followed by three equally large increments to the estimated preconsolidation pressure. Once the preconsolidation pressure is exceeded, the increments are left for 24 hours, each increment being equal to half the previous consolidation load. This test is in what follows called NGI test.

C. The third method involves daily and equal increments usually 10 or 20 kPa each with a duration of 24 hours. This test is in what follows referred to as a LIN test.

Discussion of test results

In what follows, typical test results are given for the three different incremental loading procedures and commented individually.

STD test The following increments were used for the STD tests: 10, 20, 40, 80, 160 and 320 kPa. Typical results are given in FIGs. 27a and 27b.

In FIG. 27a the log time/settlement curves for test A7-1 are plotted on two different scales. For the increments below the preconsolidation pressure, typical S-shaped curves are obtained when plotted with an accuracy of 2/1000 mm. The increment that straddles the preconsolidation pressure, in this case 40 to 80 kPa, produces a typical log time/settlement curve with no point of inflection, Hansbo (1960) and Leonards (1965). Once the preconsolidation pressure is exceeded the S-shaped curves are obtained again.

It is obvious that the consolidation process does not follow the Terzaghi theory for the increment that straddles the preconsolidation pressure, and the coefficient of consolidation can therefore not be calculated for that increment.

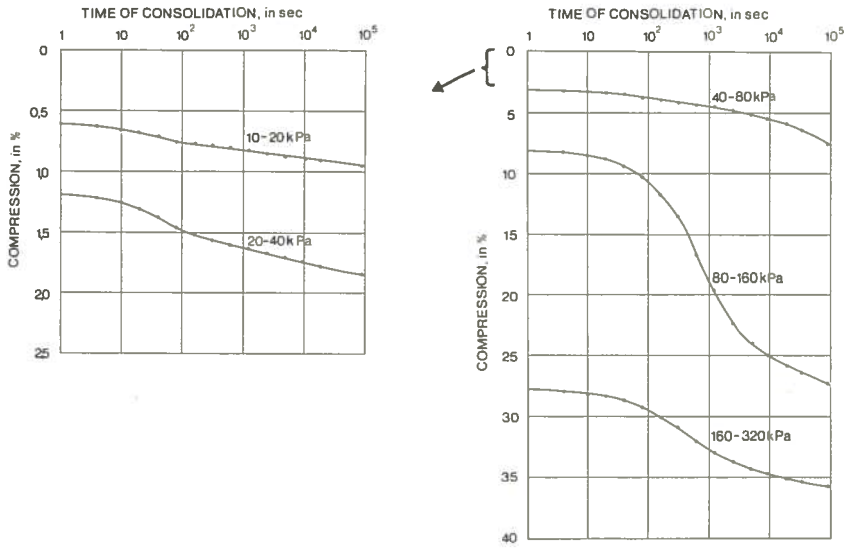

FIG. 27a Log time/settlement curves. Standard oedometer test A7-1. Figures in graphs indicate load increments.

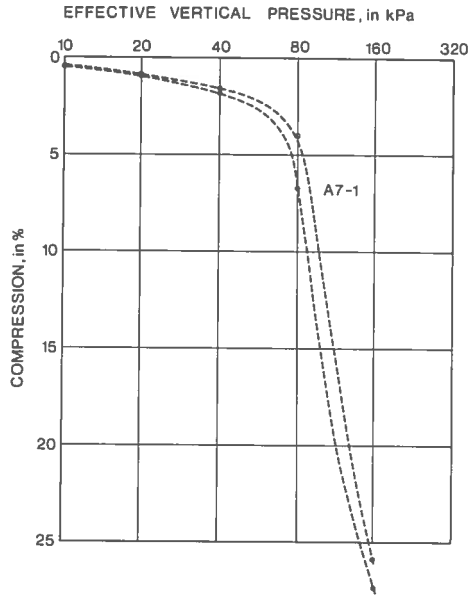

FIG. 27b Pressure/compression curve. Standard oedometer test A7-1. Black circles correspond to 24-hour readings. White circles represent deformation at 100 % primary consolidation, Casagrande method.

Pressure/compression curves are given in FIG. 27b, where the black circles represent the 24-hour readings, while the white circles represent 100 % primary consolidation determined by using the Casagrande method. The Taylor square root of time construction for 100 % primary consolidation will give somewhat lower strains. From FIGs. 27a and 27b the rate of secondary compression is found to increase significantly, once the preconsolidation pressure is exceeded.

There is only one true pressure/compression curve for a single test,but if only 6 or 7 points through which the curve passes are known, then it is possible to draw a number of different pressure/compression curves. When evaluating the preconsolidation pressure, the result can vary significantly, depending on the evaluator. An idea of possible variation can be obtained from FIG. 28, where the results of an inquiry are presented. The results of an oedometer test were sent to 28 persons working in the field of soil mechanics, and they were asked to evaluate the pre-

consolidation pressure. The histogram shows the scatter in the results and reflects not only the difficulty in determining the preconsolidation pressure but also the fact that different methods were used.

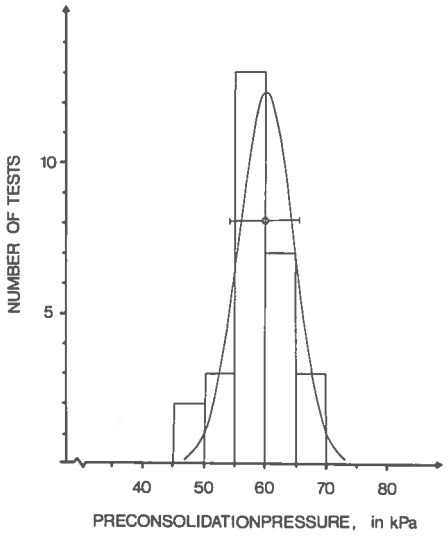

FIG. 28 Distribution of evaluated preconsolidation pressures. 80 % confidence interval. (⊢——⊣)

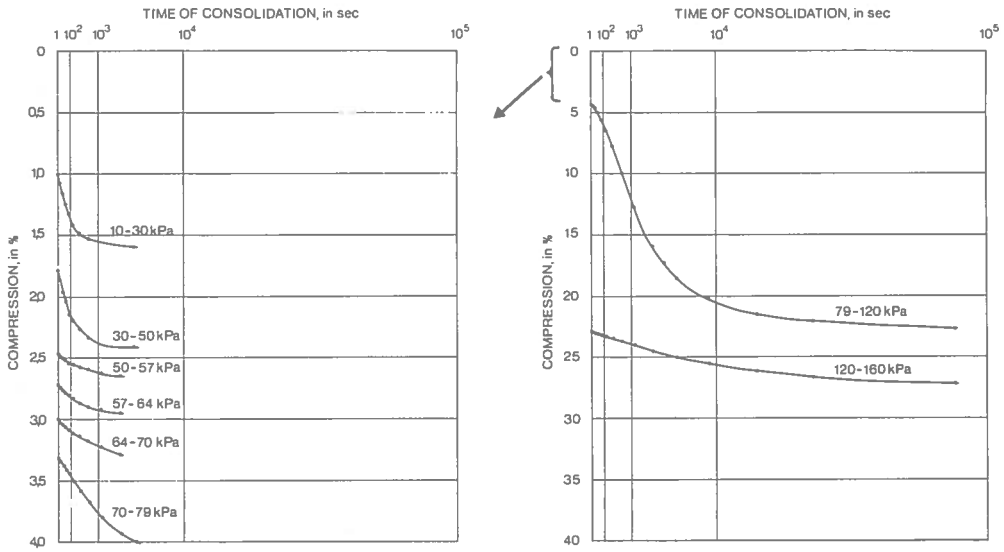

FIG. 29a Square root of time/settlement curves. NGI test A7-2. Figures in graphs indicate load increments.

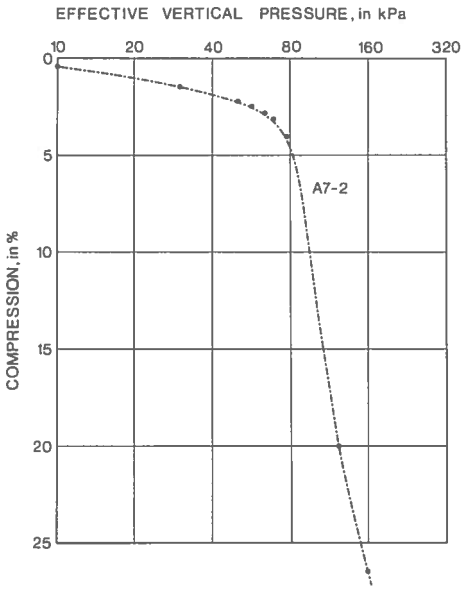

FIG. 29b Pressure/compression curve. NGI test A7-2.

NGI test Taylor's square root of time method is used for determining 100 % primary consolidation which sets the time for the next increment. Typical results are given in FIGs. 29a and b.

From FIG. 29b it can be seen that the pressure/compression curve is well defined around the preconsolidation pressure, owing to the smaller load increments. The evaluation of the preconsolidation pressure will then be more objective. The time required for a NGI test will be 3 to 4 days, as the first 6 increments can usually be completed during one working day. In return one man can at the most take care of 3 tests at a time.

LIN test Daily increments of 10 kPa were used and the log time/settlement curves for test A7-3 are given in FIG. 30a. The curves are no longer S-shaped. For loads smaller than the preconsolidation pressure, the curves are somewhat irregular and can sometimes have two points of inflection. Once the preconsolidation pressure is exceeded, the log time/settlement curves have no point of inflection and are similar in shape to the corresponding curve in the STD test, where the preconsolidation pressure is just being exceeded. This phenomenon has previously been observed by Leonards (1964) and others. An evaluation of c_v-values is no longer meaningful as the Terzaghi model is not valid.

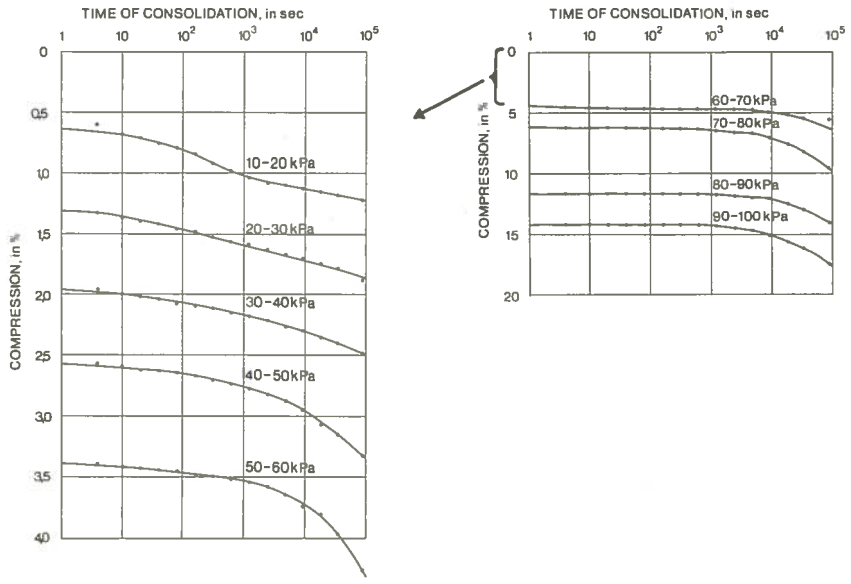

FIG. 30a Log time/settlement curves. Test A7-3. Figures in graphs indicate load increments.

The pressure/compression curve is given in FIG. 30b and, as the number of increments is larger than in the STD test, the oedometer curve is consequently better defined.

A LIN test takes 8 to 12 days depending on the magnitude of the preconsolidation pressure.

Comparison of results from oedometer tests, incremental loading

The three oedometer tests previously discussed in this section were all made on clay from Bäckebol, depths 6,90 to 7,10 m. The clay at the site is very homogeneous, but a certain natural variation in properties between the samples is to be expected. Duplicate tests were made on clay from other depths (appendix A), and the comparison and the conclusions made in the following paragraphs represent the general trend observed.

In FIG. 31 the pressure/compression curves from FIGs. 27, 29 and 30 are replotted. The 24-hour readings were used for the STD test. The preconsolidation pressure determined by using the Casagrande construction will differ with the loading procedures in such a way that the NGI test gives the highest value, followed by the values obtained from the STD test and the LIN test. This is consistent with earlier investigations (Leonards, 1964; Crawford, 1964; Kallstenius, 1963, and others); the slower the test, the lower the preconsolidation pressure. However, the difference between a STD test and a LIN test is often very small.

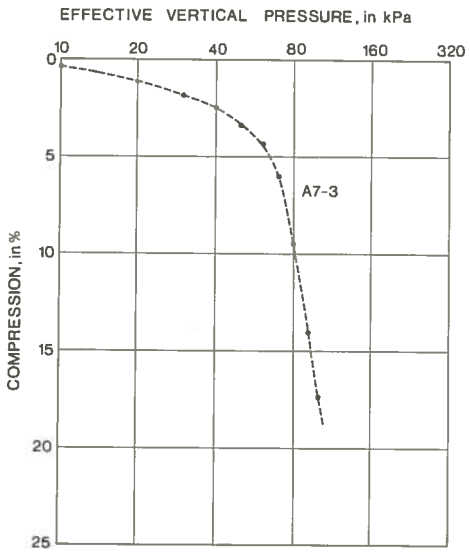

FIG. 30b Pressure/compression curve. LIN test A7-3.

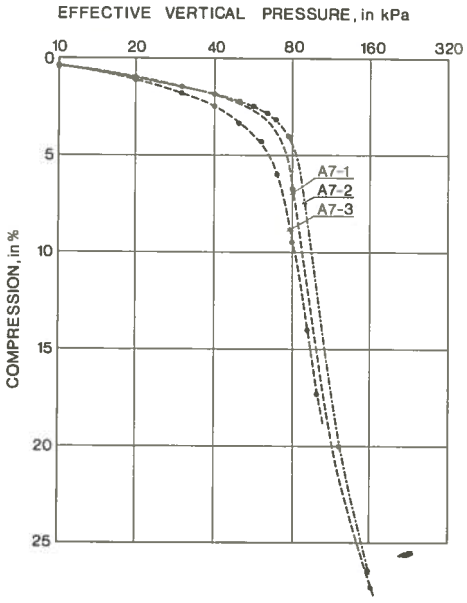

Legend

Test	Loading routine
A7-1	STD
A7-2	NGI
A7-3	LIN

FIG. 31 Pressure/compression curves. Tests A7-1, A7-2, and A7-3. The 24-hour readings are used for the STD test.

If the two curves in FIG. 27b are compared with the curve from the NGI test as in FIG. 32 the curve from the NGI test falls between the two pressure/compression curves from the STD test. The STD test is slower than the NGI test and consequently when using the 24-hour readings the STD test gives a lower preconsolidation pressure. On the other hand, if the compression corresponding to 100 % primary compression is plotted for the STD test, this curve will fall to the right of the NGI curve. This can be explained by the fact that the secondary compression that takes place in the STD test causes the structure to be more resistant to further deformation.

A comparison of the coefficients of consolidation is meaningful only for the STD and NGI tests. FIG. 33 shows the c_v-values obtained from tests A7-1 and A7-2, and the Casagrande method as well as the Taylor method is used for the STD test. The two methods agree well and the reliability of the c_v-value is good also below the preconsolidation pressure when readings are taken with an accuracy of 2/1000 mm.

The c_v-values for the increment from 125 to 160 kPa in the NGI test diverge somewhat. This can be explained by the fact that the increment is rather small and if replotted as log time/settlement it can be seen that the Terzaghi model is not valid. Hence the calculated c_v-value has no significance for this increment.

Reloading

After sampling the sample will swell somewhat, owing to the stress release. During the first loading in the oedometer test the sample is recompressed and the apparent compression is larger than that which can be expected under *in situ* conditions.

FIG. 34 gives the result of a test where the sample was loaded close to the preconsolidation pressure and then unloaded to the *in situ* vertical stress. Increments of 10 kPa, 24-hour duration, were used. When reloaded the oedometer modulus for loads smaller than the preconsolidation pressure is 4 to 6 times as great as the corresponding oedometer modulus from the first loading cycle.

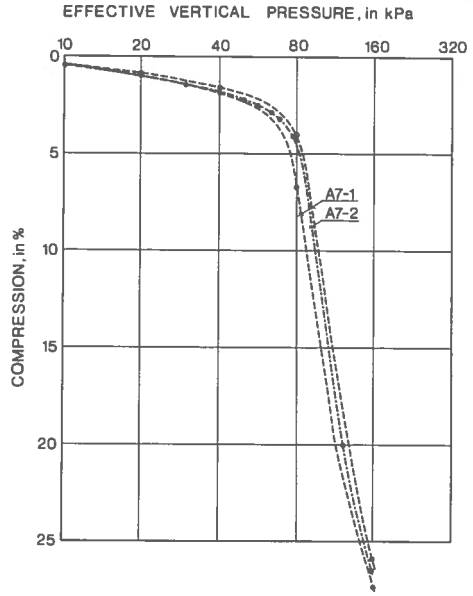

Legend

Test	Loading routine
A7-1	STD
A7-2	NGI

FIG. 32 Pressure/compression curves. Tests A7-1 and A7-2. For test A7-1, black circles correspond to 24-hour readings. White circles represent 100 % consolidation. Casagrande's method

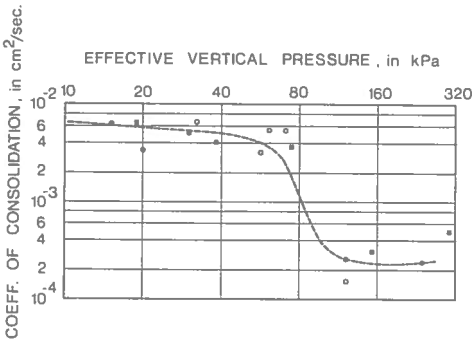

Legend

Symbol	Test Method
●	A7-1 Casagrande
■	A7-1 Taylor
○	A7-2 Taylor

FIG. 33 Comparison of c_v-values. Tests A7-1 and A7-2.

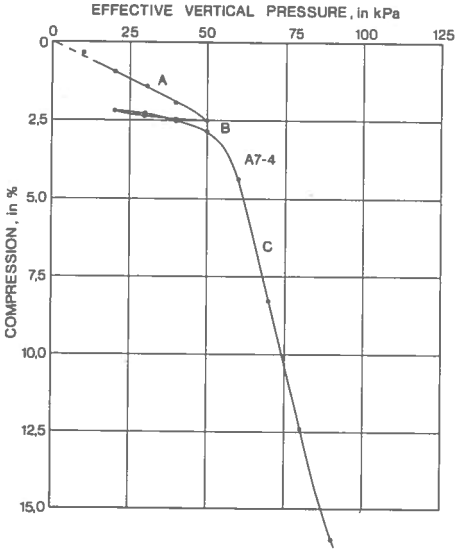

FIG. 34 Pressure/compression curve, including unloading to *in situ* stresses. LIN test A7-4.

Large errors in a settlement analysis can obviously be made for an overconsolidated deposit, if the modulus from the first loading cycle in an oedometer test is used.

FIG. 34 shows the oedometer curve on arithmetic scales.
The pressure/compression curve can be said to consist of three parts:

1. A linear part (A) from zero pressure close to pressures equal to the preconsolidation pressure. A straight line is not obtained from the very beginning of the test, and this is probably due to inefficient contact between the piston plate and the sample. In the following, the straight line A will be extended and the intersection with the zero-pressure line will be taken as the corrected starting point.

2. A curved part (B) indicating that the preconsolidation pressure is being exceeded.

3. A second, fairly linear part (C) from the preconsolidation pressure down to 10 % deformation representing virgin compression.

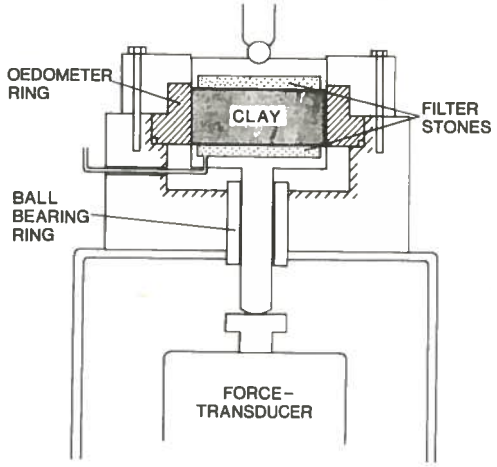

FIG. 35 Apparatus used for measuring friction between oedometer ring and clay sample.

Friction between sample and oedometer ring

A thorough investigation of the friction between the clay and the oedometer ring was made by Hansbo (1960) and Kallstenius (1963). Different materials were used for the ring and surfaces differing in smoothness were also tested. The frictional loss in applied vertical load varied from 1 to 40 % depending on ring material and surface smoothness.

The purpose of the investigation discussed in this section is only to form an idea of the magnitude of the friction between the clay and the ring for different oedometer rings.

Test apparatus

The test apparatus used for measuring the friction between the clay sample and the oedometer ring is shown in FIG. 35.

Two different oedometer rings were used, one made of acidproof stainless steel and the other of teflon. Friction was reduced by lubricating the inside of the ring either with molybdenum sulphide or with silicon grease.

A cutting device was used to trim the sample into the oedometer ring, which in this case is 45 mm in diameter. When the ring is placed in position, see FIG. 35, the bottom of the sample just barely touches the bottom filter. When the first increment is applied, there is probably a slight movement of the sample downwards, but after that the deformation takes place exactly as in the conventional oedometer.

The vertical load (P) was known for each increment and the transmitted load (P') was monitored by a force transducer. (The electronic measuring system will be explained in detail in section 3.1.2).

Discussion of test results

The results of two tests are given in FIGs. 36 and 37. The general trend is that when a new load increment is applied the friction expressed in per cent of the applied vertical load, drops somewhat and then increases again with time. The drop in friction is probably due to the fact that the clay structure is disturbed when a new increment is applied (Hansbo, 1960).

For larger vertical loads there is a certain time delay before the drop in ring friction occurs. A short time interval is obviously required before a partial breakdown of the bonding between the clay and the oedometer ring is obtained.

FIG. 36 shows the results of a LIN test performed in a stainless steel oedometer lubricated with molybdenum sulphide. The frictional loss averages about 25 % of the applied vertical load.

The results of a STD test are given in FIG. 37, where the same ring was used, now lubricated with silicon grease. The friction was was then found to be about 15 %.

These series of tests showed that the difference in frictional loss for stainless steel and teflon was about the same, when the surface smoothness was about the same. However, silicon grease was found more efficient than molybdenum sulphide.

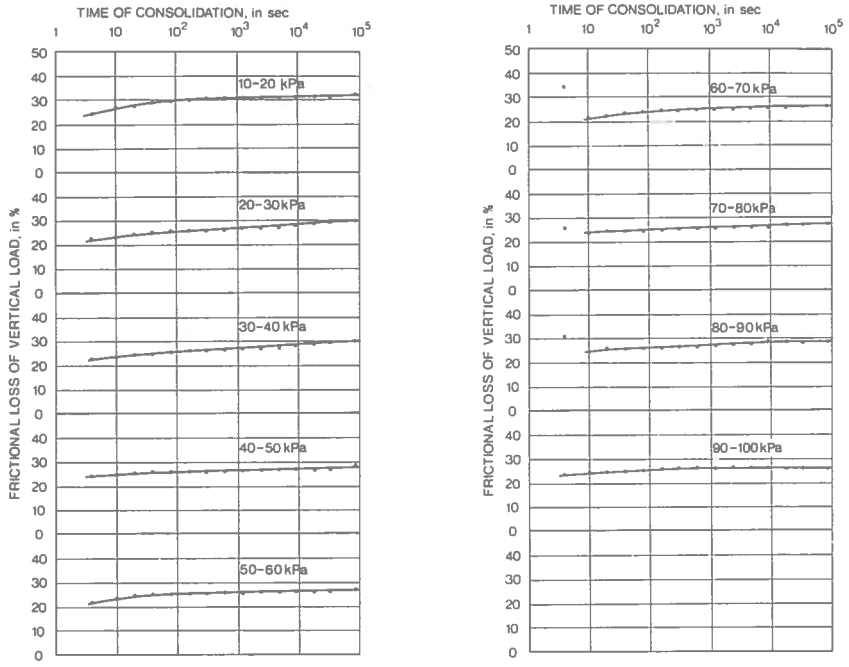

FIG. 36 Frictional loss during a LIN test. Oedometer ring of stainless steel lubricated with molybdenum sulphide.

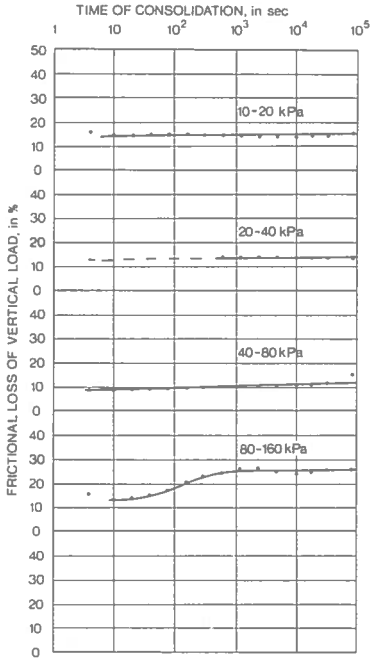

FIG. 37 Frictional loss during a STD test. Oedometer ring of stainless steel lubricated with silicon grease.

If the frictional force is assumed to be equally distributed over the oedometer ring, see FIG. 38, the average effective pressure will be reduced by half the percentage given in FIGs. 36 and 37 and this in turn would lower the preconsolidation pressure for the tests described in this section by 5 to 10 kPa.

3.1.2 Oedometer test, constant rate of strain

In the constant rate of strain test, the sample is continously deformed at a predetermined constant rate of deformation. The pressure/compression curve is obtained by taking readings of the vertical force, the excess pore pressure at the undrained bottom, and the deformation at certain definite time intervals throughout the test. In what follows, this test will be refered to as a CRS test.

Theory

The CRS test was first treated mathematically by Smith (1969) and Wissa, *et al.*, (1969). They both arrived at the conclusion that the average effective stress in the sample can be calculated with good accuracy from the equation

$$\sigma' = \sigma - \frac{2}{3} \cdot u_b$$

where u_b = pore pressure at undrained bottom.

The assumption is thus made that the pore pressure distribution in the sample is parabolic. This equation for calculating effective stresses will be used for the tests described in this thesis.

Wissa, *et al.*, (1969) derived two expressions for the coefficient of consolidation for two idealized materials, one called linear the other non-linear, see FIG. 39.

The clays treated in this investigation have a pressure/compression curve which looks more like the curve labelled "SOFT" in FIG. 39; thus, neither the linear nor the non-linear model is satisfactory. Therefore a general equation for the c_v-value will be deduced, and the linear and non-linear materials treated by Wissa, *et al.*, will be found to be special cases of this general equation.

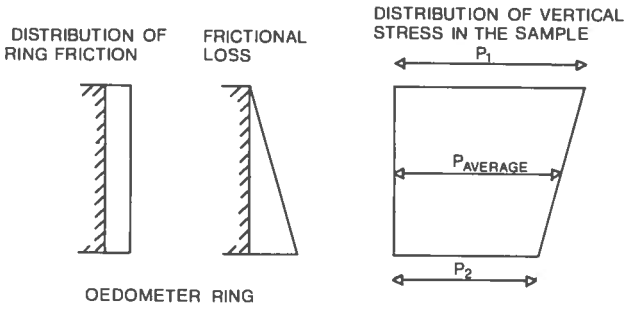

FIG. 38 Assumed distribution of frictional loss in the oedometer.

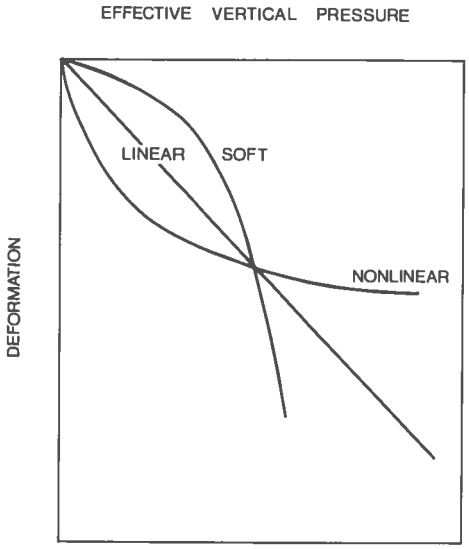

FIG. 39 Typical pressure/compression curves for linear, and non-linear materials.

In the mathematical treatment, use is made of the differential equation deduced by Janbu (1965):

$$\frac{\partial \varepsilon}{\partial t} = c_v \cdot \frac{\partial^2 \varepsilon}{\partial z^2}$$

The boundary conditions for a CRS test, with one side undrained, are (see FIG. 40):

$v = r \cdot t \cdot H$ for $z = o$

$v = 0$ for $z = H$

$\frac{\partial \varepsilon}{\partial z} = 0$ for $z = H$

where $v = \int_z^H \varepsilon \cdot dz$ (vertical displacement of a horizontal layer)

r = average rate of deformation for the sample

H = height of sample.

The differential equation was solved by Davis in 1969, (Heiberg and Wissa, 1969), who found that

$$\varepsilon(z,t) = -\frac{\partial v}{\partial z} = r \cdot t \,(1+F\{\frac{z}{H}, T_v\}) \qquad (13)$$

where $F\{\frac{z}{H},T_v\} = \frac{1}{6} T_v^{-1}(2 - \frac{6z}{H} + \frac{3z^2}{H^2}) - \frac{2}{\pi^2 \cdot T_v} \sum_{n=1}^{\infty} \frac{\cos \frac{n\pi z}{H}}{n^2} \cdot e^{-n^2\pi^2 T_v}$

and $T_v = \frac{c_v \cdot t}{H^2}$.

The distribution of ε throughout the sample can (Eq. 13) be re-written

$$\varepsilon(z,t) = -\frac{\partial v}{\partial z} = r \cdot t + \frac{rH^2}{c_v}\{\frac{1}{6}(2 - \frac{6z}{H} + \frac{3z^2}{H^2}) - \frac{2}{\pi^2} \sum_{n=1}^{\infty} \frac{\cos \frac{n\pi z}{H}}{n^2} \cdot e^{-n^2\pi^2 T_v}\} \qquad (14)$$

where $r \cdot t$ = average strain in the sample, and the second term expresses the deviation from the average strain for different values of z/H and T_v.

The second term may be said to consist of two parts

a. A steady state component of deviation given by

$$\frac{rH^2}{c_v}\{\frac{1}{6}(2 - \frac{6z}{H} + \frac{3z^2}{H^2})\}$$

b. A transient component of deviation given by

$$\frac{rH^2}{c_v}\{\frac{2}{\pi^2} \sum_{n=1}^{\infty} \frac{\cos \frac{n\pi z}{H}}{n^2} \cdot e^{-n^2\pi^2 T_v}\}$$

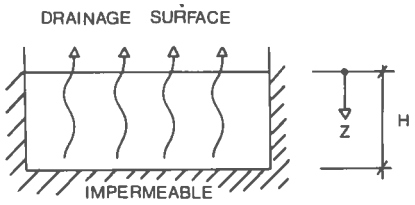

FIG. 40 Definition of boundary conditions for a constant rate of strain test (CRS).

Transient component

Assume ε to be a function of σ', known or unknown, $\varepsilon = f(\sigma')$. The ratio of strains for $z = H$ and $z = 0$ at any time t can then be written

$$\frac{\varepsilon(H,t)}{\varepsilon(0,t)} = \frac{f(\sigma(H,t) - u(H,t)) - f(\sigma(H,0))}{f(\sigma(0,t)) - f(\sigma(0,0))} = \frac{f(\sigma'(H,t)) - f(\sigma'(H,0))}{f(\sigma'(0,t)) - f(\sigma'(0,0))} = \frac{1 + F(1, T_v)}{1 + F(0, T_v)} = F_3(T_v) \qquad (15)$$

since $u(0,t) = 0$

$u(H,0) = 0.$

The function $F_3(T_v)$ can be found tabulated, Wissa, *et al.*, (1969).

Steady state part

According to Eq. (13), the strain can be written

$$\varepsilon(z, t) = r \cdot t + \frac{rH^2}{c_v}\left(\frac{1}{6}\left\{2 - \frac{6z}{H} + \frac{3z^2}{H^2}\right\}\right) \qquad (16)$$

The following definitions are used:

$$c_v = \frac{k \cdot M}{g \cdot \rho_w}$$

$$M \simeq \frac{\Delta\sigma'}{\Delta\varepsilon}$$

The difference in strain between $z = 0$ and $z = H$ at a time t can be written (see Eq. 16):

$$(\Delta\varepsilon)_1 = \varepsilon\,(0,\,t) - \varepsilon(H,\,t) = r\cdot t + \frac{rH^2}{c_v}\cdot\frac{1}{3} - r\cdot t - \frac{rH^2}{c_v}\cdot$$
$$\cdot\,\frac{1}{3} + \frac{rH^2}{c_v}\cdot\frac{1}{2} = \frac{1}{2}\,\frac{rH^2}{c_v} \qquad (17)$$

Thus $(\Delta\varepsilon)_1 = \frac{1}{2}\,\frac{rH^2}{c_v}$

Define a ratio $R = \frac{\Delta\varepsilon}{\Delta f(\sigma')} = \text{const.}$ (18)

then

$$R = \frac{(\Delta\varepsilon)_1}{\Delta f(\sigma')} = \frac{(\Delta\varepsilon)_1}{f\,(\sigma'(0,t)) - f(\sigma'\,(H,t))} \qquad (19)$$

If Eq. (17) and Eq. (19) are combined, Eq. (20) is obtained.

$$R = \frac{rH^2}{2\,c_v\,\{f\,(\sigma'\,(0,t)) - f(\sigma'\,(H,t))\}} \qquad (20)$$

On the other hand, the difference in strain at z = 0 for times t_1 and t_2 is, according to Eq. (17),

$$(\Delta\varepsilon)_2 = \varepsilon(0,\,t_2) - \varepsilon(0,\,t_1) = r\cdot\Delta t \qquad (21)$$

where $\Delta t = t_2 - t_1$.

Using the definition of R Eq. (22) is obtained.

$$R = \frac{r\cdot\Delta t}{f\,(\sigma'(0,\,t_2)) - f(\sigma'\,(0,\,t_1))} \qquad (22)$$

By combining Eq. (22) and Eq. (20) we obtain Eq. (23a), which can be solved for the c_v-value, Eq. (23b)

$$\frac{rH^2}{2c_v\cdot\{f(\sigma'(0,t)) - f(\sigma'(H,t))\}} = \frac{r\cdot\Delta t}{f(\sigma'(0,t_2)) - f(\sigma'(0,t_1))} \qquad (23a)$$

$$c_v = \frac{H^2}{2(\Delta t)}\cdot\frac{f(\sigma'(0,t_2)) - f(\sigma'(0,t_1))}{f(\sigma'(0,t)) - f(\sigma'(H,t))} \qquad (23b)$$

Substitution of $\varepsilon = k_1\cdot\sigma'$ (linear material) gives the simple expression for c_v as

$$c_v = \frac{\Delta\sigma'}{\Delta t}\cdot\frac{H^2}{2u} \quad \text{or} \quad c_v = \frac{d\sigma'}{dt}\cdot\frac{H^2}{2u} \qquad (24)$$

Substitution of $\varepsilon = k_2 \cdot \log \sigma'$ (non-linear material) gives the expression for c_v derived by Wissa, *et al.*, (Eq. (9)).

The relation $\varepsilon = e^{k_3\sigma'}$ is more likely to represent a curve which is consistent with the actual pressure/compression curves treated in this thesis. This substitution gives the following expression for the c_v-values:

$$c_v = \frac{H^2}{2\Delta t} \cdot \frac{e^{k_3\sigma'(0,t_2)} - e^{k_3\sigma'(0,t_1)}}{e^{k_3\sigma'(0,t)} \left(1 - \frac{1}{e^{k_3 u(H,t)}}\right)} \qquad (25)$$

However, if the function $\varepsilon = k_1 + k_2 \cdot \sigma'$ is substituted into equation (23b) the same result will be obtained as if the function $\varepsilon = k_1 \cdot \sigma'$ were used. This means that the simple expression of the c_v-value (Eq. 24) could be used if the oedometer modulus is constant during the time interval considered, and that a steady state is obtained.

Test apparatus

The oedometer originally used for CRS tests is shown in FIG. 41.

The oedometer ring is made of teflon, and is separated from the outer ring when the sample is mounted. Two different rings were used, one 45 mm in diameter and the other 50 mm in diameter. When the 45-mm ring was used, a cutting device trimmed the sample into the ring, whereas the 50-mm ring was centred over the sample tube and the sample was pushed directly into the ring. In both cases the ring was previously lubricated with either silicon grease or molybdenum sulphide to reduce friction between the sample and the oedometer ring. A third type of oedometer made of stainless steel, described in Section 3.2, was also used, but then the lubricant was molybdenum sulphide.

Before placing the oedometer in the bowl, the water system was flushed thoroughly with deaired water to get rid of entrapped air. Then the oedometer was fastened to the base by four bolts. The o-ring around the edge of the ring acted as a seal, making

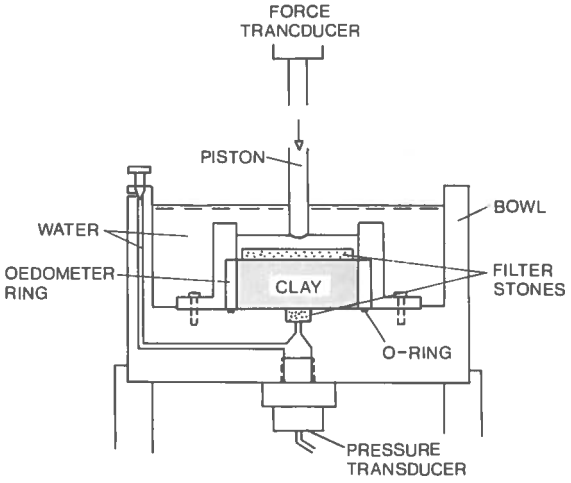

FIG. 41 Oedometer set-up used for CRS tests.

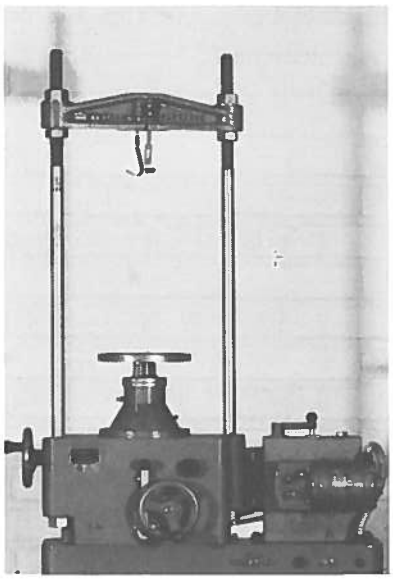

FIG. 42 Compression machine used for CRS tests.

the bottom impermeable. While the bolts were tightened, the water system was left open so as to allow excess water between the sample and the base to dissipate through the filter and the water system. This was also done to avoid large excess pressures in the water system during mounting, as the range of the pore pressure transducer is limited.

The piston plate was then placed in position, the bowl was flooded with water, and the oedometer with its elevation ring was placed in the press, see FIG. 42. A Wykeham Farrance, 1-ton compression machine was used. The rate of deformation was variable from 0,0006 to 0,2 mm/min, so as to provide 25 different discrete rate values.

The piston was placed on the piston plate, and then the table was raised so that the piston just barely touched the force transducer. The test was started by setting the press in gear. Up to a load of approximately 10 kPa the water system was left open and when good contact was ensured between the sample and the bottom the screw was tightened, making the base impermeable.

Data collecting system

As the sample in a CRS test is continuously deformed, readings of vertical force, pore pressure at the undrained bottom, and vertical deformation were taken by a data collecting system. The principle of this system is shown in FIG. 43.

Different transducers were used as measuring units. Type TYCO AB pressure transducers with a range from 0 to 350 kPa were used for measuring pore pressures, and the vertical force was measured with a Hottinger Baldwin Messtechnik force transducer, range 0 to 1000 N. These transducers are both resistive. The deformation was measured with a LVDT, type Hottinger.

Each transducer was connected to an amplifier, where the signal was calibrated. The amplifiers were in turn connected to the scanner, from which the signal was transmitted to the digital

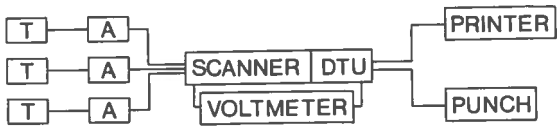

FIG. 43 Principle of data collecting system.
T = transducer, A = amplifier,
DTU = data transfer unit.

voltmeter, where it was digitalized. The scanner was used to set the number of channels to be read and also the frequency of the readings.

The scanner was connected to a data transfer unit (DTU) which administrates the output. The data collecting system used had a Type Addo printer and a Facit punching unit. The printer made it possible to check the readings at any time of the test, while the punched tape was used for transferring the data to a computer.

With the amplifiers used it was possible to calibrate the signal in such a way that the outputs were in Newtons, kPa, or millimetres.

Readings were taken with the following accuracy

Force	0,1 N
Pressure	0,05 kPa
Deformation	0,002 mm

Discussion of test results

In this section the results of a CRS test on clay from Bäckebol, depth 7 m, will be used as an example to illustrate certain points of interest.

The test was performed at a rate of deformation of 0,0040 mm/min (20 % deformation is achieved in slightly less than 16 hours). Readings of vertical force, pore pressure and deformation were taken every fifth minute. Use was made of the computer program described by Sällfors (1974).

The log pressure/compression curve, plotted by the computer (FIG. 44, full-line curve) consists of some 200 points connected with straight lines. Important is the distinct and well-defined part of the curve around the preconsolidation pressure.

This figure also shows a plot of pore pressures (+), measured at the undrained bottom, versus the log of vertical effective pressure. The pore pressure is more or less constant during the

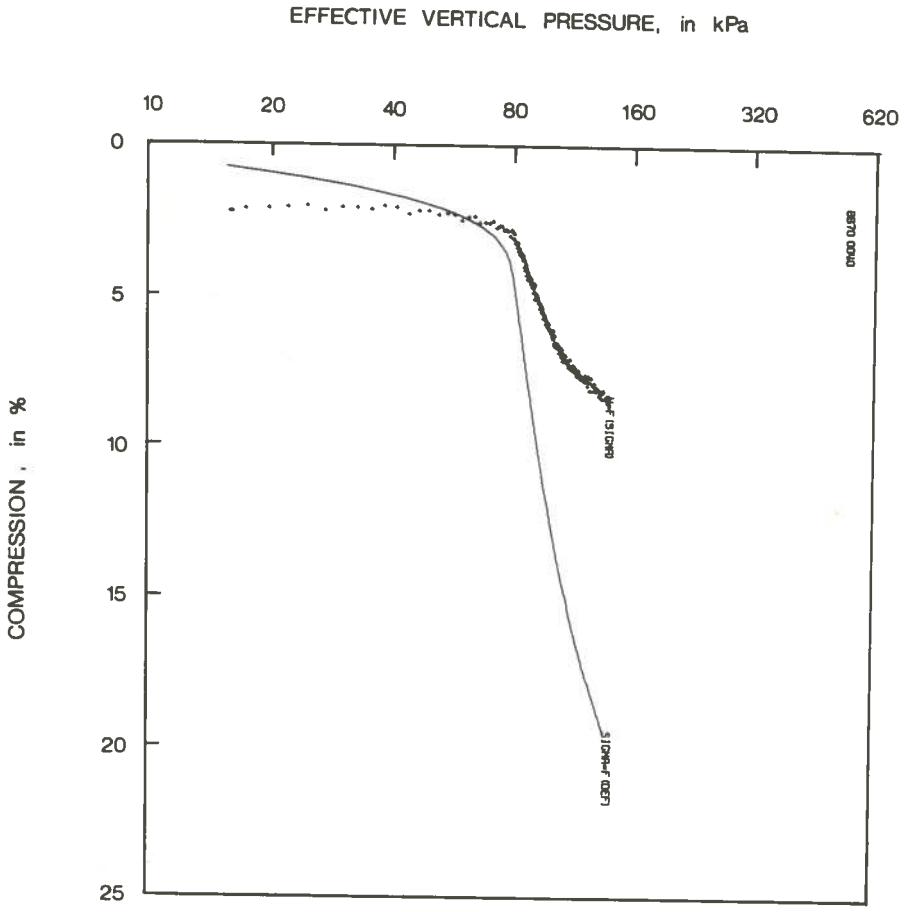

FIG. 44 Log pressure/compression curve plotted by the computer. Test C7-4. Pore pressure/log vertical pessure is also illustrated (+++).

early stage of the test. However, as the preconsolidation pressure is exceeded, the pore pressure increases rather rapidly, indicating a breakdown in the structure.

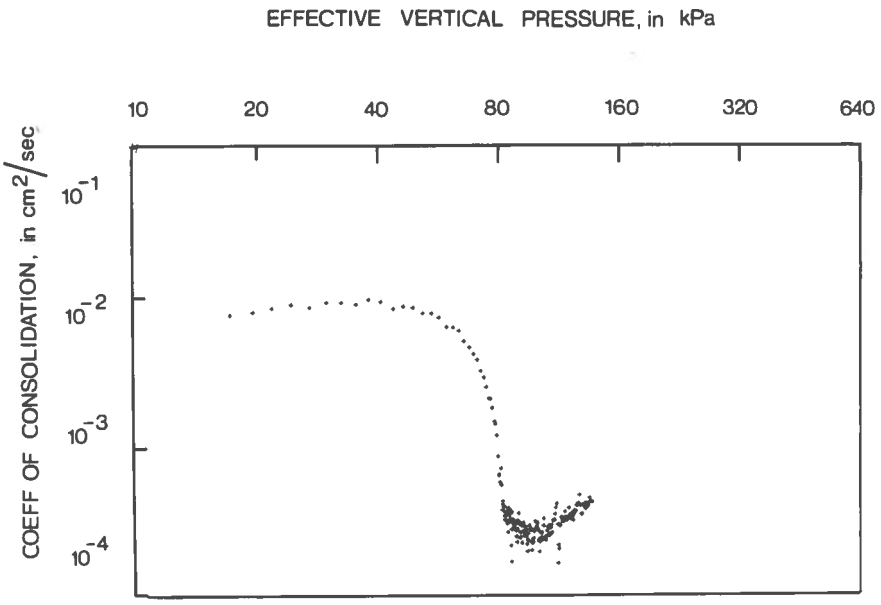

FIG. 45 Coefficient of consolidation versus log vertical pressure plotted by the computer. Test C7-4.

From Eq. (7) the c_v-value can be calculated with good accuracy if the ratio u/σ is less than 10 to 15 %. The variation in the c_v-value during the test is given in FIG. 45. The c_v-value is seen to be largely constant up to the preconsolidation pressure, where it drops very quickly to a much lower value, and then slowly increases again as the test proceeds.

As the pressure/compression curve is completely defined, the oedometer curve may very well be plotted on an arithmetic scale. This is done in FIG. 46 which gives again the pressure/compression (full-line) and pore pressure/pressure (+) curves.

The pressure/compression curve does not start from the origin because a certain definite contact pressure is needed to get good contact between the piston plate and the sample. However, once this contact pressure is established, the stress/strain curve becomes linear up to stresses close to the preconsolidation pressure. The linear part is followed by a curved line and when

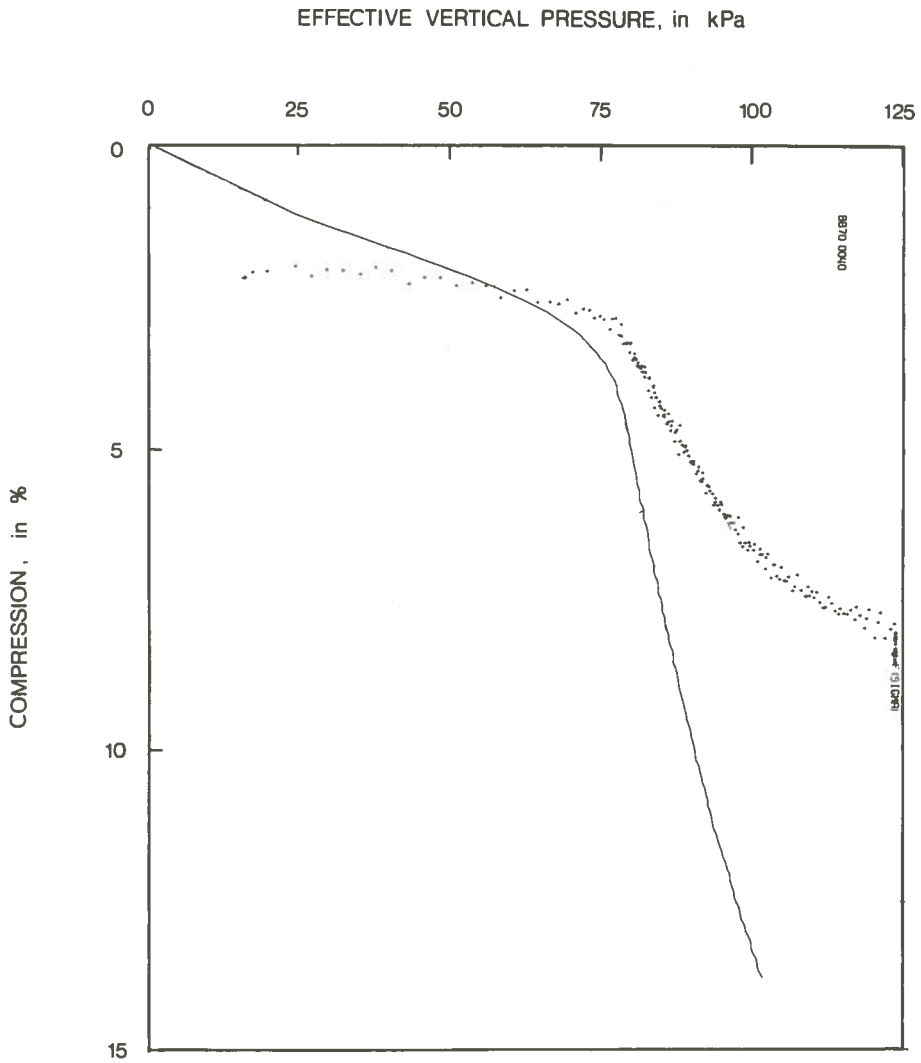

FIG. 46 Pressure/compression curve plotted by the computer on arithmetic scales. (——) Test C7-4. Pore pressure/vertical pressure is also shown (+++)

the preconsolidation pressure is well exceeded, the curve becomes linear again. For larger deformations, 10 to 15 %, the material becomes strain hardening. This general behaviour was found true also for the LIN test, see Sub-section 3.1.1.

The abrupt change in pore pressure can be clearly distinguished also when the data are plotted on arithmetic scales.

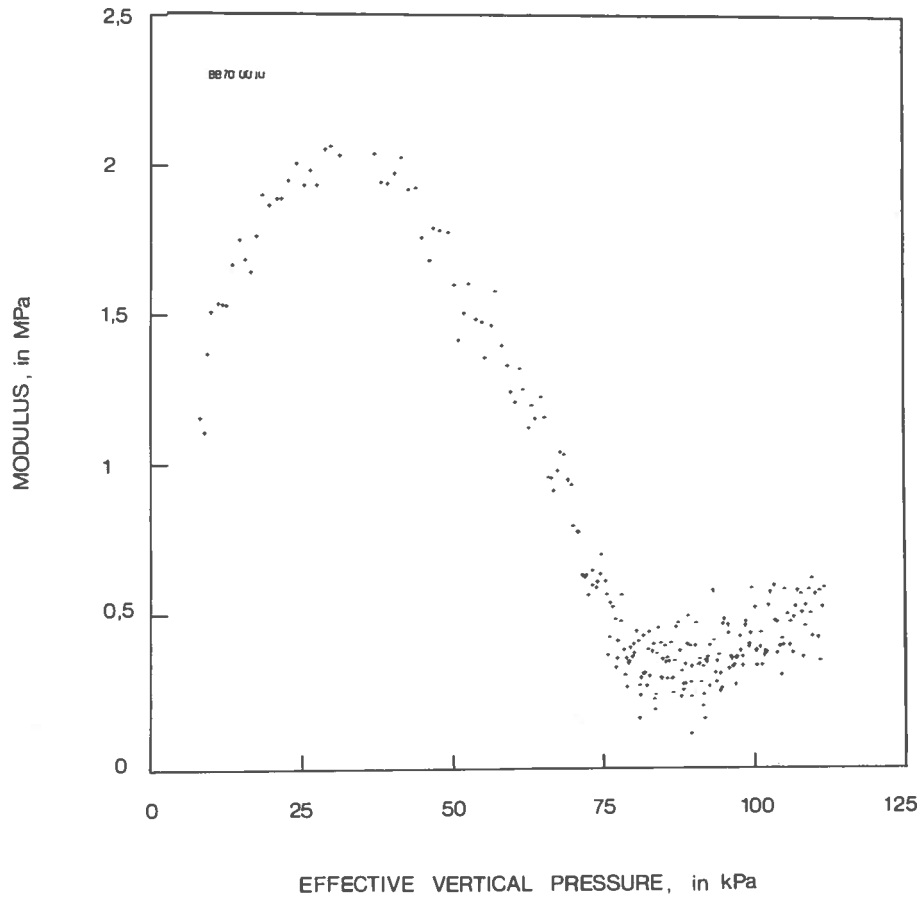

FIG. 47 Variation in oedometer modulus plotted by the computer. Test C7-2.

In this thesis oedometer curves are often compared with one another, and in the following the first straight part of the oedometer curve is therefore extrapolated, and the intersection with the axis ordinates is taken as zero deformation to fulfil the criterion of no stress, no strain.

The computer program also calculates and plots the oedometer modulus against vertical pressure, see FIG. 47. The oedometer modulus increases at the beginning of the test, probably owing to insufficient fitting between the piston plate and the clay, reaches a peak value, and then decreases rapidly, as the pre-consolidation pressure is approached, while a slight increase follows as the test proceeds.

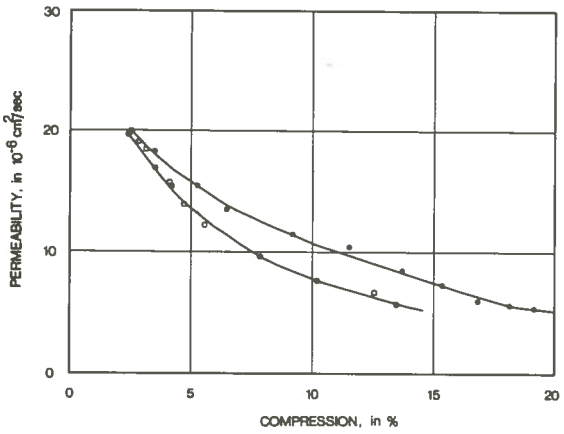

FIG. 48 Variation in permeability.

The variation in the permeability during the test can be calculated from the expression

$$k = c_v \cdot g \cdot \rho_w \cdot \frac{1}{M}$$

where M = oedometer modulus

c_v = coefficient of consolidation.

However, this expression is not yet included in the computer program.

The results plotted in FIG. 48 show the change in permeability for two tests. A slight decrease in permeability can be observed with increasing compression (decrease in void ratio). No abrupt changes are noticed as the preconsolidation pressure is exceeded. The permeability seems to be a function of the void ratio, and the increase in pore pressure as the preconsolidation pressure is exceeded is due to the decrease in the oedometer modulus.

Effect of rate of deformation

The consolidation test described in the previous section was performed at a rate of deformation equal to 0,0040 mm/min. This rate can be varied within a wide range with the compression machine used, and the effect of the rate of strain on the pressure/compression curve is illustrated in FIG. 49.

It is quite obvious that the lower the rate of strain, the lower the preconsolidation pressure will be if the Casagrande construction is used. However, the oedometer modulus below the preconsolidation pressure increases with increasing rate of strain, FIG. 50, and the necessary deformation to reach the preconsolidation pressure seems to be independent of the strain rate. The oedometer modulus for stresses higher than the preconsolidation pressure is basically independent of the strain rate.

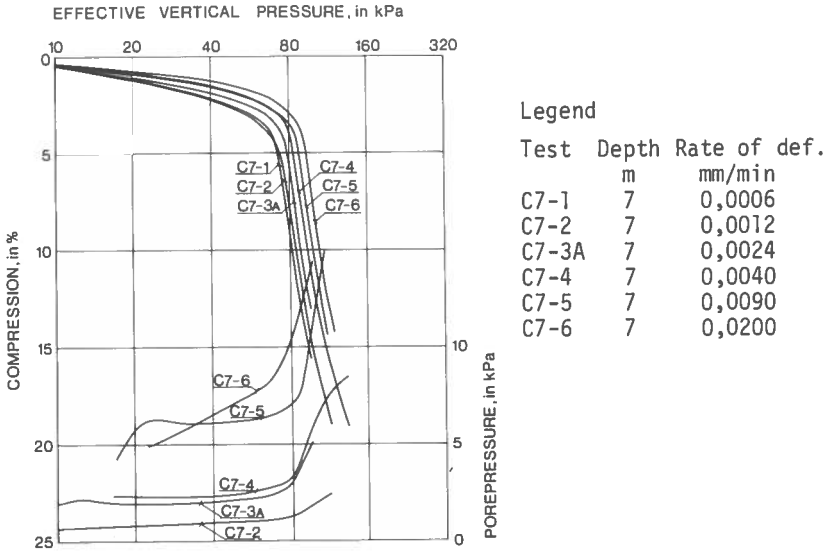

Legend

Test	Depth m	Rate of def. mm/min
C7-1	7	0,0006
C7-2	7	0,0012
C7-3A	7	0,0024
C7-4	7	0,0040
C7-5	7	0,0090
C7-6	7	0,0200

FIG. 49 Pressure/compression curves. Tests C7-1 to C7-6. The variations in pore pressures during the tests are shown at the bottom of the figure, except for test C7-1 where no excess pore pressures were measured.

At the bottom of FIG. 49 the pore pressure at the undrained bottom is plotted against the effective vertical stress except for test C7-1, where no excess pore pressures were measured. It can be noted that the positions of the pore pressure curves are dependent on the strain rate, the greater the strain rate the higher the pore pressure. The characteristic bend in the pore pressure curve appears in all the tests. Usually the breaking point in the pore pressure curve moves to the right with increasing rate of strain, reflecting the higher preconsolidation pressure.

This is explained by the fact that the greater the rate of strain, the more pore water has to dissipate in the same period of time; thus, a greater gradient is necessary, according to Darcy's law.

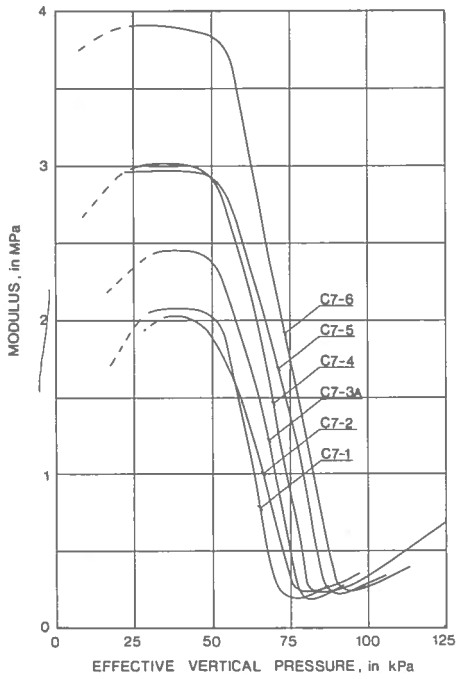

Legend

Test	Depth m	Rate of def. mm/min
C7-1	7	0,0006
C7-2	7	0,0012
C7-3A	7	0,0024
C7-4	7	0,0040
C7-5	7	0,0090
C7-6	7	0,0200

FIG. 50 Variation in oedometer modulus. Tests C7-1 to C7-6.

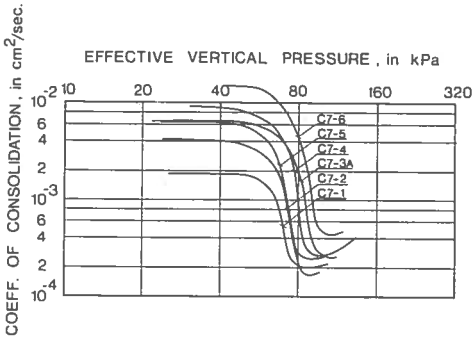

Legend

Test	Depth m	Rate of def. mm/min
C7-1	7	0,0006
C7-2	7	0,0012
C7-3A	7	0,0024
C7-4	7	0,0040
C7-5	7	0,0090
C7-6	7	0,0200

FIG. 51 Variation in coefficient of consolidation. Tests C7-1 to C7-6.

It is well known that the scatter in the coefficient of consolidation is fairly large, especially at vertical pressures lower than the preconsolidation pressure. In FIG. 51 the c_v-values for tests C7-1 to C7-6 are given, and a certain scatter is observed. No definite trend can be traced; possibly the c_v-values below the preconsolidation pressure are slightly higher at higher strain rates. Yet, this could be caused by a deviation from the assumptions that the equation for c_v is based upon. The increase in pore pressure with increasing rates of deformation is obviously at least partly balanced by a larger modulus (compare $c_v = \frac{d\sigma'}{dt} \cdot \frac{H^2}{2u_b}$)

Friction between sample and oedometer ring

Test apparatus

The apparatus used for measuring the friction between the sample and the oedometer ring was the same as that described in Subsection 3.1.1, but was now placed in the compression machine.

For these tests two force transducers were needed, one measuring the applied vertical load and the other measuring the vertical load at the bottom of the sample. The latter had a range from 0 to 10000 N (interval used 0 to 200 N) and some scatter in the results can be due to insufficient accuracy of this transducer.

This apparatus does not permit measuring of the pore pressure during the test, as both top and bottom are drained surfaces. However, the strain rates used in this investigation produced pore pressures which were less than 10 kPa when drained only on one side. The measured total stresses will therefore deviate very little from the actual average effective stresses.

Discussion of test results

Tests were performed on samples from different depths, but no significant differences were found. Therefore only results from tests on clay from a depth of 5 m are discussed here.

The results of three tests performed at different rates of strain are given in FIG. 52. The frictional loss is found to increase from a rather low value (10 %) at the beginning of the test to what appears to be a maximum value (20 %). The rate of deformation does not seem to affect the frictional loss, at least not for the rates studied.

The ring friction at the beginning of the test is greatly dependent on the testing technique. If the sample does not touch the bottom

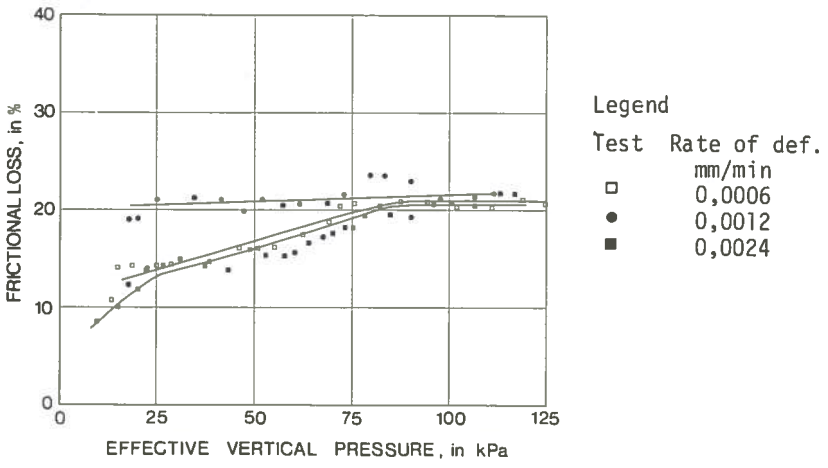

FIG. 52 Frictional loss of vertical pressure during CRS tests performed at different rates of strain. Oedometer ring of stainless steel lubricated with molybdenum sulphide. Clay from Bäckebol, 5 m.

plate, a ring friction of 100 % will be measured. On the other hand, if good contact is ensured by gently pushing the piston plate downwards before the start of the test, no frictional loss will be recorded. This is the explanation of a slight variation in ring friction found at the beginning of the test in FIG. 52.

The tests shown in FIG. 52 were performed in an oedometer ring of polished stainless steel, lubricated with molybdenum sulphide on the inside. FIG. 53 gives results of two tests, where the oedometer ring was lubricated with silicon grease. Lubricating the ring with silicon grease obviously reduced the frictional loss to between 6 and 8 % of the applied vertical force.

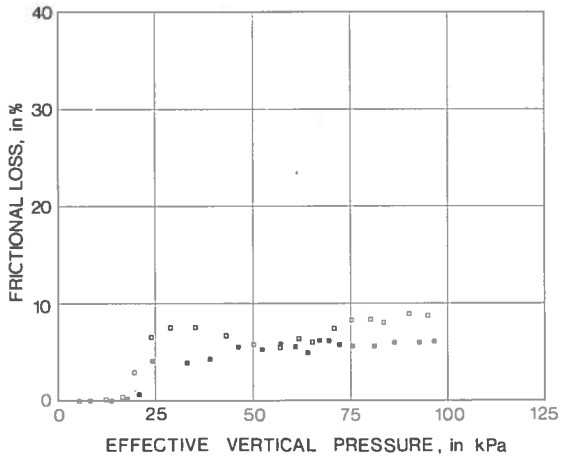

FIG. 53 Frictional loss in per cent of applied vertical pressure during two CRS tests. Rate of deformation 0,0024 mm/min. Oedometer ring of stainless steel lubricated with silicone grease. □ 5m, ■ 7m,

3.1.3 Oedometer test, constant pore pressure gradient

In the Constant Pore Pressure Gradient Test, in what follows called CGT test, the sample is loaded in such a manner that the pore pressure at the undrained bottom is kept at a predetermined constant value. The pressure/compression curve can than be plotted if readings are taken of applied pressure and vertical deformation only, as the pore pressure is known.

Theory

A comprehensive study of the CGT test was made by Lowe (1969), who arrived at the following formula for the coefficient of consolidation:

$$c_v = \frac{d\sigma'}{dt} \quad \frac{H^2}{2u_b}$$

where $\frac{d\sigma}{dt}$ = rate of loading

u_b = preset pore pressure

H = sample height

Just as for the CRS test, the average effective stress can be calculated from the expression

$$\sigma' = \sigma - \frac{2}{3} u$$

on the assumption that the pore pressure distribution in the sample is parabolic.

Test apparatus

A Rowe consolidation cell, 75 mm in diameter, was used for the CGT tests. The reason was that the vertical pressure in this cell can be applied directly as an air pressure, and this was found suitable for the servo-system used.

The sample was trimmed from a 100-mm sample directly into the oedometer ring with a cutting edge (FIG. 54). The samples were 25 mm in height.

The consolidation cell, the loading device, and the servo-system are schematically shown in FIG. 55. The base of the consolidation cell is impervious, with a filter, 10 mm in diameter at the centre, connected to a pressure transducer by a water system. On the top of the sample there is a 1 mm thick bronze filter underlaying the rubber membrane. Water can dissipate into the filter through the centre of the piston. The vertical pressure is applied by in-

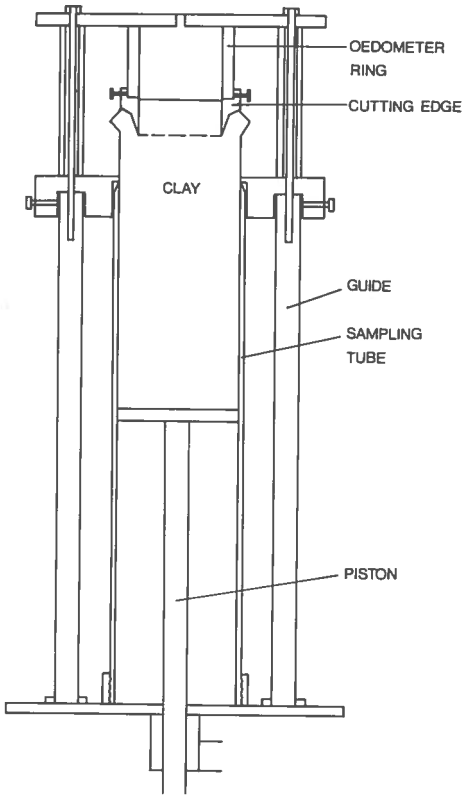

FIG. 54 Cutting device used for mounting clay samples in 75 mm oedometer ring.

creasing the pressure in the chamber. During the test the piston follows the top of the sample downwards and the deformation is monitored by a LVDT on the piston.

The servo-system works in the following manner. A certain definite pore pressure gradient is chosen, and the corresponding signal from the pressure transducer, which is connected to the relay, is set as switch point on the relay, see FIG. 55. The air pressure is slowly increased as the air passes through regulator A, regulator B, magnetic valve C, and the needle valve D into the chamber in the consolidation cell. A pressure transducer is connected to the tube between the magnetic valve and the chamber, thus measuring the applied total pressure.

As the pressure in the chamber is increased, the pore pressure at the bottom of the sample also increases, see FIG. 56. When the

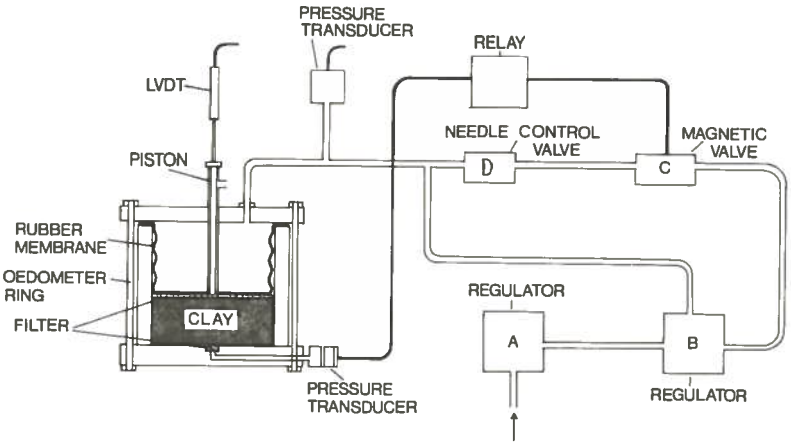

FIG. 55 Oedometer and servo-system used for the CGT tests.

pore pressure reaches the preset value, the relay causes the magnetic valve to close. The pressure in the chamber then remains fairly constant and, as consolidation progresses, the pore pressure starts to dissipate. A slight decrease in pore pressure causes the relay to switch and the magnetic valve opens, the pressure increases, etc. The pore pressure will oscillate between an upper and a lower value as the test proceeds, while the pressure in the chamber increases stepwise (see FIG. 56).

It was possible to trim the servo-system to such a degree that the difference between the upper and lower values of the pore pressure was of the order of a few hundredths of one kPa, the distance between the lines A and B in FIG. 56 was then of the order of 0,3 kPa. The mechanism of the servo-system was fairly simple, but worked extremely well.

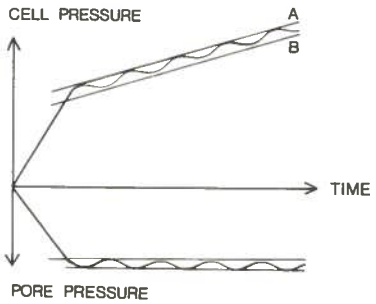

FIG. 56 Variations in cell pressure and pore pressure during a CGT test.

Discussion of test results

The samples used for the tests described here were taken at Bäckebol from a depth of 5 m.

The same data collecting system was used as for the CRS tests. Readings were taken every ten minutes up to the preconsolidation pressure and then at longer time intervals.

The results in FIG. 57a were obtained from test B5-2, where the pore pressure at the bottom of the sample was kept at 3 kPa. FIG. 57b presents the corresponding c_v-values.

The remarks made on the results of a CRS test are also valid for a CGT test, except that no change in the pore pressure occurs.

FIG. 57c shows that the increase in vertical pressure is rather rapid at the beginning of the test but the rate of loading is drastically reduced as the preconsolidation pressure is reached. The CGT test is comparatively slow, once the preconsolidation pressure is exceeded, as the pore pressure would otherwise start to increase.

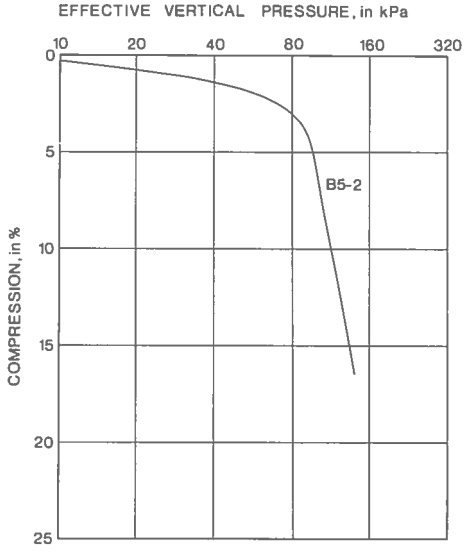

FIG. 57a Pressure/compression curve. Test B5-2. Pore pressure kept at 3 kPa at the undrained bottom. Clay from Bäckebol, 5 m.

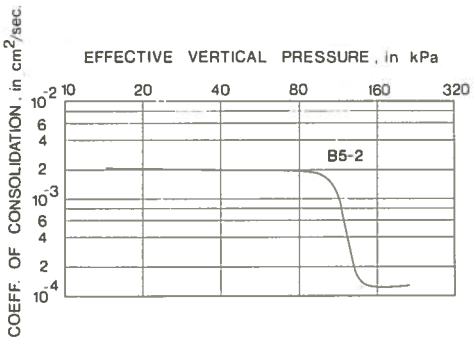

FIG. 57b Variation in coefficient of consolidation. Test B5-2.

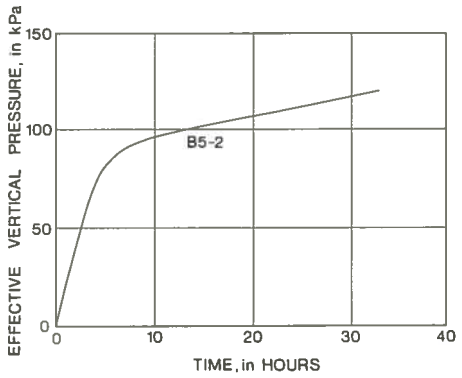

FIG. 57c Increase in vertical effective pressure with time. Test B5-2.

Effect of pore pressure gradient

In test B5-2 a gradient of 1,2 kPa/cm was used on the 25 mm thick sample. FIGs. 58a and b give the results of three CGT tests, where the gradients were 0,3, 1,2 and 5 kPa/cm. It is obvious that the higher the gradient, the higher the preconsolidation pressure will be if the Casagrande construction is used. This is in agreement with earlier investigations: the higher the rate of deformation, the higher the preconsolidation pressure. What was stated concerning the oedometer modulus in connection with the CRS test is also valid here.

Unfortunately a comparison with other loading routines is complicated by the fact that the rubber membrane used was too stiff, and not all the applied pressure was transmitted to the sample. Between 10 and 20 % of the applied pressure was carried by the membrane. Attempts were made to calibrate the membrane, but the reliability was poor owing to difficulties in reconstructing the deformation pattern. Therefore some incremental loading tests were made in the Rowe cell which was used as a reference material in a comparison, and will be discussed in the next Sub-section 3.1.4.

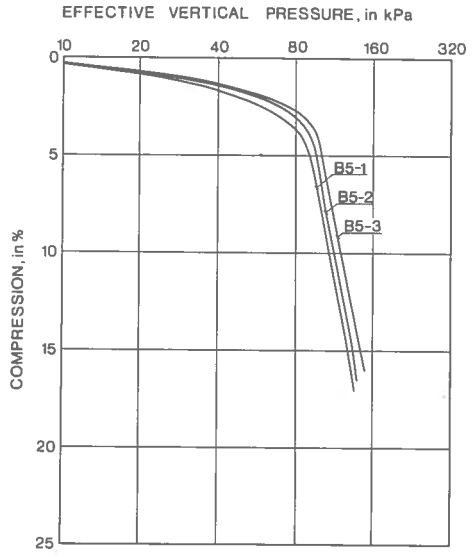

Legend

Test	Depth m	Gradient kPa/cm
B5-1	5	0,3
B5-2	5	1,2
B5-3	5	5,0

FIG. 58a Pressure/compression curves. Tests B5-1 to B5-3.

3.1.4 Comparison of different loading routines

The main object of a comparison of the different oedometer routines described is of course to find out whether the results are in agreement or not, but, for practical purposes, the apparatus and laboratory technique involved are also important. First the results will be discussed, and then some practical points will be made concerning the future application of the different methods.

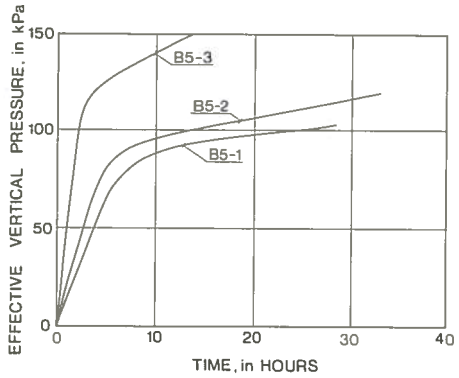

FIG. 58b Increase in vertical effective pressure with time. Tests B5-1 to B5-3.

Results

FIG. 59 shows pressure/compression curves for CRS tests and incremental loading tests (data taken from FIGs. 27b, 29b, 30b, and 49). The curves obtained with different routines are very similar in shape, but give different preconsolidation pressures. As was pointed out in Sub-section 3.1.1 the NGI test includes only primary consolidation according to the Taylor method, while the STD test, when plotted with the 24-hour readings as in this case includes some secondary compression. It was also stated before, in Sub-section 3.1.2, that the strain rate in the CRS test affected the stress/strain curve. In terms of primary and secondary compression, a slower CRS test could be said to include a larger part of secondary compression.

The same conclusions can be drawn from a comparison of the CGT tests with incremental loading tests, as shown in FIG. 60.

The friction between the clay and the oedometer ring was previously discussed and the smoothness of the surface was found to be more important than the choice of material for the oedometer ring. Lubricating the inside with silicon grease reduced the friction more efficiently, than the use of molybdenum sulphide.

The frictional loss in the CRS tests was smaller than in the STD tests. The reason is probably that towards the end of each increment in the STD test the rate of strain is very low and bonds are probably formed between ring and clay (Hansbo, 1960). This is partly prevented in the CRS test owing to the higher rate of strain.

It is interesting to note that the CRS test and to a certain extent the CGT test cover a slightly wider span in FIGs. 59 and 60 than the incremental loading tests.

In FIG. 61 a comparison is made between the c_v-values obtained from the tests treated in FIG. 59. The agreement is very close, and it is obvious that the c_v-value before the preconsolidation pressure is fairly constant and then drops to a much lower value as the preconsolidation pressure is reached, gradually increasing again as deformation becomes larger.

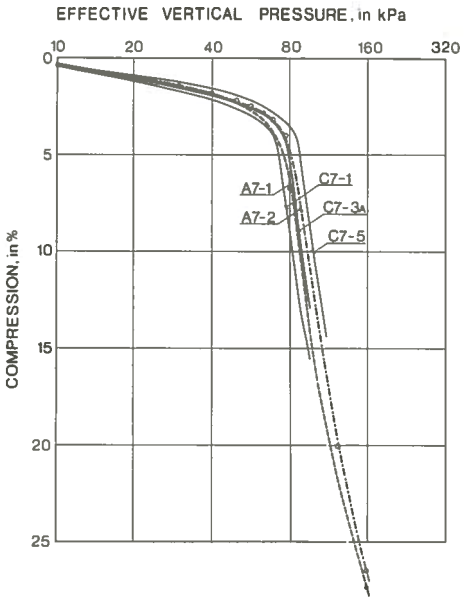

Legend

Test	Loading routine	Rate of def. mm/min
A7-1	STD	--
A7-2	NGI	--
C7-1	CRS	0,0006
C7-3A	CRS	0,0024
C7-5	CRS	0,0090

FIG. 59 Pressure/compression curves. CRS tests and tests with incremental loading. Bäckebol 7m.

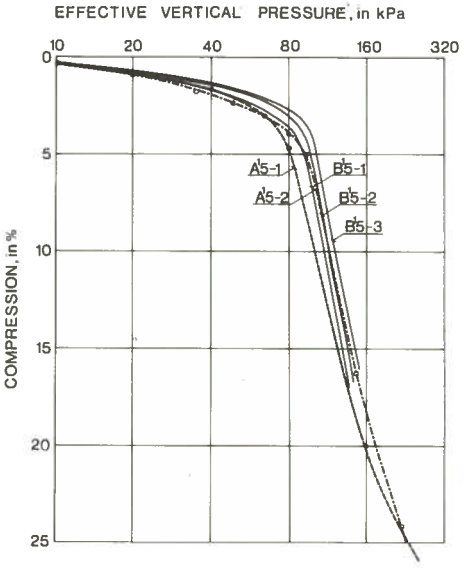

Legend

Test	Loading routine	Gradient kPa
A'5-1	STD	--
A'5-2	NGI	--
B'5-1	CGT	0,3
B'5-2	CGT	1,2
B'5-3	CGT	5,0

FIG. 60 Pressure/compression curves. CGT tests and tests with incremental loading.[1]All tests made in a Rowe consolidation cell. Bäckebol 5m.

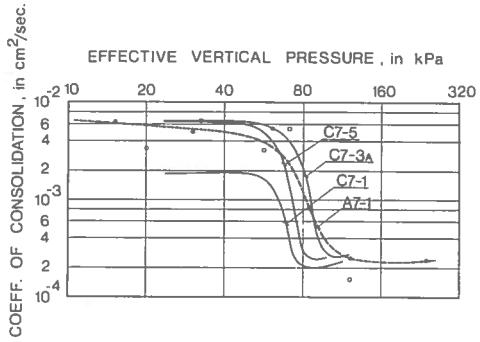

Legend

Test	Loading routine	Rate of def. mm/min
A7-1	STD	--
A7-2	NGI	--
C7-1	CRS	0,0006
C7-3A	CRS	0,0024
C7-5	CRS	0,0090

FIG. 61 Comparison of c_v-values obtained from CRS tests at different rates of strain on samples loaded in increments.

The equation deduced for the coefficient of consolidation was identical for the CGT test and the CRS test, if in the latter case the material was assumed to be linear in the interval considered. This implies that a steady state is attained, but that is not quite true for the CRS test once the preconsolidation pressure is reached as the pore pressure then increases with time.

In the CGT test the pressure/compression curve and the pressure/time curve are both linear at stresses moderately above the preconsolidation pressure, and this implies that the rate of deformation then is constant. As the pore pressure is constant, the process progresses under steady state conditions and the requirements for Eq. (12) are thus fulfilled.

No systematic differences between the c_v-values from the CGT tests and CRS tests have been found, and the error involved in the CRS test is believed to be small if the excess pore pressure is low in comparison with the vertical stress. If the rate of strain in a CRS test is small enough, a steady state will also be obtained after the preconsolidation pressure is exceeded.

Apparatus and techniques

The consolidation cell used for incremental loading does not differ significantly from the cell used for the CRS tests, while the Rowe cell used for the CGT tests is somewhat more complicated.

The laboratory techniques required for mounting the sample are comparable in all three tests.

The loading devices used are also simple in all these tests, except for the CGT tests, where the servo system is rather sensitive to trimming.

The total time required for a test with load increments is somewhat dependent on the magnitude of the preconsolidation pressure. For the clay considered here, the STD test requires 6 to 7 days, the NGI test 3 to 4 days, and the LIN test 10 to 12 days.

For the continuous loading tests, the time required is dependent on the chosen rate of strain and on the preset gradient. If a curve corresponding to the STD curve is wanted, the CRS test requires 25 to 30 hours for 20 % deformation, and this is enough considering the well-defined pressure/compression curve. With the same criteria a CGT test will take 3 to 4 days.

The CRS and CGT tests can be readily automated, and this is a great advantage as they need not to be supervised during the test.

The accuracy in deformation and pressure readings can today be extremely high in all kinds of tests, but the reliability of the results is much greater in the continuous loading tests, as the complete pressure/compression curve is defined, in contradistinction to the incremental loading tests, where only 6 to 10 points are obtained.

The results obtained from the CRS and the CGT tests are very similar and of the same quality. These two tests were also found to be identical, theoretically, if the oedometer modulus is constant, which it is with good accuracy up to the preconsolidation pressure. It is not until after the preconsolidation pressure that these two methods differ. As the preconsolidation pressure is the main interest in this thesis, the CRS test was chosen for a detailed study in view of its simpler loading device and the fact that the same amount of information is obtained as from a CGT test in less time.

3.2 Three-dimensional stress/strain analysis

In an oedometer test, deformation takes place only vertically. This is obtained by using a stiff oedometer ring, which is able to sustain stresses without significant horizontal strains. With reference to stresses, the consolidation test is a three-dimensional problem, which can be reduced to two dimensions owing to the axi-symmetric sample, as $\sigma_2 = \sigma_3$.

As was stated in the survey of the literature, Roscoe, *et al.*, (1963), Hansbo(1960), and Berre and Bjerrum(1973) pointed out the importance of the shear stress and its possible connection with the preconsolidation pressure. The best way to investigate this phenomenon would be to run consolidated, drained triaxial tests, where the diameter of the sample is kept constant during compression. A single test on the Bäckebol clay takes about two weeks. For this reason and because a rather complicated servo-system was needed, the Author chose a slightly different procedure, where the horizontal stress is measured in the oedometer.

A natural clay exhibits a certain degree of scatter which can complicate an analysis. To eliminate this scatter, an artificial clay was prepared and used for the series of tests described in this section.

A clay with a water content of 80 % was mixed with distilled water to a slurry with a water content of 140 %. The slurry was poured into a large consolidation cell, FIG. 62, where the load was gradually increased to a final value of 31 to 33 kPa. Primary consolidation was completed in a month, and the clay was left with the load on for another month and a half. Clay samples were then carfully taken in the box by means of stainless steel tubes.

Table 2. Geotechnical properties of artificially sedimented clay

ρ	τ_{fu}	w	σ_o'
1,70 t/m^3	9 kPa	83 %	31-33 kPa

The geotechnical properties of the clay are given in Table 2. Although the microstructure of the artificially sedimented clay probably has little resemblance to that of a naturally deposited clay, it is homogeneous and offers a good possibility of making comparative tests.

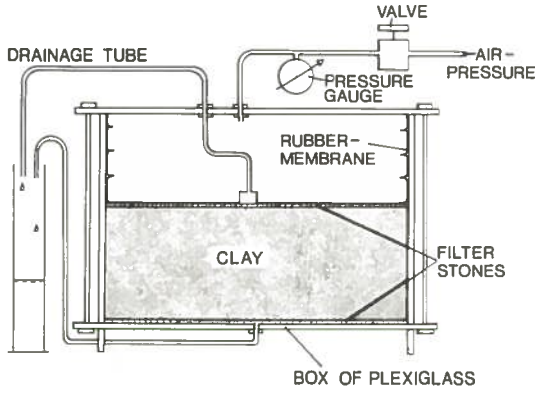

FIG. 62 Consolidation cell used for preparation of artificially sedimented clay.

3.2.1 Critical shear stress

Apparatus

The horizontal stresses in an oedometer have been measured by Brooker and Ireland (1965), Som and Simons (1969), and others. The system most commonly used is a semi-stiff oedometer ring with strain gauges on the outside. To avoid problems due to calibration and zero drift of the gauges another system was chosen.

The oedometer ring, made of stainless steel, was machined down at the centre, as shown in FIG. 63, so that the ring, from 5 to 15 mm in height, was only about 1/10 mm thick. Strain gauges were than glued on the outside of the membrane, and the chamber was closed by an outer ring and sealed with o-rings. The strain gauges were then used as null indicators in such a manner that when the horizontal stress inside the oedometer increased, the air pressure in the chamber was increased accordingly so that the strain gauges gave the same readings all the time. Exactly the same servo-system that was employed in the CGT test, discussed in Sub-section 3.1.3 was used, but the strain gauges were now connected to the relay and not the pressure transducer, FIG. 64. The valve B in FIG. 64 continuously monitored the pressure in the chamber and admitted a pressure 5 kPa higher than that in the chamber. In this way shock in the air system was avoided when the magnetic valve opened.

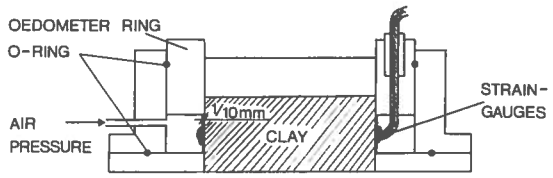

FIG. 63 Oedometer used for measuring the development of horizontal stresses during an oedometer test.

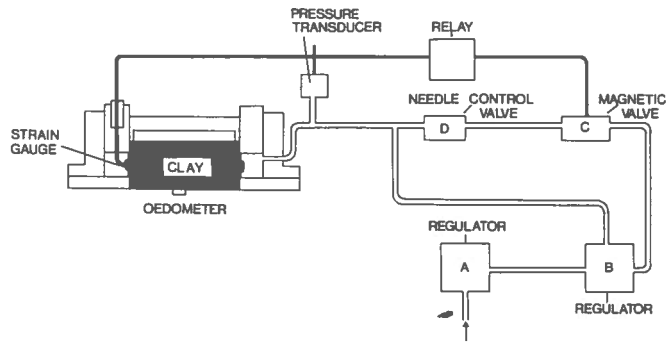

FIG. 64 Principle of oedometer and servo-system used for measurement of horizontal stresses during an oedometer test.

All tests described in this section were made as CRS tests and the test procedure was the same as that outlined in Sub-section 3.1.2. The only difference was the start of the test. Up to a vertical pressure of 5 to 10 kPa, the horizontal pressure was manually operated before the relay was set and the servo-system was allowed to operate.

In a test where the horizontal stresses are measured it is extremely important that perfect contact should be ensured between the clay sample and the oedometer ring. A cutting device shown in FIG. 65 was therefore constructed and used in the following manner. A clay sample 26 mm in height was extruded from the sampling tube and placed on a cutting board on the pedestal shown in FIG. 65. The cutting edge, which is machined to exactly the same diameter as the oedometer ring (45 mm), was lowered, and was kept in a horizontal position by the guide. Then the oedometer was centred on the cutting edge by the notch, and the cutting board was slowly pulled out and the system lowered. The pedestal then pushed the sample into the oedometer. Finally 6 mm of clay outside the oedometer was trimmed off, leaving a 20 mm high sample inside the oedometer.

The data collecting system described in Sub-section 3.1.2 was used for monitoring stresses and strains.

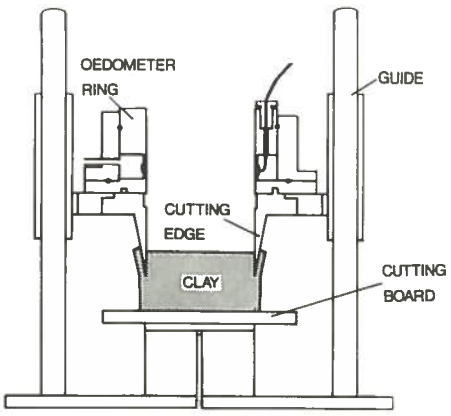

FIG. 65 Cutting device used for trimming 50 mm samples into an oedometer ring, 45 mm in diameter.

Discussion of test results

The horizontal stresses measured with the apparatus described in the previous section may not be the true horizontal stresses at rest. After all it is only the 10 mm in the centre of the sample that is influenced. Even if the cutting device produces good contact between the sample and the oedometer ring, there is bound to be a thin zone around the edge which is slightly disturbed and which can to a certain degree influence the results (Larsson, 1975*a*), so that the measured horizontal stresses are too low. In spite of this it is the Author's opinion that the measured stresses are a fairly good indication of the change in horizontal stresses during an oedometer test.

To begin with, test C7-4, previously treated in Sub-section 3.1.2, will be considered in order to illustrate the accuracy and the type of curves used.

FIG. 66 shows the stress path plotted by the computer. The maximum shear stress $(\sigma_v - \sigma_h)/2$ in the sample is plotted as a function of the effective horizontal stress, calculated from the relation

$$\sigma_h' = \sigma_h - \frac{2}{3} u_b$$

The test was performed in a climate-controlled room, where the temperature was kept at $7^oC \pm 0{,}5^o$. The oscillation of the curve is due to the following. Two strain gauges were fastened on the membrane and, to obtain full bridge, two dummy gauges were used. These were glued onto a steel plate outside the oedometer and were not surrounded by water and therefore affected by the slight change in temperature. The oscillation has the same period as the change in temperature in the room and is not caused by instability elsewhere in the system. The most probable stress path is drawn as a full-line curve in FIG. 66. In the comparisons made in what follows, only this most probable stress path will be used.

The shear stress in the sample increases rather quickly during the early stage of the test, but when it reaches a certain definite value, the stress path bends off, and the sample cannot sustain any further shear stresses without undergoing large vertical de-

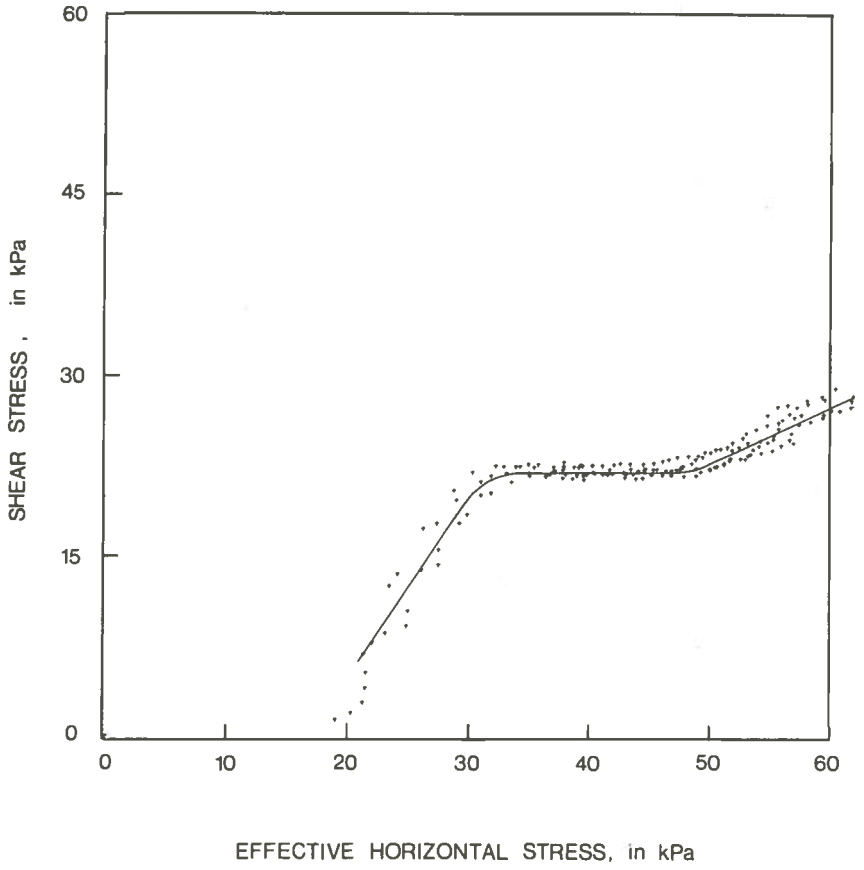

FIG. 66 Stress path plotted by the computer. Test C7-4.

formations. The stress path bends off at an effective vertical pressure of 65 kPa and becomes a straight line again at 80 kPa. If the pressure/compression curve is checked, see FIG. 46, the corresponding values would be 60 kPa and 80 kPa. This is the interval where the preconsolidation pressure will be found, and it is evident that reaching the preconsolidation pressure also means reaching a critical shear stress.

General model of a stress path

FIG. 67 gives what is believed to be a general model of a stress path followed during an oedometer test on clay. The build-up of shear stresses is rather rapid at the beginning of the test up to the preconsolidation pressure, where a critical shear stress is reached and the curve bends off. The second part of the curve is also fairly straight but eventually turns concave upwards.

The slope of the steep part of the curve represents the increase in the horizontal stress caused by an increase in the vertical stress in the overconsolidated region ($\Delta\sigma'_h/\Delta\sigma'_v = K''_o$). The slope of the second part of the curve consequently represents the increase in the horizontal stress caused by an increase in the vertical stress in the normally consolidated region ($\Delta\sigma'_h/\Delta\sigma'_v = K'_o$). The K_o (σ'_h/σ'_v) *in situ* will be found where line A in FIG. 67, which represents *in situ* vertical effective stress, intersects the stress path, if hysteresis effects during unloading and reloading can be neglected. If the clay is normally consolidated this line should intersect the stress path where it bends off, as indicated by the dash-and-dot line in FIG. 67.

The principle of this model has been found true also for clays with lower clay content (Janbu, 1973).

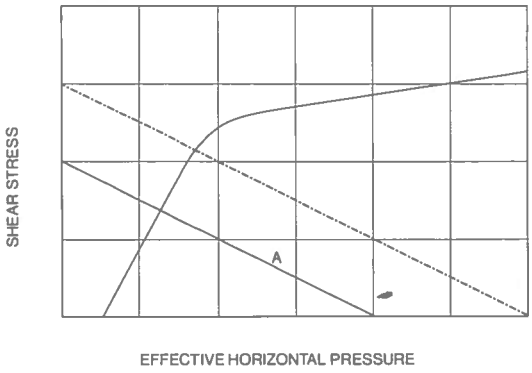

FIG. 67 General model of a stress path.

Effect of rate of strain

In Sub-sections 3.1.2 and 3.1.3 the preconsolidation pressure was found to vary with the rate of strain. A series of tests was therefore performed to investigate the effect of the strain rate on the critical shear stress. The previously described artificially sedimented clay was used in order to avoid discrepancies due to a natural variation of the clay.

The results of tests A1 to A4 are plotted in FIG. 68, and the critical shear stress is found to decrease with decreasing rate of strain just as the preconsolidation pressure. The parameters K_0' and K_0'' do not seem to be significantly affected by the rate of strain.

The critical shear stresses for strain rates of 0,0012 and 0,0006 mm/min do not differ significantly, and this suggests that a lower limit for the critical shear stress may exist.

This is in agreement with earlier investigations made at Chalmers University of Technology, where Torstensson (1973, 1975) found that the shear strength determined by vane boring also decreased with decreasing strain rate.

Again there is evidence for the hypothesis that the preconsolidation pressure should be very closely related to a critical shear stress.

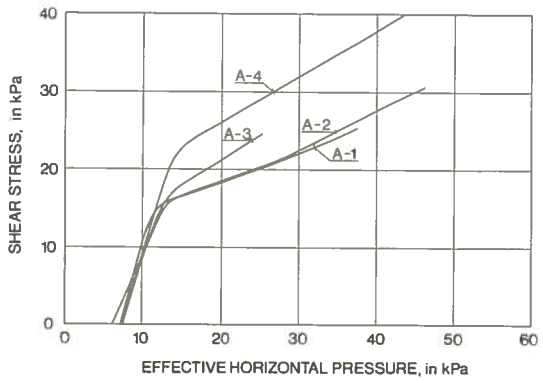

Legend

Test	Rate of def. mm/min
A-1	0,0006
A-2	0,0012
A-3	0,0024
A-4	0,0040

FIG. 68 Stress paths for tests A-1 to A-4. Artificially sedimented clay.

3.2.2 Effect of stress path

Test procedure

In Sub-section 3.2.1 it was explained how a CRS test with measurements of the horizontal stress was started, by manually adjusting the pressure in the chamber to a value of 5 to 10 kPa according to the vertical pressure. The membrane is thin and rather flexible around its vertical position. When the clay sample was trimmed into the oedometer ring, an increase in the readout signal from the strain gauges was to be observed, and this indicated an outward deflection of the membrane, probably due to the swelling pressure of the clay. As the pressure in the chamber is increased, together with the vertical pressure, the membrane is forced inwards, causing a kind of isotropic consolidation. If this procedure is carried out further, the stress path will start from a different point. A series of tests was performed with different starting-points for the stress path.

Discussion of test results

The results are plotted in FIG. 69, and it is obvious that the critical shear stress is greatly dependent on how far the isotropic consolidation is carried in the laboratory; the higher the isotropic consolidation pressure, the lower the critical shear stress.

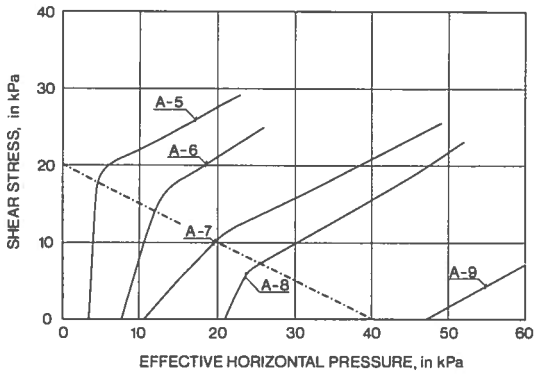

FIG. 69 Stress paths. Tests A-5 to A-9. All tests performed at a rate of deformation of 0,0024 mm/min. Artificially sedimented clay.

There are several objections that can be made against the valid of the results of these tests. As the membrane deflects it wil be gradually stressed, and parts of the applied pressure in the chamber will be transmitted by the membrane itself. Attempts have been made to account for that by calibrating the system without any sample in the oedometer. Another objection against the validity of the results is that only parts of the sample are affected by the movement of the membrane. Nothing could be done to account for that.

Therefore great precautions must be observed when the results ar interpreted. No numerical values will be used in the following discussion, only the general trend will be commented on. If the general model presented in Sub-section 3.2.1 is valid, the slope of the stress path is large in the overconsolidated region and much smaller in the normally consolidated region. Thus, if the sample were loaded from zero stress, while the diameter is kept constant, a stress path would be obtained in accordance with the model, looking somewhat like the curve from test A-5 in FIG. 69. If an identical sample were mounted in a triaxial cell, and if the cell pressure were then increased under drained conditions beyond the preconsolidation pressure, the structural collapse wo be obtained when the horizontal or vertical preconsolidation pressure, whichever is the lowest, was exceeded. If the sample were then loaded vertically, while the cell pressure was adjuste in such a manner that the diameter of the sample was kept consta the slope of the stress path would be small as the clay would th be in the normally consolidated region, and the stress path woul be in accordance with that obtained from test A-9 in FIG. 69. Fo starting-points between those two extreme cases, the results pre sented in FIG. 69 appear to be very logical.

Another reason to believe the general trend in FIG. 69 to be correct is that a very close connection between the preconsolida tion pressure and the critical shear stress was found in the pre vious section. If the preconsolidation pressure is assumed to b unaffected by the horizontal stresses, the critical shear stress obtained with different starting-points of the stress path will fall on a straight line parallel to the dot line in FIG. 69. Th reason why such a line would bend off at higher isotropic pressu is believed to be the fact that the horizontal preconsolidation pressure is lower than the vertical preconsolidation pressure

Consequence of variation in critical shear stress

When evaluating the coefficient of earth pressure at rest, K_0, from FIG. 69, the various stress paths give different results. For a soil sample *in situ*, only one value can be the true value. All the stress paths obtained in the laboratory are thus fictitic except the one path which passes through the true K_0 point. For a sample at the centre of a load in the field where only vertical deformation takes place, the real critical shear stress should be comparable to the stress determined by the stress path in the laboratory. This fact illustrates the extreme importance of knowing the horizontal stress *in situ*. It may not be so importar for consolidation tests as for K_0-consolidated triaxial tests. Investigations made at Chalmers University of Technology (Larsson 1975*b*) have proved that a change in K_0 in a K_0-consolidated undrained triaxial test greatly affects the determined shear streng

3.2.3 Three-dimensional considerations

There is a very definite relation between stresses and strains, a in this section the void ratio is introduced as a third axis to visualize the stress/strain behaviour of a clay in a three-dimensional plot. The results of tests A-5 to A-9 in FIG. are used. The same type of diagram as in FIG. 18 is used with me normal stress (p), deviator stress (q), and void ratio (e) as coordinates.

FIG. 70 shows the three-dimensional stress path for test A-7. During the "isotropic consolidation" the stress path follows the p-e plane, but then, when the diameter of the sample is kept constant, the shear stress in the sample increases rapidly up to the critical shear stress, where the curve bends off "into the plane of the paper". The projection of the stress path on the p-e plane is represented by the dash line in FIG. 70.

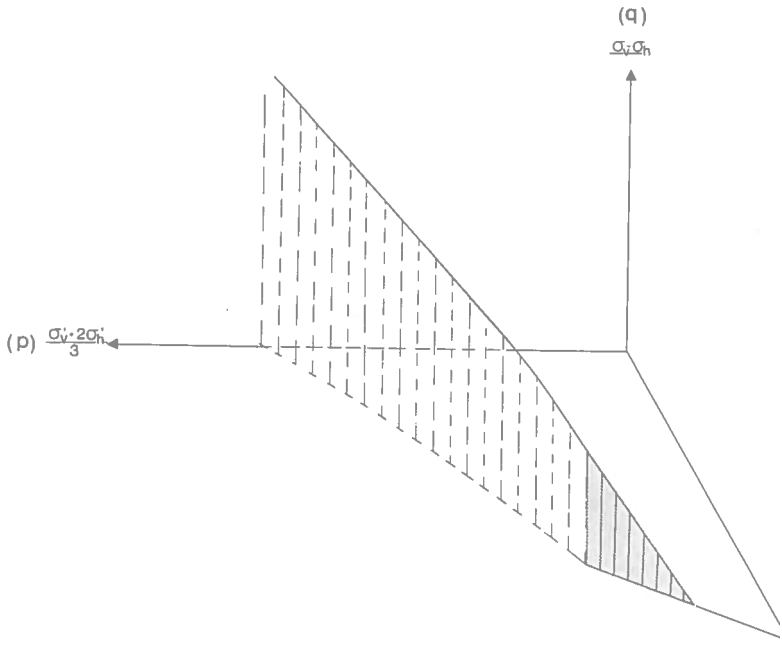

FIG. 70 Three-dimensional stress path. Test A-7.

Test A-5 through A-9 are replotted in the same type of diagram in FIG. 71. FIG. 20 is included as a reference. The resemblance is evident.

All stress paths seem to follow the plane A B_1 C D E. When the critical shear stress is reached, the stress path follows the state boundary surface,C C" D" E" E

In this graph there is also a single point that represents the *in situ* conditions, namely (σ'_{ho}; σ'_{vo}; e) and it is the stress pa that goes through this point that represents *in situ* conditions. Since the critical shear stress is dependent on the strain rate, we arrive at the conclusion that there exists a number of state boundary surfaces each in a different vertical position

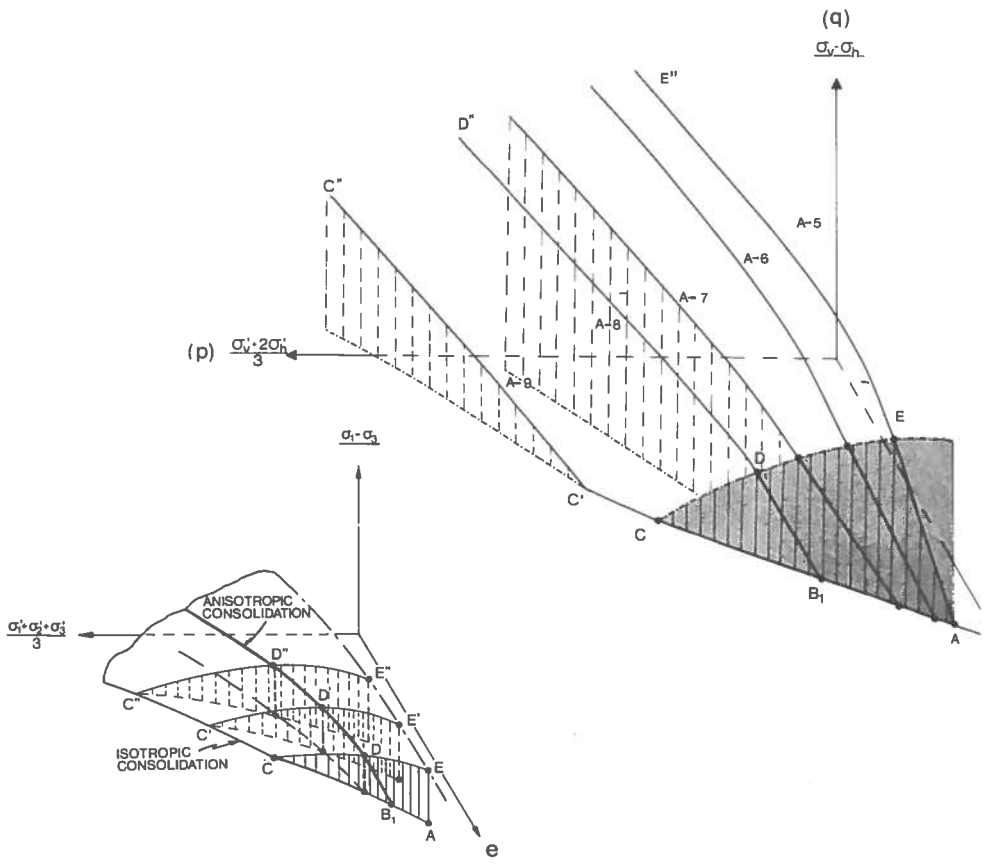

FIG. 71 Three-dimensional stress paths. Tests A-5 to A-9. FIG. 20 is included as a reference.

Reloading

A few samples were unloaded and reloaded in the oedometer which measured the horizontal stresses. The unloading was complicated as stresses only can be changed by adjusting the deformation. Reloading was carried out at a constant rate of strain.

The oedometer modulus was found to be larger during reloading, just as for incremental tests. The stress path was steep up to the previous consolidation load, and then followed the state boundary surface very logically, as illustrated in FIG. 72. The difference in oedometer modulus is found in the projections on the p-e plane, angles α_1 and α_2.

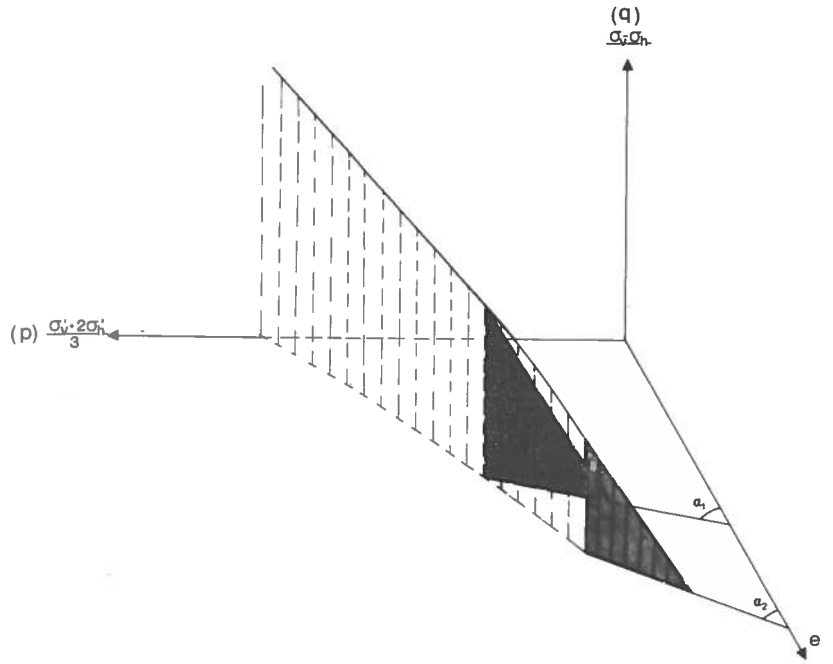

FIG. 72 Three-dimensional stress path for a sample unloaded to *in situ* stresses. Reloading made at a constant rate of strain.

Increased preconsolidation pressure due to secondary compression

As was pointed out in the survey of the literature, a clay under going secondary compression under a constant vertical stress can develop an increased preconsolidation pressure.

FIG. 73a illustrates the general behaviour of such a clay. The *in situ* conditions are given by point A having the coordinates (σ'_{vo}, σ'_{ho}, e_o). When the vertical stress is increased, the shear stresses increase until the stress path hits the state boundary surface (B). A further increase in the vertical stress causes the clay to follow the surface to C. Then the vertical st is kept constant, represented by the plane I. The void ratio wi decrease, and which of the three stress paths the clay will foll depends entirely on the development of the horizontal stresses. Unaltered horizontal stresses result in stress path D. A slight increase in the horizontal stress is represented by D', while D" represents a decrease in the horizontal stress. After that a further increase in the vertical stress will result in the stres paths represented by E, E' and E" respectively. The increased p consolidation pressure will be found where the stress paths agai hits the state boundary surface. The corresponding oedometer curves are found by projecting the stress paths on a plane perpendicular to plane I.

This discussion explains the development of an increased pre-consolidation pressure, but no definite conclusions can be drawn concerning the change in the horizontal stresses during secondar compression. However, it is shown that moderate changes in the horizontal stresses do not significantly affect the developed pr consolidation pressure, but that a large increase or decrease in the horizontal stresses would preclude an increase in the pre-consolidation pressure.

It was earlier stated that owing to the time-dependence of the critical shear stress, there exists a number of state boundary surfaces. This is illustrated in FIG. 73b, where the position of the stress path is dependent on the rate of strain. Just as in FIG. 73a, the *in situ* conditions are represented by point A. When the vertical stress is increased the stress path hits the state boundary surface at B and then follows this surface to C.

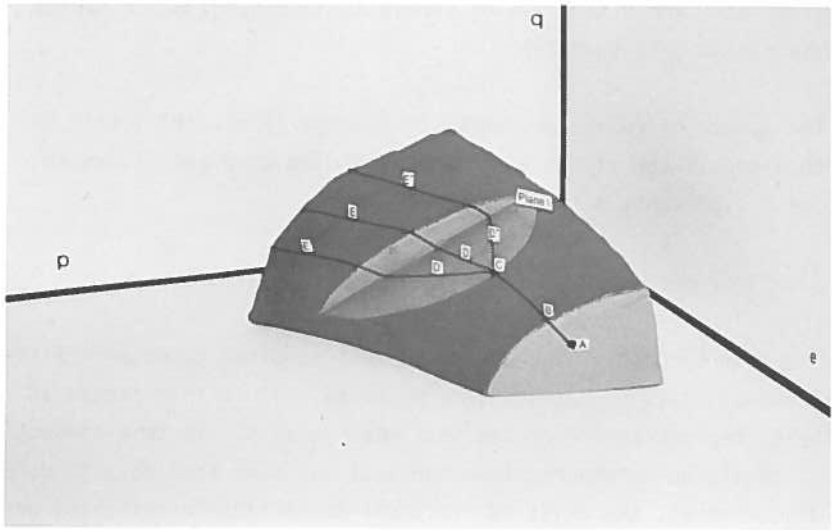

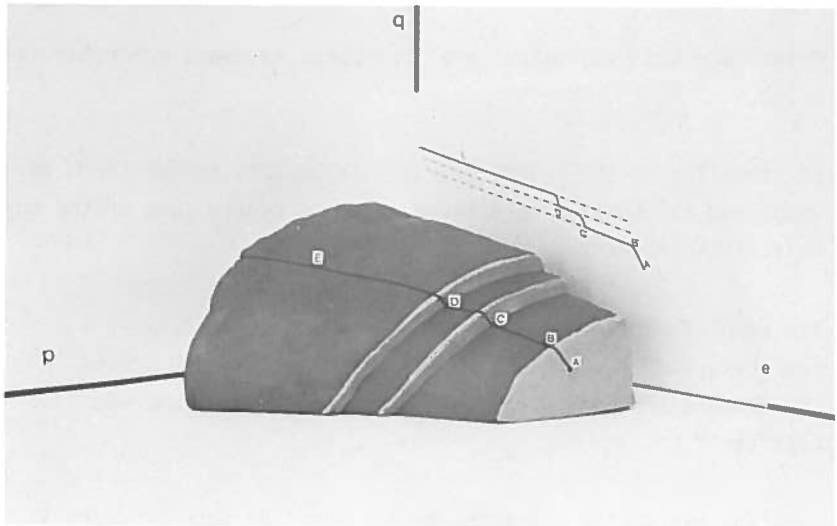

FIG. 73 Clay model modelled in clay.

a. The model illustrates the stress/strain behaviour of a clay during secondary compression.

b. The model illustrates the effect of rate of strain on the critical shear stress and the preconsolidation pressure.

At point C and D the rate of strain is increased, which causes the stress path to raise.

The system of curves presented by Bjerrum (1967, 1973) will be obtained if the stress paths are projected on plane II, which again represents $\sigma_h' = 0$.

3.3 Interpretation of the preconsolidation pressure

The main purpose of the oedometer test is often to determine the preconsolidation pressure of a material. It is interpreted as being representative of the soil mass *in situ*. In this connectio it should be remembered that the soil has been sampled with possi disturbances, the existing vertical and horizontal stresses were released and followed by swelling of the material, and then the sample had been stored for some time before it was trimmed into the oedometer ring.

Great care has been taken in all respects to avoid erroneous results.

For sampling in the field, the Swedish piston sampler St I was used, and all samples were taken from the centre tube or the uppe half of the lower tube.

The samples were stored in a room with 100 % humidity at a temperature of 7^{o} C, the same temperature as in the ground. The temperature in the room where the tests were made was also kept at 7^{o} C.

Swelling was partly prevented by the negative pore pressure in th sample, and horizontal stresses were not completely removed owing to the stiff sampling tubes used. It is the Author's experience that storing does not significantly affect the sample as long as oxidation is prevented. Some swelling occurs vertically, as may be concluded from FIG. 34.

The most commonly used method for evaluating the preconsolidation pressure is the Casagrande method applied to results of STD tests When other loading routines are used, the preconsolidation pressu

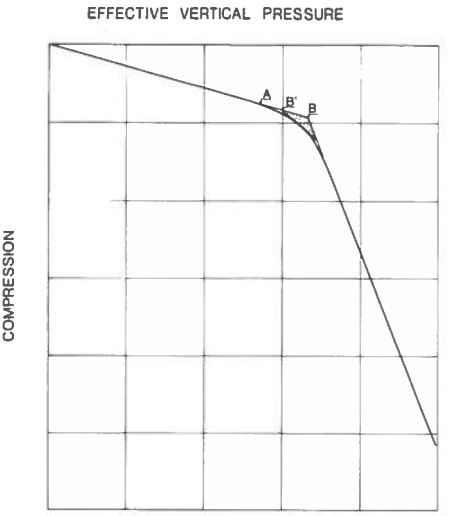

FIG. 74 Principle of suggested method for determination of preconsolidation pressure from a CRS test.

is affected because of the time dependence of the preconsolidatio pressure and the fact that smaller or larger amounts of secondary compression are included.

The introduction of the CRS and the CGT tests afforded a possibility of studying the pressure/compression curve more in detail. In Sub-section 3.1.1 the pressure/compression curve was found to consist of three main parts, see FIG. 34. Up to a certain definit pressure the curve is almost perfectly linear, and then becomes curved. Just when the curve starts to bend at point A in FIG. 74 the first yield probably occurs and theoretically this is believe to be the preconsolidation pressure. The use of this criterion wo require a perfect sample. Even a minor disturbance causes the point A in FIG. 74 to move to the left, and that criterion can therefore not be used in practice. It is the Author's opinion that a Casagrande construction or even point B (the intersection of the two linear parts of the pressure/compression curve) is an interpretation which is too optimistic, and the following procedu is therefore suggested. The two linear parts of the pressure/compression curve are extended and intersect each other at point B, FIG. 74. An isosceles triangle is inscribed (shown shaded). The intersection at point B' is taken as representing the preconsolidation pressure.

The point B' has been found to be rather insensitive to a slight disturbance of the sample, and an important feature of this meth is that it is straightforward and not dependent on the evaluator

If the described method is used for interpreting the preconsolid tion pressure in tests C7-1 to C7-6 in FIG. 49, Sub-section 3.1. the preconsolidation pressures will be found to be 62, 62, 65, 68, 71, and 75 kPa, respectively; and the preconsolidation pressure is obviously not significantly affected by strain rates lower than 0,0024 mm/min. This implies that if the method is valid, the preconsolidation pressure could be determined from a CRS test requiring no more than 24 hours, at least for the clay studied.

If the method described in the previous paragraph is applied to the tests made on the artificially sedimented clay, preconsolida tion pressures of 33, 35, 35, 36, 36, 36, and 37 kPa are ob tained, see Table 2, for rates of deformation not higher than 0,0024 mm/min.

The actual effective vertical pressure for the artificial clay w 31 to 33 kPa, and was kept for two and a half months, allowing some secondary compression to take place, and a preconsolidation pressure of 35 kPa seems reasonable.

If the Casagrande construction were used, the preconsolidation pressures would be around 43 kPa, which is rather high in compar son with the assumed value of 35 kPa. This does not necessary mean that the Casagrande method gives a less reliable value. If a a standard test were made on this clay, giving 5 or 6 points of the pressure/compression curve, the results could be different. is the Author's experience that soil engineers in general draw a pressure/compression curve that falls to the left of the CRS cur around the preconsolidation pressure even if individual points coincide with the CRS curve, see FIG. 75. A Casagrande construc tion will then give a value of the preconsolidation pressure whi is of the same order as that evaluated from a CRS curve by using the previously described method.

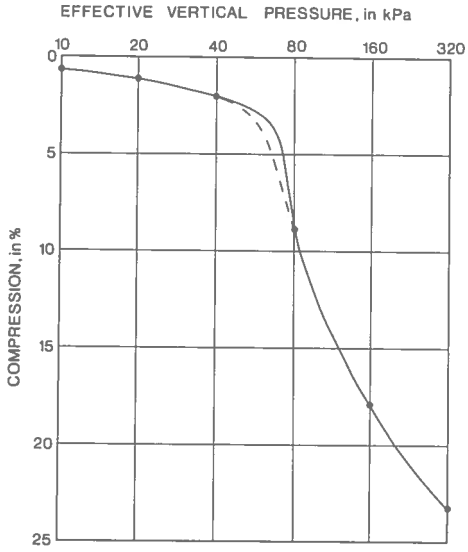

FIG. 76 Pressure/compression curves from CRS (——) and STD (---) tests.

Indications of the points where the preconsolidation pressure was reached were also obtained in a CRS test from the variation in th excess pore pressure at the undrained bottom. The pore pressure started to increase as the preconsolidation pressure was reached. This increase in the pore pressure is usually found for slightly higher values of the calculated average effective vertical stress than those obtained by means of the method described above. This is explained by the fact that the effective vertical stress at the bottom of the sample is lower than the average effective stre because of the friction between the sample and the oedometer ring If that is taken into account, the agreement between the two criteria is much closer.

3.4 Clay microstructure

The generally accepted picture of the microstructure of a marir clay is shown in FIG. 76 (Pusch, 1970; Hansbo, 1975). The clay is believed to consist of aggregates connected by bridges or li The aggregates are dense clusters of particles and function mechanically mainly as larger particles, while the links connec the aggregates are less resistant to stresses. When the sample is stressed, whether in compression or in shear, the stresses i the links increase. The links are believed to have a certain resistance to compression, and up to a certain definite level little deformation occurs. Once the stresses exceed this value sliding occurs between particles in the links. Fairly large de formations are then needed in the links, before considerable strength is gained. Eventually domains will be formed and the material becomes strain hardening, as little deformation occurs in the aggregates.

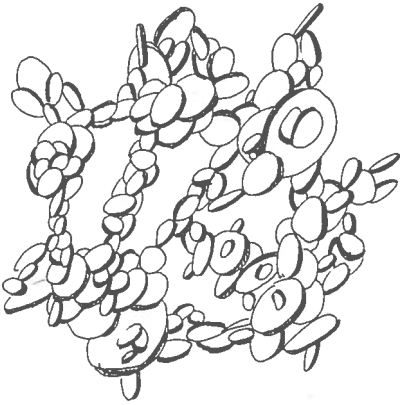

FIG. 76 Microstructure model of a clay sedimented in salt water.

Bjerrum (1973) and others explain the same phenomenon in terms mobilized effective friction and effective cohesion. This micr structure model agrees very well with the previous presented macro model for the stress path. In the overconsolidated regio where the stress path is steep, the links are subjected to a st increase resulting in total stresses which are lower than they have been subjected to before. Once the preconsolidation press and hence the critical shear stress, is reached, sliding occurs in the links and rather large deformations are required for the formation of domains, when a significantly higher stress can be carried or further friction is mobilized.

The phenomenon of decrease in critical shear stress with increa isotropic consolidation pressure is also explained by this micr structure model. The higher the isotropic consolidation pressu is, the higher the stresses in the links. Thus, the lesser is remaining strength in the links, and the smaller the additional shear stress that can be carried before a structural breakdown. In other words, the critical shear stress is the sum of the mobilized effective friction and the available effective cohesi The preconsolidation pressure can be regarded as a failure in t microstructure under drained conditions.

4 FULL-SCALE TESTS AT BÄCKEBOL

4.1 Test field

4.1.1 Geology

Two full-scale tests were performed at Bäckebol, 10 km north of the city of Göteborg. Several other investigations have been made at this site in connection with other research projects carried out in the Geotechnical Department, and the clay is know to be very homogeneous. Of course some natural variation is to be expected, and may sometimes complicate the interpretation of test results.

The geology in the test area has been described by Torstensson (1973), and only a short summary is given here.

The test area is situated in the Göta river valley, on the weste bank, 200 m from the river. The ground has an elevation of 5 m with reference to the river, and the clay deposit is some 40 m deep.

A representative soil profile is shown in FIG. 77.

The uppermost metre consists of a dry crust followed by a grey clay. Down to 3,5 m root threads are quite common. The clay co tent ranges from 55 to 75 %, and the organic content determined chemical analysis (Pusch, 1973) is 0,5 to 1 %. Table 3 gives th presence of different clay minerals at two different depths (Pus 1973).

Table 3. Presence of clay minerals at Bäckebol. (Pusch, 1973)

Depth m	Dominant minerals in the clay fraction						
	Illite	Chlorite	Kaolinite	M_m^a	Quartz	Feldspars	Carb
4	+++	+	+	(+)	+	+	+
7	+++	+	(+)		+	+	+

^aM_m = Swelling: +++ = dominant; ++ = abundant
\+ = Moderately abundant; (+) = slight amount

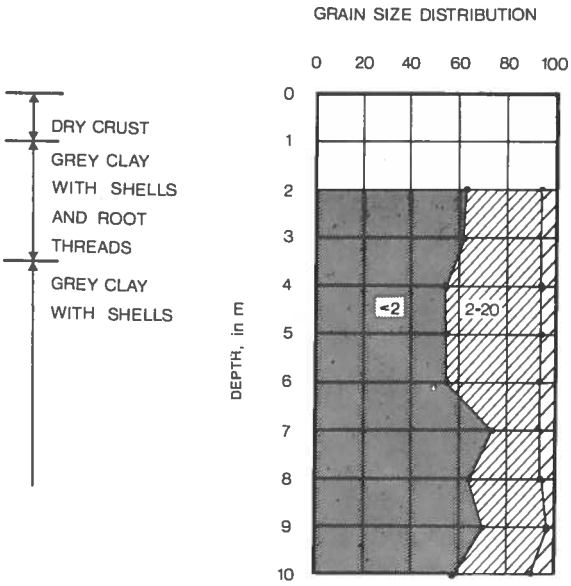

FIG. 77 Clay at Bäckebol. Geological profile and particle size distribution. Figures in graph indicate particle sizes in μm.

4.1.2 Geotechnical properties

Water contents

The water contents are listed in FIG. 78. The natural water co
varies from 75 to 105 %. It is fairly constant, around 80 % fo
2 to 6 m but at 7 m it increases to somewhere around 100 %. Th
reflects the higher percentage of clay particles at this depth.
The plasticity index is about 55 %.

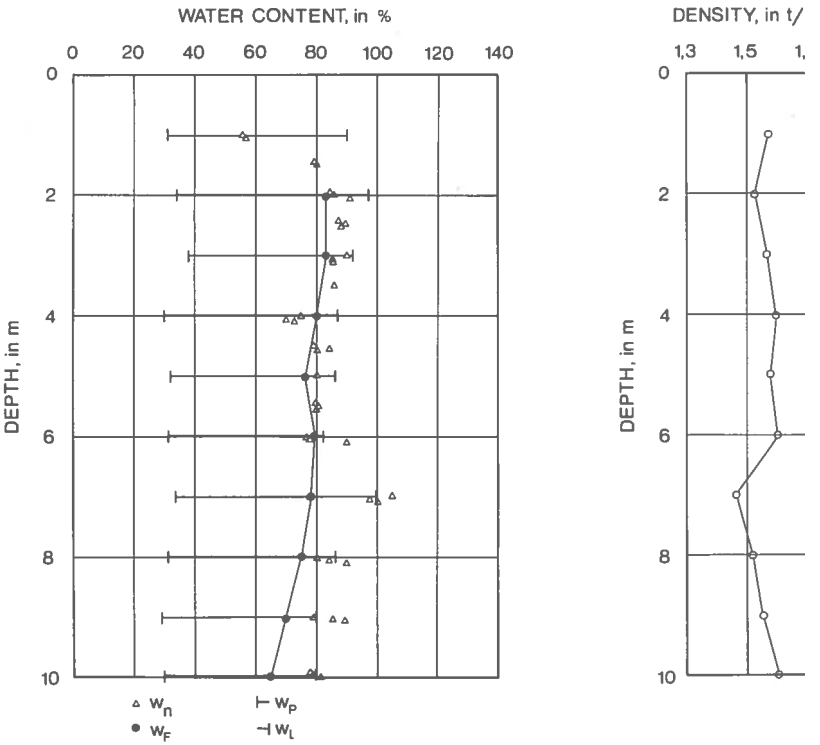

FIG. 78 Water contents of the clay situated in the depth range from 0 to 10 m below ground surface at Bäckebol.

Shear strength

An extensive test program has been carried out at Chalmers in o to determine the shear strength of this soft, high-plastic clay (Torstensson, 1973; Larsson, 1975*c*; Bengtsson, 1975).

FIG. 79 shows the undrained shear strength determined by fall-c test. The shear strength is seen to be fairly constant with de and has a mean value of 16 kPa.

Triaxial K_0-consolidated undrained tests performed at different rates of strain give a lower limit value which increases slight with depth, Larsson (1975*c*). The same time dependence is found true for vane boring tests made at different rates of angular r tion, Torstensson (1973).

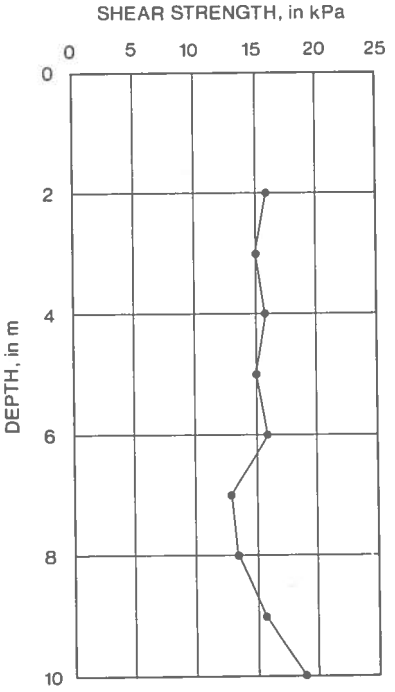

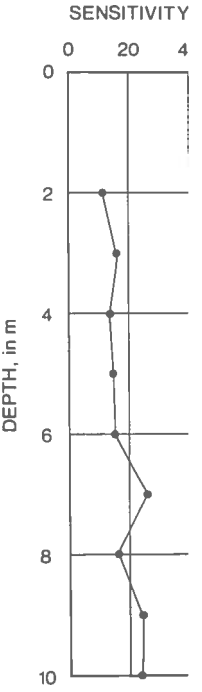

FIG. 79 Variation in shear strength. Profile at Bäckebo Fall-cone test.

4.1.3 Inhomogeneities

When a clay deposit is built up the sedimentation conditions var and one millimetre of clay can represent a period of one month o perhaps ten years. Parts of the deposit can be eroded, and the clay is bound to be varved, even if it appears to be homogeneous

When determining the water content of a clay, usually a 20 mm th slice is extruded from the sample tube. The natural water conte determined in this way is the mean value of the two centimetres involved.

In order to investigate the variation in the water content more in detail, four different depths, 3, 4, 5, and 7 m, were exami as follows. The water content was determined on some 50 pieces 2 mm thick consecutive slices taken from each depth. The result are given in FIG. 80.

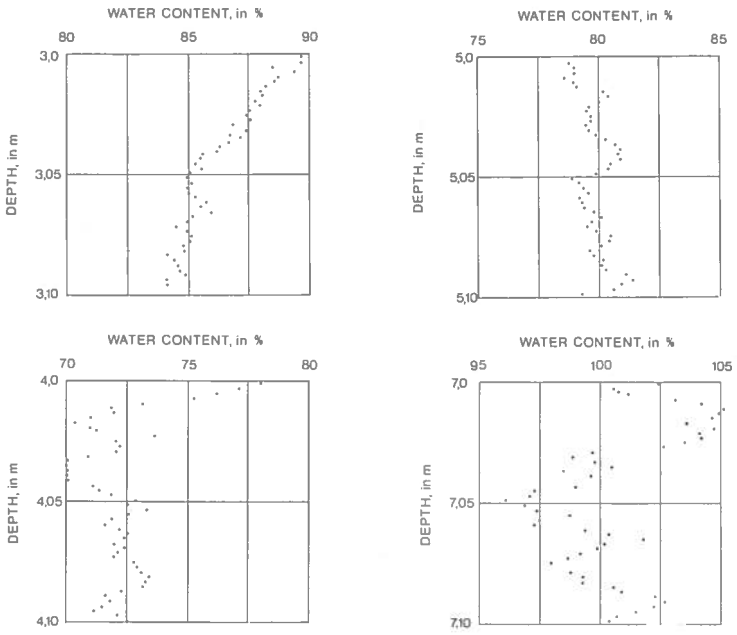

FIG. 80 Variation in natural water content at four different depths.

The water content is found to vary continuously through the sampl reflecting the difference in sedimentation conditions. Even if the water content can vary as much as 7 to 8 % in 100 mm, the cla can be considered very homogeneous.

Unfortunately it is impossible to repeat the same type of investi gation to determine the preconsolidation pressure, in order to se the effect of change in water content.

Three duplicate consolidation tests were made on clay from 7 m. They were made as CRS tests at a rate of strain of 0,0024 mm/min. and the pressure/compression curves are given in FIG. 81. By using the evaluation method suggested in Section 3.3, the preconsolidation pressures were found to be 62, 65 and 65 kPa. Th water content of the clay next to the sample was between 98 and 105 %.

The preconsolidation pressure is thus found to be little affected by slight variations in water content.

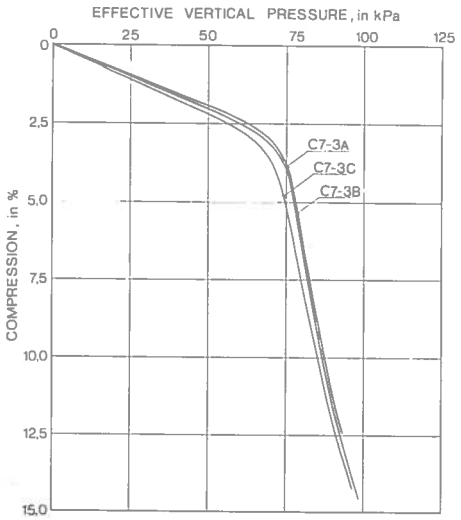

FIG. 81 Pressure/compression curves. Test C7-3A, B and C. Depth 7 m, rate of deformation 0,0024 mm/min.

4.1.4 Oedometer tests

More than a hundred oedometer tests have been made on clay from the test field. The different methods described in Chapter 3 were used. Only results from CRS tests are presented in this Sub-section.

First, the results of a few CRS tests are discussed to validate the model presented in Section 3.2. Then the preconsolidation pressures for the soil profile in the test field will be discusse

Critical shear stress

The apparatus described in Section 3.2 was used for measuring the horizontal stresses during the CRS tests.

In the following analysis two depths will be treated simultaneous 4,5 and 7 m. Pressure/compression curves are given for these two depths in FIG. 82. The difference between these two curves is th the 7-m curve has a very distinct and well-defined preconsolidati pressure, compared with the 4,5-m curve. This is not due to any difference in the quality of the samples. The upper five metres

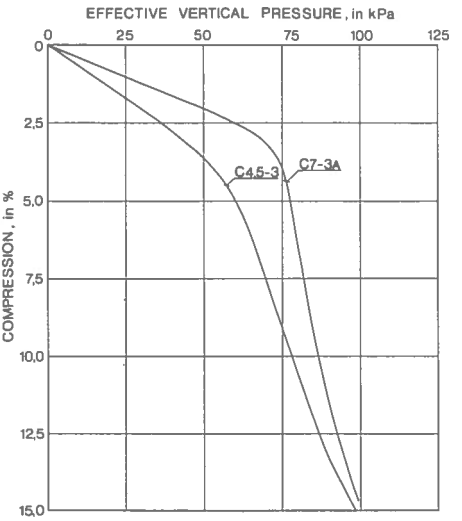

FIG. 82 Pressure/compression curves. Tests C4,5-3 and C7-3

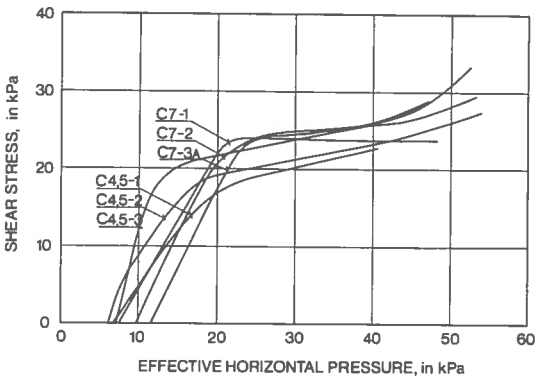

Legend

Test	Depth m	Rate of d mm/min
C4,5-1	4,5	0,0006
C4,5-2	4,5	0,0012
C4,5-3	4,5	0,0024
C7-1	7,0	0,0006
C7-2	7,0	0,0012
C7-3A	7,0	0,0024

FIG. 83 Stress paths. Tests C4,5-1 to C4,5-3 and C7-1 to C7-3A.

of clay are probably influenced chemically by infiltrating water, and form part of the weathered zone where the pressure/compressior curves are constantly more arched.

The above-mentioned difference is also found when stress paths frc the two different depths are compared.

The stress paths at different rates of strain are presented in FIG. 83. For this naturally deposited clay, the critical shear stress is also found to decrease with decreasing rate of strain down to a probably existing lower limit value.

A few CRS tests have been made on the 7-m clay at different "isotropic consolidation" pressures. The flexibility of the membrane in the oedometer presents a limitation, and again there are many objections against the test procedure. The curves only illustrate that what was said in Sub-section 3.2.2 about the artificially sedimented clay is probably also valid for this clay.

In FIG. 84 three stress paths are plotted. The horizontal preconsolidation pressure is shown on the axis of abscissæ as a black circle. The probable surface of critical shear stresses is represented by a dash-and-dot-line curve.

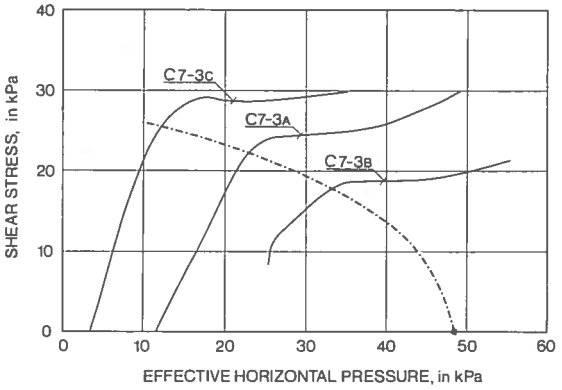

FIG. 84 Stress paths. Test C7-3A, B and C. Depth 7 m, rate of deformation 0,0024 mm/min.

The stress paths shown in FIG. 84 agree well with the three-dimensional model previously presented, but even slight variations in void ratio will render the interpretation difficul and a three-dimensional plot is therefore not presented.

Preconsolidation pressures

It was earlier pointed out that the preconsolidation pressure determined by using the Casagrande construction was greatly dependent on the evaluator, and that the interval of possible values was rather wide. The Author has therefore not determinec the preconsolidation pressures from incremental loading tests. However, in Appendix A the results of incremental loading tests are given together with CRS curves determined at a rate of deformation of 0,0024 mm/min as reference.

In Appendix A the pressure/compression curves for CRS tests are also listed. Only the tests made at a rate of deformation equal to 0,0024 mm/min or lower are included. The preconsolidation pressures were determined with great accuracy directly on the computer plot (250 x 250 mm^2), and are listed in Table 4. The method suggested in Section 3.3 was used.

Table 4. Preconsolidation pressures evaluated from CRS tests

Depth in m	Rate of deformation in mm/min		
	0,0006	0,0012	0,0024
2,5	44	47	{45 49
3,0	{45 42	--	43
3,5	--	--	42
4,0	--	--	53
4,5	47	47	48
5,0	44	53	{54 44
5,5	36	--	{50 61
6,0	--	--	{67 72
7,0	63	62	65 {62 65
8,0	--	--	65
9,0	--	--	63
10,0	--	--	66

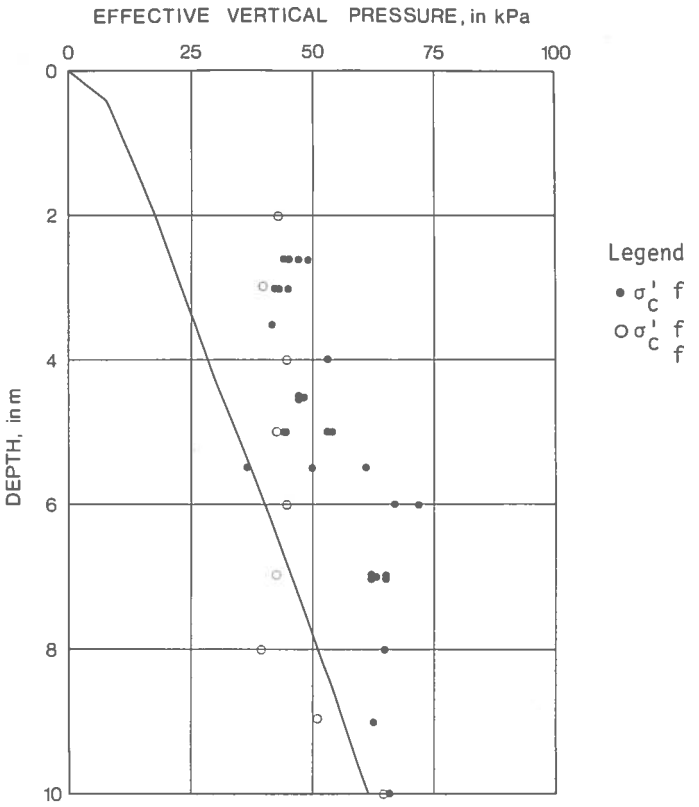

FIG. 85 Variation in preconsolidation pressure determinec from CRS tests at Bäckebol, Table 4. Distributic of effective overburden pressure also given, ful' line.

In FIG. 85 the preconsolidation pressures in Table 4 are plotte versus the depth. The effective overburden pressure is also give

The tests on clay from 2,5 to 7,0 m were carried out in an oedo- meter ring made of steel, lubricated with molybdenum sulphide, a the preconsolidation pressures should be reduced by 10 %. In th tests on clay from 8 to 10 m a teflon ring lubricated with silic grease was used, and the friction was then negligiable.

There is very little scatter in the results. The deviation is generally less than 5 % of the mean value. For 7 m, six tests, some at different rates of strain, give preconsolidation pressur from 62 to 65 kPa. One exception is the depth 5,5 m, where the

scatter is very large. Further comments on that will be made in Section 4.3. FIG. 85 also gives the preconsolidation pressure calculated from the expression

$$\sigma_c' = \frac{\tau_{fu}}{0{,}45\ w_F} \quad \text{(Hansbo, 1957)}$$

The correspondence with the oedometer values is very good for the uppermost 5 metres.

4.1.5 *In situ* horizontal stresses

In Sub-section 3.2.2 it was demonstrated that the *in situ* horizontal stress is an extremely important parameter. This has been known for some time, but perhaps only in the last few years the need for determining it has become quite obvious. More refined analysis, such as stress path methods and finite element methods require a good estimate of the horizontal stresses *in situ*.

Various equipments have been constructed for the purpose of measuring horizontal stresses *in situ*, such as hydraulic fractur different kinds of pressuremeters, and also pressure cells have been used.

A thorough investigation of the horizontal stresses *in situ* has been carried out at Bäckebol in the last few years, (Larsson, 19

The methods used were the Cambridge Pressuremeter, the Ménard Pressuremeter and a modified Glötzl cell (Massarsch, 1975).

The results are presented in FIG. 86. The Menard Pressuremeter i not a self-boring device, and a slight disturbance of the hole seemed to give rather high values of σ_h'. Therefore, only the min values are given for this method. The dash-line curve was obtain by using the equation proposed by Schmidt(1967).

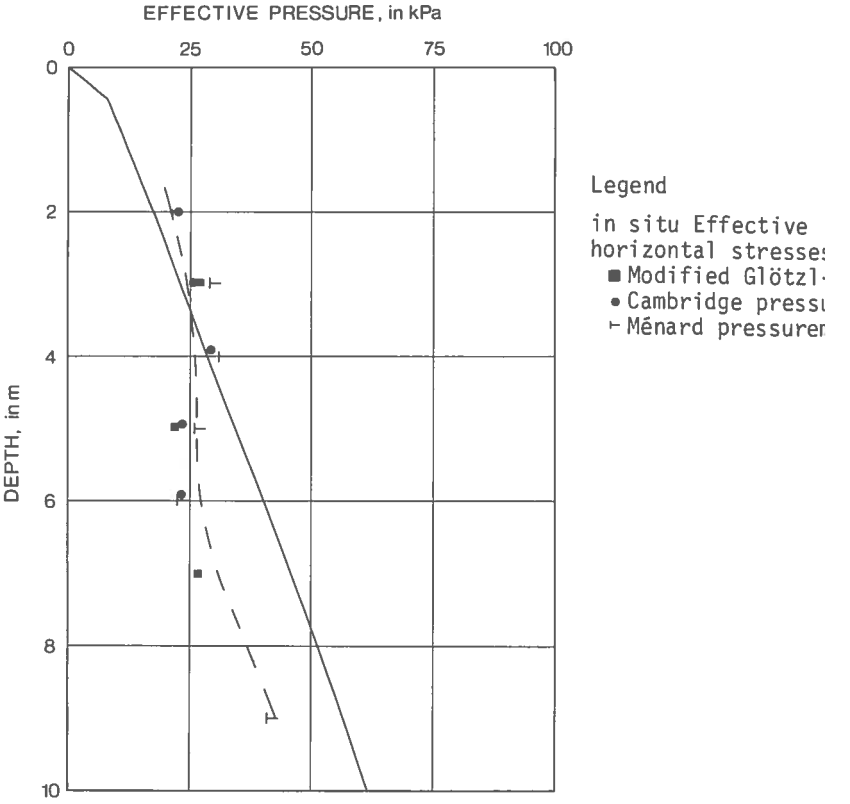

FIG. 86 Distribution of *in situ* effective stresses at Bäckebol. (Larsson, 1975*b*). Effective vertical pressure: full-line curve, effective horizontal pressure, see Eq. (26): dash-line curve.

$$K_{rb}^{o} = K_{o}' \left\{\frac{\sigma_c'}{\sigma_v'}\right\}^{1,2 \sin \phi'} \qquad (26)$$

where σ_c' = preconsolidation pressure (from oedometer tests)

K_o' = incremental coefficient of earth pressure (from oedometer tests)

ϕ' = effective angle of internal friction(from triaxial

The agreement between the values measured in the field and those calculated from laboratory tests is very close.

Those values of K_0 which can be calculated from the data present will be used later in Sub-section 4.3.2 when the *in situ* shear stresses are used in the analysis.

4.2 Loading arrangements and results

4.2.1 Introduction

The laboratory oedometer test is performed under external circumstances which in many respects differ from the *in situ* condit The sample is unloaded and might be slightly disturbed. Furthern the sample is small, the drainage paths are short, and the rate of loading is very high compared with loading rates at construction sites. It is therefore necessary to be able to compare results of laboratory tests with those of full-scale *in situ* loading tests, in order to appreciate the validity of the laboratory tests.

The *in situ* tests must be full-scale and performed at loading rates that are comparable to those used during construction. If the interpretation is simple and straightforward, this is an advantage.

The *in situ* loading tests described in this chapter were performe in the summer and fall of 1974.

4.2.2 Testing tank and loading procedure

In Chapter 3, the CRS test was found very powerful as a laborator test. In the field a loading test can hardly be performed at a constant rate of strain, owing to purely practical difficulties. A more suitable loading test for field conditions is to load the soil at a constant rate of loading. Besides, it was stated in Sub-section 3.1.4 that a constant rate of strain test and a const rate of loading test are identical if the oedometer modulus is co stant. The pressure/compression curves in Appendix A clearly sho that the oedometer modulus is constant up to the preconsolidation pressure for the clay at Bäckebol, and the two types of tests wil not differ from each other until the preconsolidation pressure is reached.

As the main purpose of this investigation is to study the preconsolidation pressure, the *in situ* tests were performed as constant rate of loading tests.

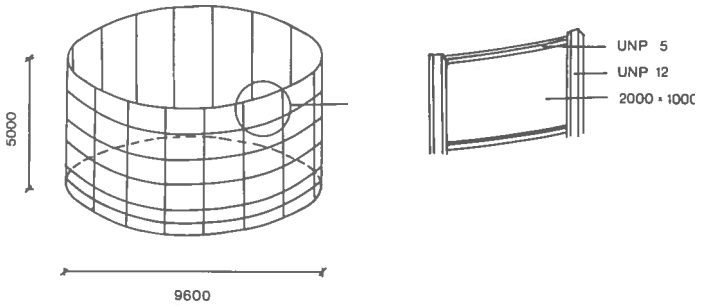

FIG. 87 Loading tank consisting of 15 segments (2x5 m^2).

For this purpose a dismountable tank was constructed. The tank consists of 15 segments, connected to each other by bolts formir an envelope surface 9,6 m in diameter and 5 m in height, see FIG The tank was placed on a 10 cm precompacted sand layer and made waterproof by an inside tarpaulin bag, having an area of 250 m^2.

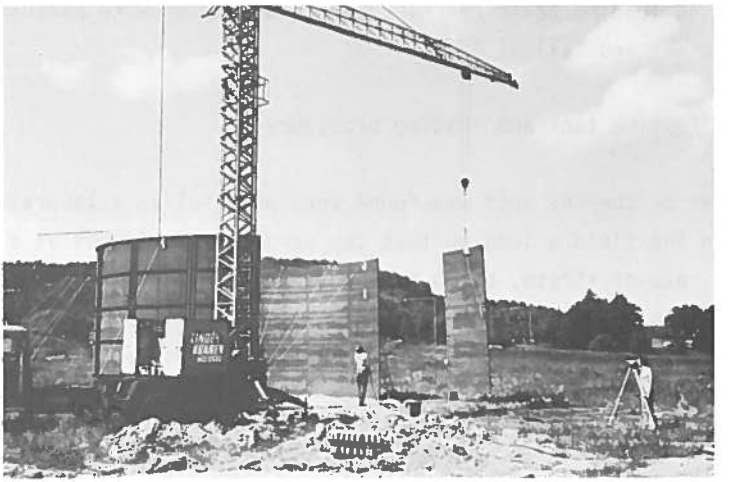

FIG. 88 Assemblage of loading tank at Bäckebol.

The assemblage of the tank, which is shown in FIG. 88 takes less than one day for four persons. After the assemblage of the tank a 1 m deep trench was dug around the tank, thus cutting through the dry crust and hence ensuring a well-defined stress distribution throughout the underlying homogeneous clay. Once the tank is assembled the loading test can start by slowly filling the

tank with water from a nearby fireplug. The load can be accurat determined throughout the test by taking readings of the water-meter on the fireplug.

Two tests were performed at loading rates of 1,3 (test I), and 0,8 (test II) kPa/day. The two test areas were not more than 25 apart.

4.2.3 Instrumentation

During the test, readings were taken of settlements and pore pressures. In this Sub-section a brief description is given of the different measuring systems used.

Settlements

The use of a tank rendered the measurement of settlements difficult as no readings could be taken from above the loaded area.

Two systems were used, one measuring the settlement along a horizontal tube embedded in the sand layer below the tank, the other measuring the variation in settlement with depth under the edge of the tank, FIG. 89.

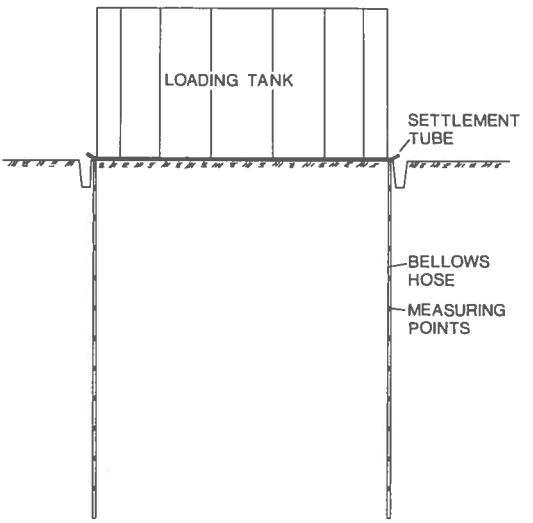

FIG. 89 Loading tank with settlement tube and bellows hos

Settlement tube

A settlement tube described by Bergdahl & Broms (1967) was used. The principle of the system is shown in FIG. 90. A measuring ur is inserted into its position in the tube. When the air pressur in the system is increased, the rubber membrane starts to expanc when the air pressure equals the pressure in the water system. By taking readings of the air pressure on the U-tube and levelli the water table (A), the elevation of the measuring unit can be calculated. The accuracy is within ± 3 mm.

Bellows hose

The variation in settlement with depth was measured by means of a bellows hose. The principle of this system had been described by Wager (1972), but several improvements have been made by the Author.

The measuring system is shown in FIG. 91. A plastic bellows hos with measuring points every metre is installed in the ground ins a 1 1/4" tube. A 10 x 14-mm^2 steel rod is inserted in the bello hose, which is stretched and attached to the inside rod. The outer tube is withdrawn, and the inner rod is left in the ground for a few days before it is taken away, allowing the clay to re-consolidate around the hose. A reference tube 1,5 m in length i used as base for the measurements.

Readings are taken by lowering the sensor. When the two springs (FIG. 91) are in contact with the stainless steel ring in a cage the circuit is closed, and this is indicated on the voltmeter. The sensor is fastened in a measuring cable and the depth from t reference level to the cage can be measured. By levelling the reference tube, the elevation of each cage can be calculated.

The accuracy of the system is good (± 1 mm).

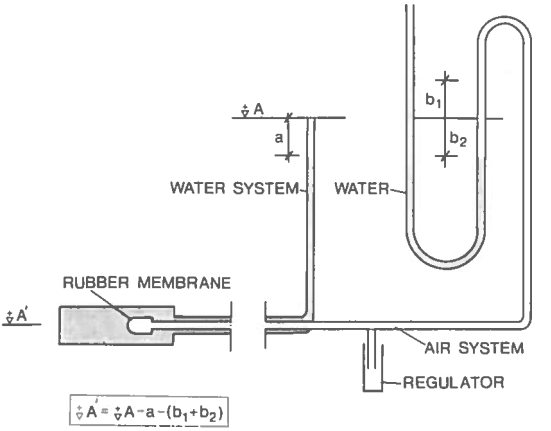

FIG. 90 Principle of apparatus for levelling the settlement tube.

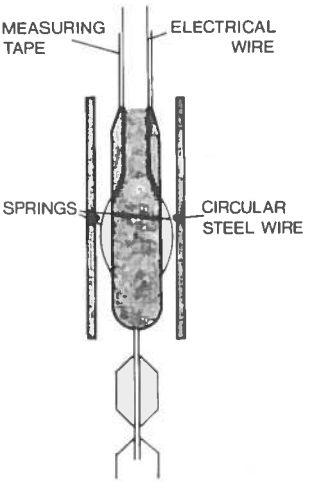

FIG. 91 Sensor used for levelling the bellows hose.

Pore pressures

The piezometers used were of the Geonor vibrating wire type. Fou
older piezometers, with a range from 0 to 400 kPa, were made of
stainless steel, while the others, with a range from 0 to 200 kP
were made of a brass alloy.

The piezometers were installed in the ground in the following manner. The piezometer with its 600 mm long casing, FIG. 92 was pushed down by means of 1 1/4" tubes, the cables and a wire following outside the tube. When the piezometer reached the des depth, the tubes were withdrawn leaving the piezometer in place and the cables and wire being the only connection with ground surface. This procedure was chosen in order to prevent "piling" of the soil below the loading area. Besides, a slight downward movement of the piezometer would produce an excess pore pressure which could hardly be separated from excess pore pressures cause by loading. The 600-mm casing was used for sealing the piezomet

At the end of the test the piezometers were recovered by pulling the wires.

The location of the piezometers is shown in FIG. 93.

The accuracy was extremely good when, as in this case, the objec was to record a change in pore pressure. One unit on the readou device corresponded to approximately 0,2 kPa for the piezometers with a range from 0 to 200 kPa.

A few of the piezometers were equiped with a zero-check device. When this was used, some irregularities were observed for some time afterwards. As the readings were very logical most of the time, no further zero-checks were made during the tests.

Test II was performed during a very rainy period. The readout device was very sensitive to weather conditions, and a tent was built on the site and heated by a fan. In spite of this, readin were occasionally lost for some of the piezometers.

4.2.4 Typical results

Settlements

The settlement record for one of the bellows hoses, placed next to the edge of the tank, is given in FIG. 94. The settlements are rather small, and it is obvious that little primary consolid tion is included.

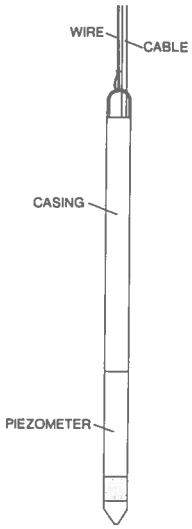

FIG. 92 Piezometer with 600-mm casing.

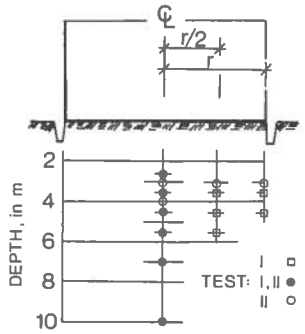

FIG. 93 Location of piezometers. Tests I and II at Bäckebol.

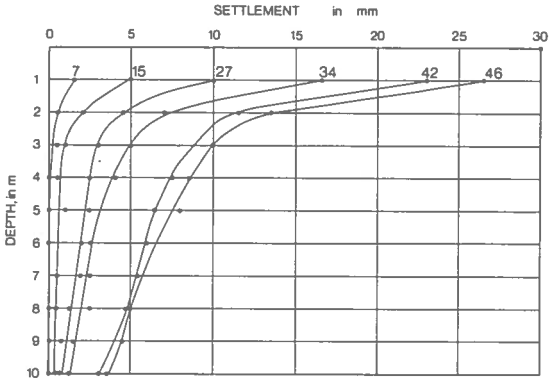

FIG. 94 Settlement record for one of the bellows hoses. Test I.

An attempt was made to separate the compression of each metre of clay by taking the settlement of one cage, subtracting the settlement of the following cage, and dividing by the initial distance between the cages. However, this was not possible as the differences were of the same order as the accuracy of the measuring system.

The readings taken with the settlement tube are shown in FIG. 95 for test I. This method gives values of the settlements that ar higher than the results obtained from the bellows hose. This is due to a deformation of the pedestal which the tank rested on, a the validity of the readings can therefore be questioned.

Pore pressures

Pore pressure readings were taken for every one or two kPa of additional load, to ensure a good continuity of the curves. Typical results from tests I and II are given in FIG. 96. The excess pore pressure is plotted as a function of the surface load. All the pore pressure curves are listed in Appendix A, an the curves in FIG. 96 are taken as representative of the two tes so as to point out a few important characteristics.

FIG. 96 gives the results relating to two piezometers at a depth of 3,5 m. In test II the increase of the excess pore pressure a the beginning of the test is about 6 kPa. This is partly due to the fact that a period of very rainy weather began just before test II. Earlier the ground water table had been around 0,4 m be the ground surface. However, the trench around the tank was filled with water because of the rain and the ground water table rose to the ground surface or perhaps slightly above. All exces pore pressures in the graphs are given with reference to a groun water table at 0,4 m below the ground surface. This was done in order to facilitate the comparison with test I and with the pre-consolidation pressures determined in the laboratory.

Very shortly after the start of the test a steady state is reach as the excess pore pressure remains constant in spite of the in-creasing vertical load. Then rather suddenly the pore pressure

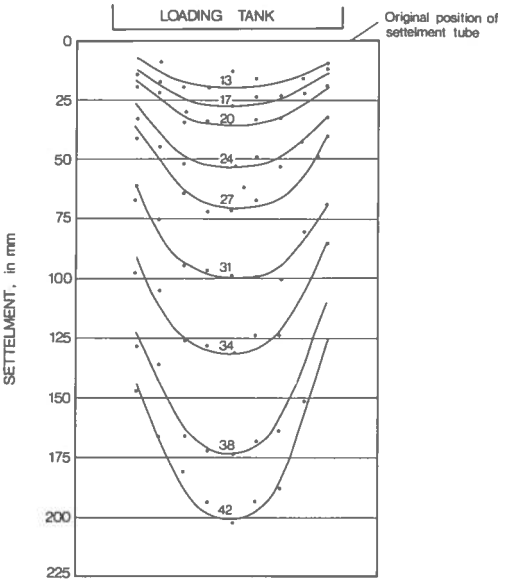

FIG. 95 Settlement record for one of the settlement tubes. Test I. Figures in graph indicate surface load in kPa.

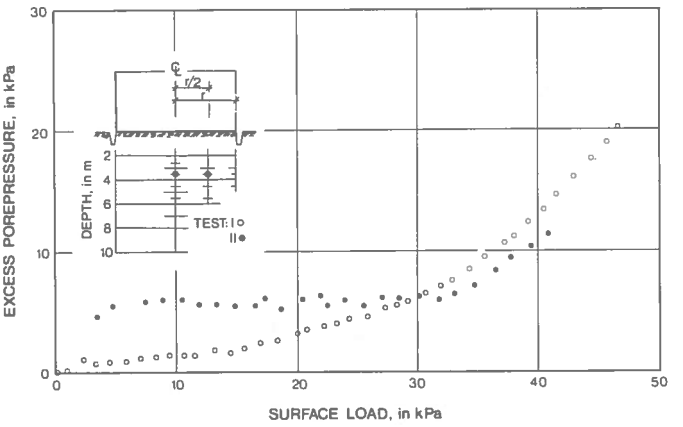

FIG. 96 Development of excess pore pressures in full-scale loading tests at Bäckebol.

starts to increase rapidly, and this indicates a change in the behaviour of the material. This is very similar to the results obtained in the CRS test. The pore pressure at the undrained bottom of the oedometer shows exactly the same trend (FIG. 49) and this sudden increase in pore pressure was proved in Sub-sect 3.1.2 to be associated with a breakdown in the structure and wit the fact that the preconsolidation pressure was reached. The bend-off of the curve can therefore be interpreted as indicating that the preconsolidation pressure is reached.

In test I, the rate of loading was higher, 1,3 kPa/day against 0,8 kPa/day in test II, and a true steady state was never obtair The pore pressures increased slightly all the time. Yet, a chan in behaviour can be observed around a vertical load of 30 kPa, where an increase in excess pore pressure is evident.

A thorough discussion of the results follows in Sub-section 4.2.

Most of the piezometers worked well during tests I and II. Howev some of them showed certain peculiarities, especially at the beginning of test I. FIG. 97 gives the results obtained from the piezometer at 4,5 m, test I. This piezometer had been installed 9 days before the start of the test, yet a rather large excess pore pressure was present. It decreased with time and an appare steady state was obtained. From then on the behaviour of the piezometer was quite normal.

These excess pore pressures are believed to be due to the produc tion of gas in the piezometer. This phenomenon occurred only in the new piezometers, which were made of a brass alloy which is known to react chemically with the salt water in the clay so as to produce gas. This reaction probably ceased after some time owing to the fact that a protecting oxide had been formed.

The possible presence of some gas in the piezometer is not believed to affect the results significantly as this test is comparatively slow.

The results obtained from the piezometers at a depth of 5,5 m, test I and test II, are given in FIG. 98. These curves differ f

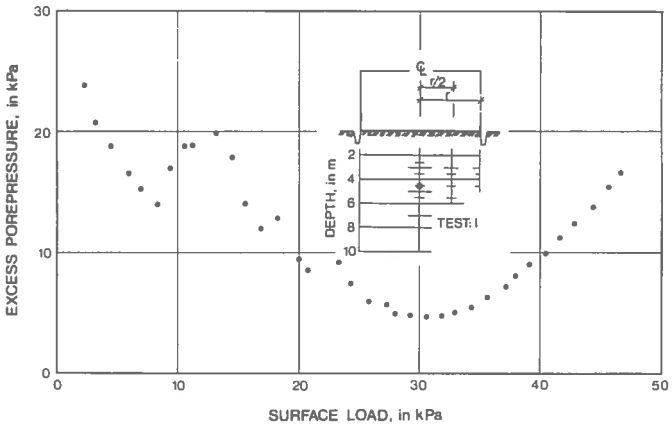

FIG. 97 Results obtained from piezometer at 4,5 m. Test I.

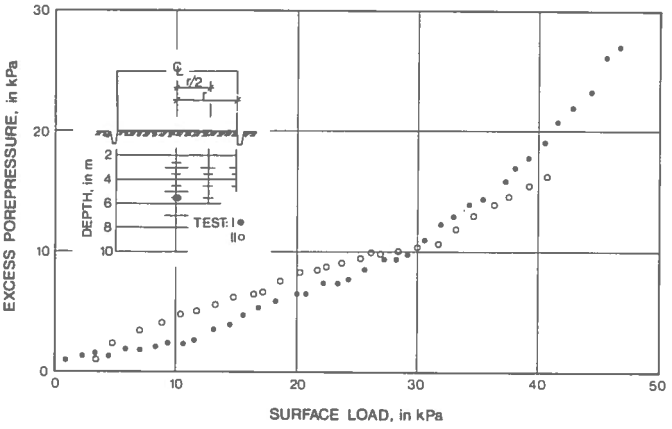

FIG. 98 Excess pore pressures. Piezometers at 5,5 m. Test I and test II.

all other curves in one respect, namely that the pore pressure increases constantly. The increase in the pore pressure due to the breakdown in the structure occurring when the preconsolidatic pressure is reached seems to be superimposed. No explanation of this behaviour was found, and the pore pressure build-up in the CRS test did not show the same trend.

4.2.5 Stress distribution

Before any calculation of *in situ* preconsolidation pressures can be made the stress distribution throughout the soil mass must be known. This problem may be far more difficult than that of determining the preconsolidation pressure. As the clay is visco-elastoplastic no existing stress distribution theory can be used over the whole range of stresses. Limitations must be introduce

The main object of this study was to determine the preconsolidat pressure. From the CRS tests described in Sub-section 3.1.2 the stress/strain relation was found to be linear up to the pre-consolidation pressure. The use of the theory of elasticity is therefore considered to be justified for stress levels lower tha the preconsolidation pressure, as the material is "elastic" in this region. The distribution of stresses above the preconsolid tion pressure will hardly be given any attention.

The graph used is showed in FIG. 99, Harr (1966), and gives the distribution of vertical stresses under a flexible circular surface load on a homogeneous semi-infinite body. For horizonta and shear stresses, the graphs presented by Hansbo (1966) were used.

The assumptions made are believed to be satisfactory fulfilled. The clay has a fairly constant undrained shear strength in the interval considered, and hence also a constant E-modulus as the elastic modulus usually is written as a constant times the un-drained shear strength.

However, this is not true for the dry crust, but the crust was c through by a trench around the tank, and the influence of the cr should therefore be eliminated. The load was applied one metre below the surface, but as the depth over the width of the load w only 1/10 its effect on the stress distribution can be neglected The bottom of the tank was completely flexible and the load is assumed to be uniformly distributed by the 1 m thick pedestal of crust. The depth of the deposit is 40 m which is large in relati to the diameter of the tank.

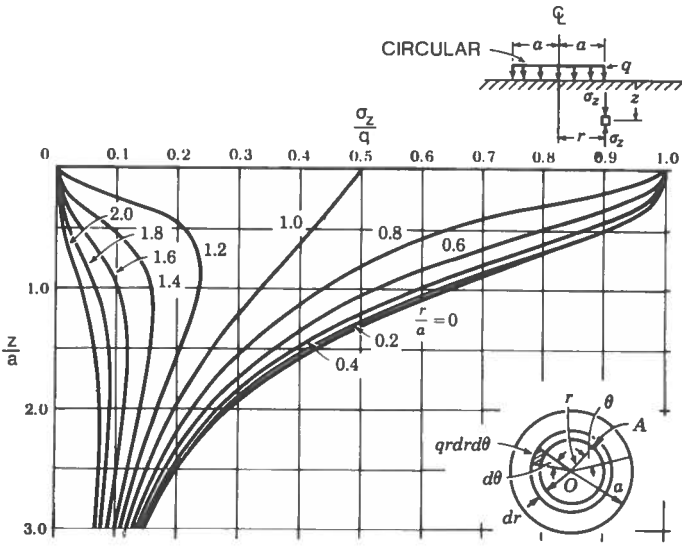

FIG. 99 Stress distribution in an elastic medium under a circular flexible load. (Harr, 1966).

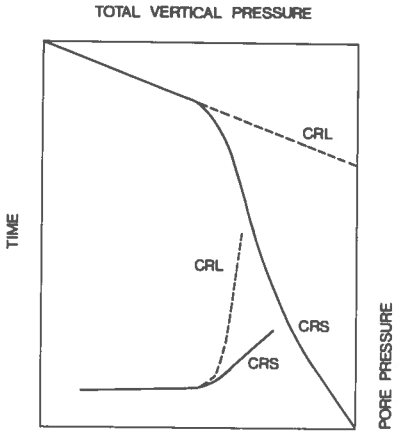

FIG. 100 Comparison of loading rate and excess pore pressure in a constant rate of strain test and a constant rate of loading test.

4.2.6 Discussion of test results

Results of a CRS test are schematically shown in FIG. 100, where (full-line curves) total stresses are used instead of effective stresses. As this test was performed at a constant rate of deformation, the vertical axis in FIG. 100 can be said to represent time on an arithmetic scale. The corresponding load/tim curve for the field tests, which were performed at a constant ra of loading, is shown by a dash-line curve. A more drastic chang in pore pressures is to be expected when the preconsolidation pressure is exceeded. This is illustrated by the assumed (dash- pore pressure curve in FIG. 100.

The curves given in Sub-section 4.2.4, where the excess pore pressure was plotted versus surface load, did not show this abru change in the development of excess pore pressures.

If the curves in FIG. 96 are replotted so that the stress distri tion is taken into account on the basis of the theory of elastic $\Delta\sigma$ is given at the level treated, and the existing pore pressure is subtracted, then the excess vertical effective stress ($\Delta\sigma'_v$) w be obtained. FIG. 101 shows the results for the 3,5-m piezomete Now the excess pore pressure is represented as a function of the vertical effective stress increase at the level of the piezomete The expected abrupt change in the development of pore pressure i now obvious. As the preconsolidation pressure is reached, the effective stress hardly increases at all, in spite of the increasing total pressure. Evidently, once the preconsolidation pressure is reached, all additional loads are carried as pore pressures.

In FIG. 102 the build-up of pore pressures at the piezometer at depth of 10 m is represented as a function of the surface load a the vertical effective stress increase. From the latter curve i can be seen that the effective vertical stress does not increase during the test; the stress increase is totally carried as a pc pressure increase already from the beginning of the test. The c is therefore believed to be normally consolidated at the depth.

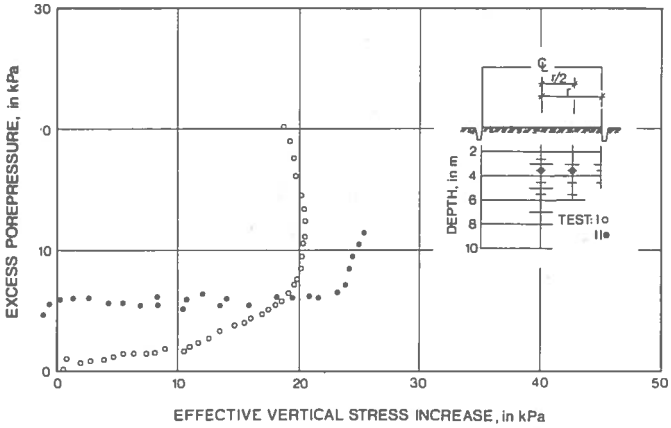

FIG. 101 Increase in excess pore pressure as a function of effective vertical stress increase. Piezometers I:3,5B and II:3,5A.

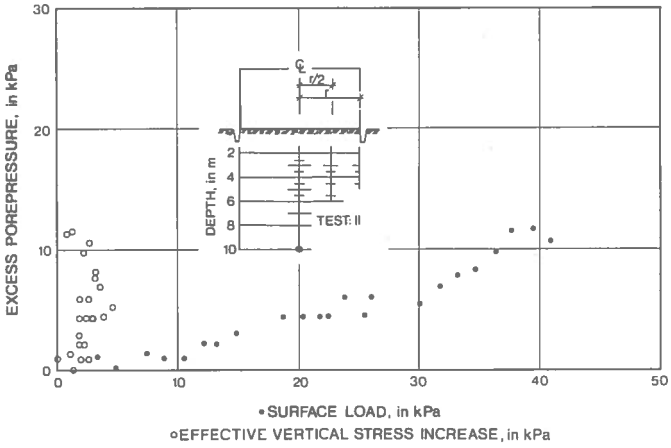

FIG. 102 Variation in excess pore pressure with effective vertical stress increase. Piezometer at 10 m. Test II.

It seems a little strange that the excess vertical effective str in test I, FIG. 101, decreases at the end of the test, and water is nevertheless poured into the tank. A plausible explana tion of this is that the method used for calculating the stress distribution is no longer valid as the preconsolidation pressure is exceeded in some regions. The preconsolidation pressure is reached first along the centre line and then gradually further o

The preconsolidation pressure was previously proved to be closel related to a critical shear stress, and once the critical shear stress is reached, large deformations were found to be necessary before the clay could sustain any further stress. As the load i distributed because of the presence of shear stresses, it is qui logical that the stress distribution based on the theory of elasticity gives a distribution that is too large once the criti shear stress is reached. For example, in FIG. 101, curve from test I, a load distribution factor of 0,84 is used for the appli load according to the theory of elasticity. A decrease in effec tive stress is avoided if this factor is increased from 0,84 to 0,88 at the end of the test.

The bend-off in the pore pressure curve will be interpreted as i dicating that the preconsolidation pressure is exceeded. Most c the curves are fairly linear at the beginning of the test. The curves for test II remain horizontal until they suddenly start t rise. This change in behaviour is very well defined and the int pretation presents no difficulties.

The curves for test I are more arched, and a true steady state flow is never reached. Several of these curves have two linear parts in the beginning, before the drastic change occur. In thes cases the bend-off from the second linear part is interpreted as the preconsolidation pressure.

It is to be borne in mind that the preconsolidation pressure is the existing overburden pressure plus the excess effective press as interpreted in the preceding section. An error of, say, 5 kP can appear to be large but is totally only an error of about 10

As can be seen from FIG. 101, the effective stress increases up the preconsolidation pressure, and then almost all excess load i carried by an increasing pore pressure. Hardly any settlement will be due to primary consolidation. The increase in settlemen occurring when the preconsolidation pressure is reached must be due to a horizontal deformation in the soil mass. The settlemen will therefore not be analyzed any further.

All pore pressure curves for tests I and II are listed in Appendi
The evaluated excess effective stresses at the preconsolidation
pressures are given in Table 5. The following code is used: Roma
numerals = test number, Arabic numerals = depth. Letters: A = c
line, B = half the radius, C = under the edge of the tank.

Table 5. Excess effective stress at the time when the preconsoli
tion pressure was reached during *in situ* tests.

I	2,5	A	22	kPa			B	10	kPa
II	2,5	A	30	"			C	7,5	"
II	3,0	A	23,5	"		II	4,5	A 14,5	"
		B	23	"		I	5,5	A 10	"
		C	11	"				B 9,5	"
I	3,5	A	(17)	"		II	5,5	A 11,5	"
		B	18,5	"		I	7,0	A 12,5	"
		C	9	"		II	7,0	A 10,5	"
II	3,5	A	23	"		I	10,0	0	"
II	4,0	A	20,5	"		I	10,0	0	"
I	4,5	A	11	"					

The value for piezometer I 3,5 A is bracketed because the bend-of
is believed to be caused by a defect of the piezometer rather tha
by the fact that the preconsolidation pressure was exceeded, sinc
extremely high excess pore pressures were obtained (50 kPa).

Effect of rate of loading

By using Table 5, a comparison can be made between test I (1,3 kP
and test II (0,8 kPa/day) to determine the effect of the rate of
loading. The differences in the evaluated preconsolidation
pressures are small, indeed so small that natural variation in th
clay very well could cause differences of the same order of magni
tude. It is therefore believed that a lower rate of loading woul
not significantly affect the evaluated preconsolidation pressures

Effect of induced shear stresses

Most of the piezometers were placed along the centre line of the
tank to avoid the influence of horizontal deformations; thus, the
deformation conditions were equivalent to those in the oedometer.

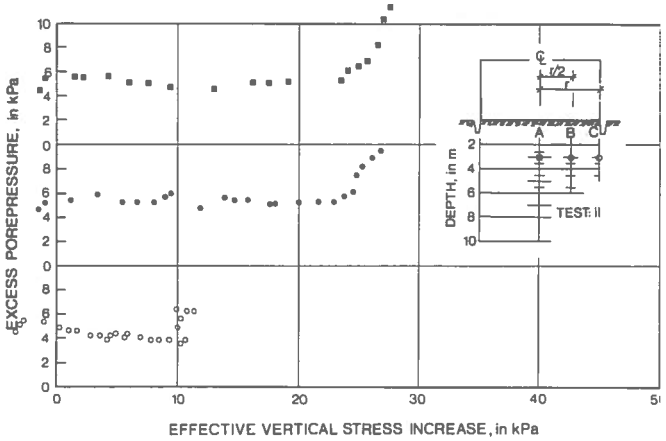

FIG. 103 Variation in excess pore pressure with effective vertical stress increase. Three piezometers at a depth of 3 m. Test II.

Some piezometers were installed at a radial distance of half the radius, and some others at the radius, from the centre line. This was done for 3,5 m and 4,5 m in test I and 3 m for test II. The build-up of pore pressures during test II is shown in FIG. 103 for the piezometers at 3 m.

At a depth of 3 m, i.e. 2 m below the dry crust, the respective load distribution factors determined from the theory of elastici are 0,95, 0,89, and 0,45 for piezometers A, B and C, FIG. 103. The respective excess effective stresses corresponding to the points where the curves bend off are 23,5 23, and 11 kPa.

Piezometers A and B are closely in agreement, while piezometer C bends off at an additional effective stress of less than half th of piezometers A and B, and cannot possibly be interpreted as in dicating that the vertical preconsolidation pressure is exceeded

The shear stresses below the tank have to be considered. First the existing stresses must be known. The effective overburden pressure at 3 m is 23 kPa, and K_0 is believed to be 1,10, Larsso (1975*b*). This gives an effective horizontal *in situ* stress of 25 kPa.

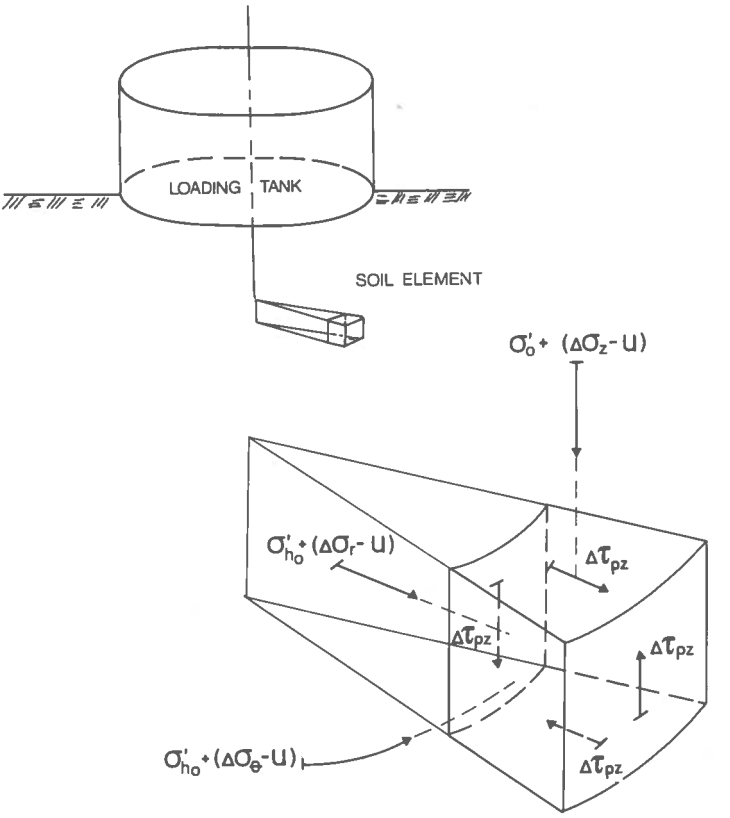

FIG. 104 Definition of stresses in an axi-symmetrical element.

Just as before, the theory of elasticity is taken to be valid fo loads below the preconsolidation pressure. The excess shear stresses in the ρ-z plane, see FIG. 104, will be 0 on the centre line, 3,2 kPa for $\rho/a = 1/2$, and 10 kPa for $\rho = a$, where a equal the radius of the loaded area. On the assumption that $\nu = 0{,}25$, the respective values of the increase in horizontal stresses determined from the theory of elasticity are 8, 8, and 7 kPa.

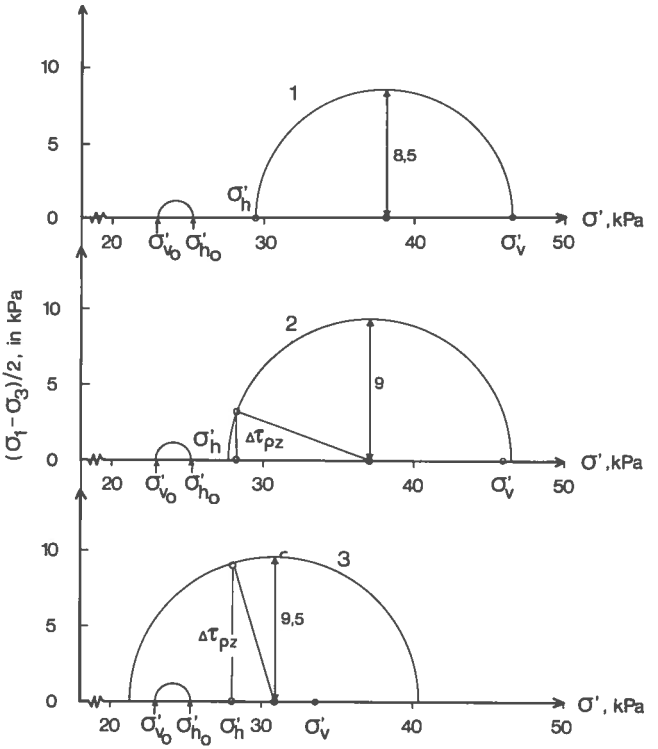

FIG. 105 Mohr's circles illustrating the stress conditions around the three piezometers at a depth of 3 m at the time when the pore pressure curves bend off, see FIG. 91. Distance from center line 1: 0r 2: 2,5 m, 3: 5 m.

A stress analysis is made by means of Mohr's circles in FIG. 105. On the centre line the principal axis remains vertically orientec but as the distance of the points from the edge of the loaded area decreases, the rotation of the principal axis will increase.

The calculated maximum shear stresses at the time when the pore pressure curves bend off are 9,5, 9, and 8,5 kPa. It seems that the pore pressure curves change in shape when a certain definite critical shear stress is reached. This critical shear stress was previously proved to be closely connected with the preconsolidati pressure. A similar analysis of the results of test I, 3,5 m, will give 10 and 9,5 kPa for piezometers B and C. The value for piezometer A was not used as it was believed to give erroneou results.

It may be noted that, according to the theory of elasticity, the increase in horizontal stress caused by an increase in vertical stress, corresponds very well with K_0'', (see Sub-section 3.2.1) determined by the CRS test with measurement of the horizontal stresses if ν is assumed to be 0,25.

When the excess effective stress needed for the preconsolidation pressure to be reached is known, the *in situ* preconsolidation pressure can be determined if the existing overburden effective pressure (σ_0') is known.

The density of the clay was determined for every half metre down to 6 m and then for every metre, and thus the variation in effective overburden pressure can be calculated. The pore water pressures correspond to a ground water table 0,4 m below ground surface.

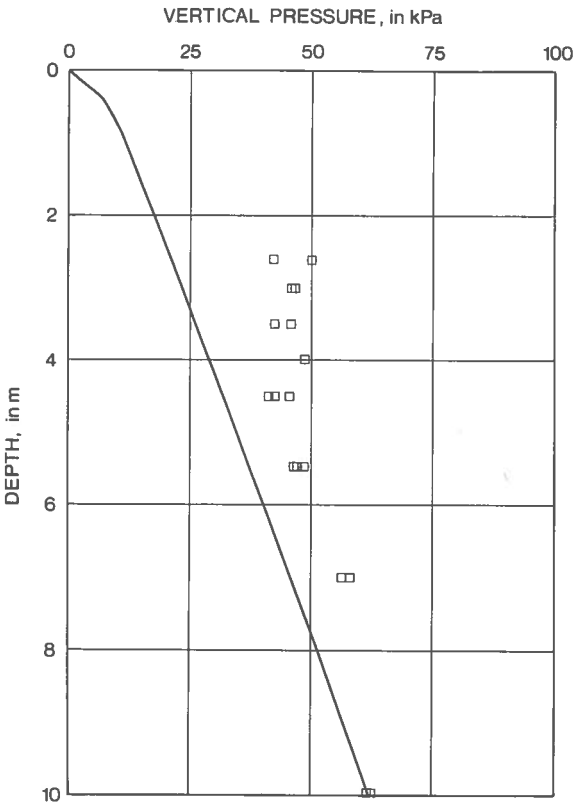

FIG. 106 *In situ* preconsolidation pressure calculated as the sum of the effective overburden pressure and the value presented in Table 5.

Appendix A gives the excess pore pressure as a function of the surface load and of the effective vertical stress increase. The effective stress increase necessary for the preconsolidation pressure to be reached was evaluated as previously described. The variation in the *in situ* preconsolidation pressure with dept is plotted in FIG. 106.

4.3 Comparison of results of laboratory and field tests

In Chapter 3 a comparison was made between the results of oedometer tests using different loading routines. No contradictory results were obtained, and the differences that were found were interpreted as being caused by a time dependence of the clay. Th CRS test was found superior to incremental loading tests, mostly because the complete pressure/compression curve was obtained frc the CRS test.

In this section the results of CRS tests on clay from the test field at Bäckebol are compared with the results of the field loading tests. The incremental loading tests are not discussed, but are indirectly treated as they have previously been compared with the CRS tests in Chapter 3.

4.3.1 Preconsolidation pressures

In Chapter 3, where the CRS test is thoroughly treated, the preconsolidation pressure was traced as a bend-off in the pressure/compression curve as well as in the pore pressure/press curve. Measurements of the horizontal stresses during the oedometer test revealed a close relationship between the critical shear stress and the preconsolidation pressure. It is important to appreciate the mechanical behaviour on a microscale. As the preconsolidation pressure is reached, the material starts to yie and this is followed by large deformations as well as by an increase in pore pressure.

A method was suggested for evaluating the preconsolidation press from the laboratory curve. These results, together with the *in situ* preconsolidation pressures interpreted from the field tests are plotted in FIG. 107.

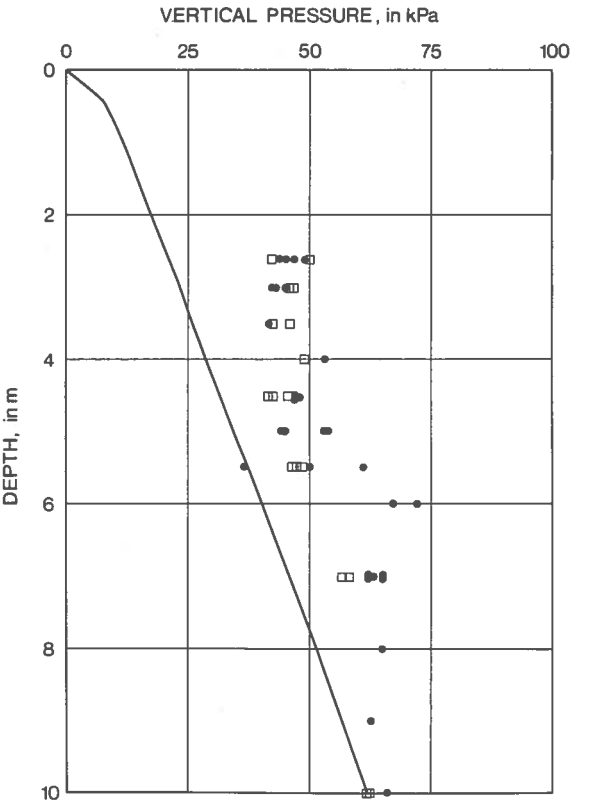

FIG. 107 Preconsolidation pressures determined from field and laboratory tests, see FIG. 85 and FIG. 106. ● σ'_c determined from CRS tests; □ σ'_c determined from full-scale field tests.

The correspondence of the laboratory and field results is good indeed with one exception. The difference between the preconsolidation pressure determined in the laboratory and in the field is less than 10 %, except for 5,5 m, where the variation in the results of CRS tests is large. The pore pressure curves obtained from the field tests at this level show a comparatively large increase in excess pore pressure before the bend-off of th curve. This increase in pore pressure could indicate that the clay is normally consolidated, and this was also found in one of the CRS tests. On the other hand, the bend-off of the curves corresponds well with the preconsolidation pressure determined from laboratory test C5,5-3B which in turn is in good agreement with the incremental loading tests (Appendix A), while test C5,5- indicates a larger overconsolidation ratio, comparable to that obtained at a depth of 6 m.

It is obvious that the variation in properties of the clay at 5, is larger than in the deposit in general. At present this quest is subjected to a thorough investigation involving chemical and geological test methods.

However, it is important to point out the extremely good correspondence at the other depths, but also to realize that knowledge about secondary compression and creep is necessary to enable a prediction of long-term settlements.

No significant time dependence of the *in situ* preconsolidation pressure was found by comparing the values obtained at the two loading rates used for the field tests. This seems credible when we compare the preconsolidation pressures evaluated from CRS tests made at different strain rates. The preconsolidation pressures determined by using the suggested method of evaluation were little affected by a change in the rate of strain when it was lower than 0,0024 mm/min. This corresponds to a loading rat of 15 to 20 kPa/hour, while it was 0,8 and 1,3 kPa/24 hours in the field tests.

4.3.2 Critical shear stresses

Measurements of the horizontal stresses during a CRS test showed that a critical shear stress was reached at the same time as the preconsolidation pressure.

From the data presented in FIGs. 105 and 106 it was concluded tha the bend-off in the excess pore pressure curve from the field test occurred when the vertical preconsolidation pressure was exceeded at the piezometer in the centre. The piezometer situat at the same level but under the rim of the tank gave readings of the excess pore pressure that were far less. A calculation of shear stresses showed that all three pore pressure curves bent off when the shear stresses were about 9 kPa.

FIG. 108 gives two stress paths with different "starting-points" for the clay from a depth of 3 m. If a probable stress path is drawn from the *in situ* point (K_0 = 1,10), see the dash-line curv a critical shear stress of 8 kPa is obtained. Again it should b

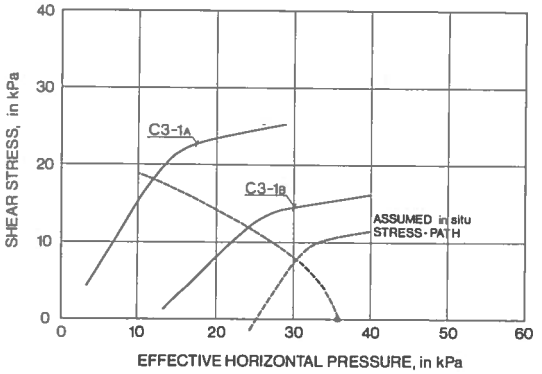

FIG. 108 Stress paths. Bäckebol clay, depth 3 m. Assumed variation of the critical shear stress is represented by the dash-line curve. Black circle represents horizontal preconsolidation pressure.

noted that great care must be taken when the different stress pa are interpreted. Still the results are of the right order of magnitude.

These results agree well with the previously discussed micro model of the clay where the increase in stresses, compression as well as shear stresses, are mainly carried by the links or bridges.

5 FULL-SCALE TEST AT VÄLEN

5.1 Test field

A full-scale loading test was made at Välen, in the southern par of the city of Göteborg. This complementary site was chosen in view of the high organic content of the clay (5 to 6 %).

The laboratory work has not been as extensive as in the tests on clay from Bäckebol, but enough data are given to facilitate a comparison of the preconsolidation pressures determined by oedometer tests with those determined in the field.

5.1.1 Geology

The test area is situated 10 km south of the city of Göteborg, 100 m north-west of the river Stora ån. The ground has an eleva tion of 2 m with reference to the river, and the deposit is some 20 m deep. The soil profile is given in FIG. 109.

The uppermost metre consists of a dry crust, followed by a green-grey organic postglacial clay. Shells are common and at a depth of 6 m there is a dense band of shells in the clay. The clay content varies from 50 to 55 %, and the organic content determined by ignition loss is 5 to 6 %.

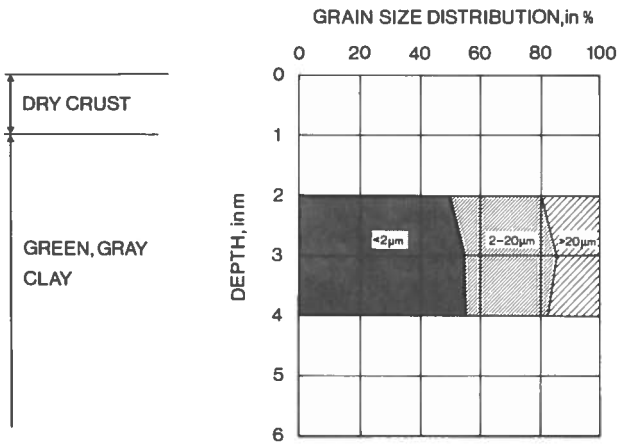

FIG. 109 Clay at Välen. Geological profile and particle size distribution. Figures in graph indicate particle sizes in µm.

5.1.2 Geotechnical properties

Water content

The water contents are given in FIG. 110. The natural water content varies from 110 to 130 %, slightly decreasing with depth. The liquid limit is of the same order of magnitude as the natural water content, and the plasticity index is around 80 %. The variation in density is also given in FIG. 110.

The variation in natural water content of a 100-mm sample is give in FIG. 111. Relatively large differences can evidently be found in this clay even for small variations in elevation.

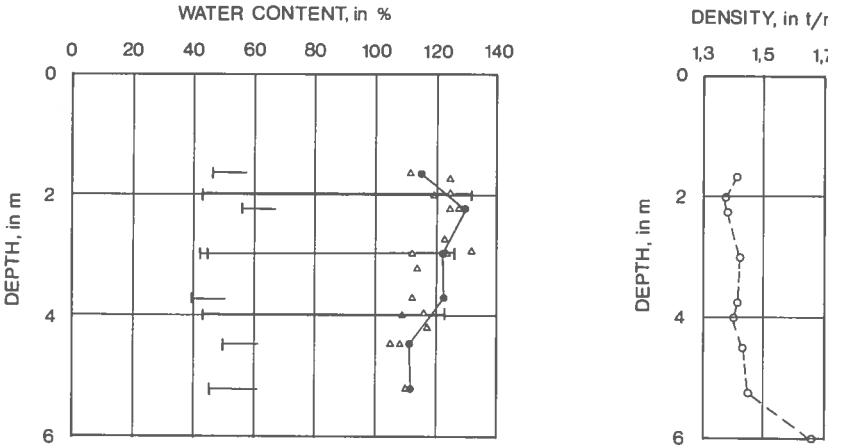

FIG. 110 Water contents of the clay situated in the depth range from 0 to 6 m below ground surface at Välen. $\triangle$ w_n • w_F ⊢ w_P ⊣ w_L

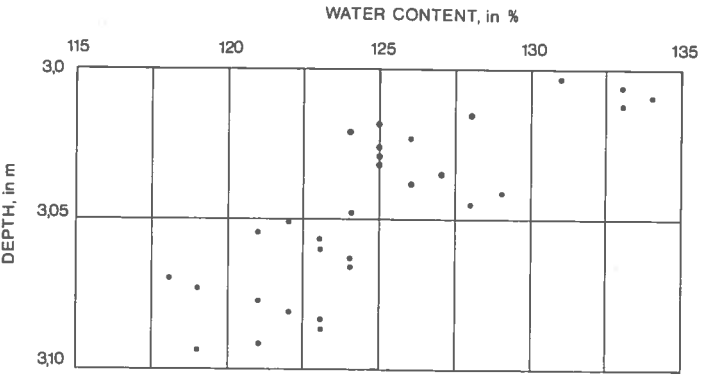

FIG. 111 Variation in natural water content at a depth of 3 m.

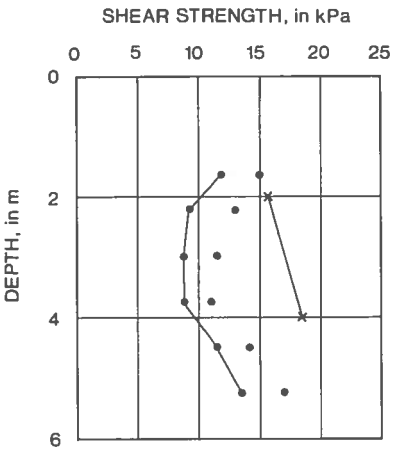

FIG. 112 Shear strength of the clay situated in the depth range from 0 to 6 m below ground surface at Välen. • Fall-cone test; ↘ Fall-cone test, reduced values; x vane boring.

Shear strength

The clay from depths of 2 to 5 m has been thoroughly investigate in connection with other research projects carried out in the Geotechnical Department, Bengtsson (1975) and Torstensson (1975) FIG. 112 gives the shear strength determined by fall-cone test and vane boring test. The shear strength determined by vane boring test varies from 16 to 18 kPa. Slightly lower values are obtained from the fall-cone test.

5.1.3 Oedometer tests

Only the uppermost 5 m of the deposit were investigated and as preconsolidation pressure there is very low, smaller than 40 kPa no STD tests were made. The interest was focused on the CRS tes and the preconsolidation pressure determined by using the constr tion suggested in Section 3.3. Six LIN tests were made, and are given for comparison in Appendix B, (Bengtsson, 1975).

Typical results of a CRS test are given in FIG. 113. The pressure/compression curve is very flat, and the oedometer modulus is low. It is interesting to note that a deformation of almost 5 % was needed for the preconsolidation pressure to be

Table 6. Preconsolidation pressures evaluated from CRS tests

Depth in m	Rate of deformation in mm/min		
	0,0006	0,0012	0,0024
1,65	--	--	43
2,0	25	26	27
2,25	--	--	24
3,0	--	--	19
3,75	--	--	17
4,5	--	--	29
5,25	--	--	32

5.2 Loading arrangements and results

5.2.1 Introduction

The clay at the test site at Välen is fairly homogeneous and has a low permeability. The same type of loading test as used at Bäckebol was therefore chosen. The loading rate was set at 0,5 kPa/day. This low value was chosen for two reasons.

- The low loading rate at Bäckebol (0,8 kPa/day) gave very well-defined excess pore pressure curves.
- The overconsolidation ratio was believed to be small, and a certain number of pore pressure readings was wanted before the preconsolidation pressure was reached.

The same kind of instrumentation was used but with a different location of the piezometers, see FIG. 117.

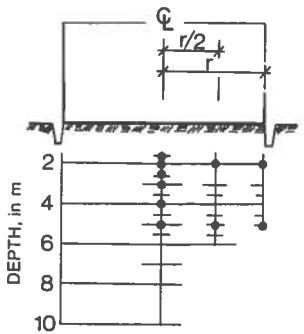

FIG. 117 Location of piezometers. Field loading test at Välen.

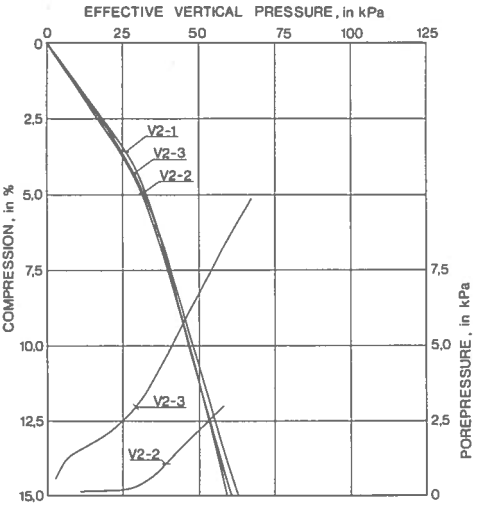

Legend

Test	Depth m	Rate mm
V2-1	2	0
V2-2	2	0
V2-3	2	0

FIG. 115 Pressure/compression curves. Tests V2-1, V2-2, and V2-3. Vertical pressure/pore pressure curves, lowe curves. No excess pore pressures were measured in test V2-1.

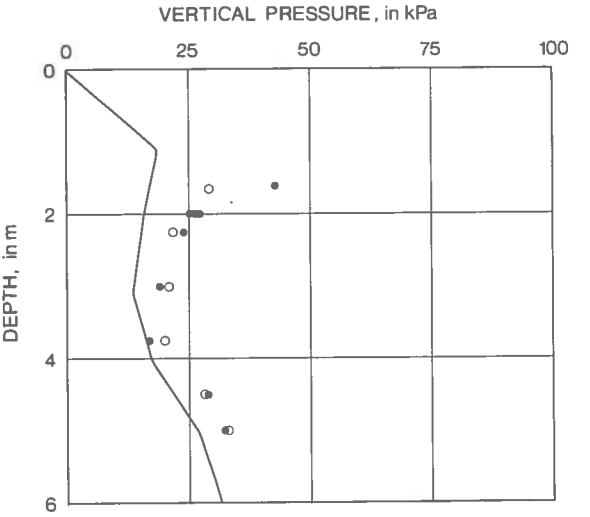

FIG. 116 Variation in preconsolidation pressure at Välen.

• σ_c' from CRS tests; o $\sigma_c' = \frac{\tau_{fu}}{0{,}45\ w_F}$

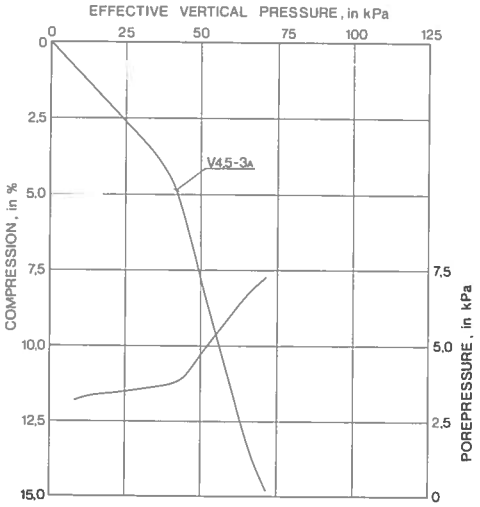

FIG. 113 Pressure/compression curves. Test V4,5-3A. Vertical pressure/pore pressure is also shown, lower curve.

reached, against 2,5 to 3 % for the clay from Bäckebol. However, if the sample is unloaded to *in situ* stresses and then reloaded, a much larger modulus and hence a smaller strain will be obtained for this clay too.

The pore pressure developed at the undrained bottom of the sample varies in the same way as in the clay from Bäckebol. A fairly constant value is obtained in the early stage of the test. Howev once the preconsolidation pressure is reached, the pore pressure starts to increase again.

The stress path followed during the test just described is given in FIG. 114. It is in agreement with the general model suggested in Section 3.2. However, hardly any increase in horizontal stres can be found in the overconsolidated region, and this would be th same as a Poisson's ratio (ν) equal to zero. It is also possible that the disturbance of the rim of the sample is large enough to disguise the real increase in horizontal stress, which probably is rather low, considering the low value of K'_o.

The preconsolidation pressure can be traced as a bend-off in the pressure/compression curve as well as in the pore pressure/pressu curve and in the stress path.

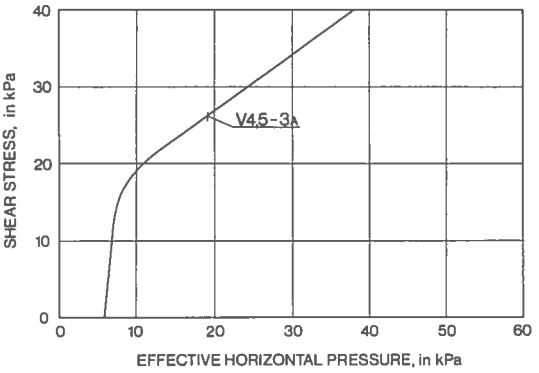

FIG. 114 Stress path. Test V4,5-3A.

The test just described, V4,5-3, was performed at a rate of deformation equal to 0,0024 mm/min.

The effect of the rate of deformation on this organic clay is illustrated in FIG. 115. The preconsolidation pressures are 25, 26, and 27 for rates of deformation of 0,0006, 0,0012, and 0,0024 mm/min, respectively. This seems to be comparable to the strain rate effects on the Bäckebol clay.

Oedometer curves obtained from CRS tests and LIN tests are given in Appendix B. The evaluated preconsolidation pressures are lis in Table 6 and given in FIG. 116 together with the effective ove burden pressure. The preconsolidation pressures are also given as values calculated from the equation

$$\sigma_c' = \tau_{fu}/0,45\ w_F \text{ (Hansbo, 1957).}$$

Extremely close agreement is found between the preconsolidation pressures evaluated from oedometer tests and the above empirical equation.

The pore pressures were measured in the field on two different occasions and a non-hydrostatic pore pressure distribution was observed on both both occasions. This resulted in the somewhat peculiar variation in effective overburden pressure with depth, see FIG. 116.

5.2.2 Discussion of test results

As was pointed out in Sub-section 4.2.4, an analysis of the sett ments was rendered difficult by the fact that the bellows hose was placed under the edge of the tank, and the settlement readin from the settlement tube were affected by a change in shape of t dry crust pedestal. The settlements will therefore not be considered here.

The stress distribution throughout the soil mass was discussed in Sub-section 4.2.5. What was said there is taken as valid als for the clay at Välen.

In FIG. 118 the build-up of pore pressures during the test is gi for two piezometers at depths of 2 m and 5 m. The piezometer at 2 m exhibits the same general behaviour as in the test at Bäckebol, i.e. a slight increase in pore pressure at the beginni of the test, followed by a steady state phase with a constant excess pore pressure. Once the preconsolidation pressure is reached, the pore pressure starts to increase again rather rapid The piezometer at 5 m shows a different trend, namely the pore pressure increases constantly throughout the test and no bend-of can be observed.

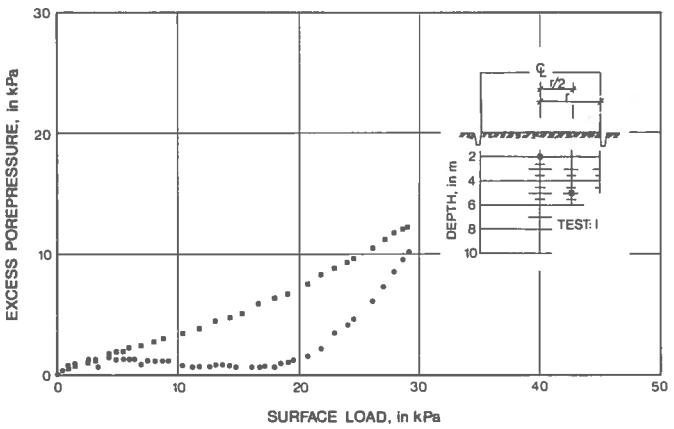

FIG. 118 Build-up of pore pressures at piezometers at depths of 2 and 5 m. Field loading test at Välen.

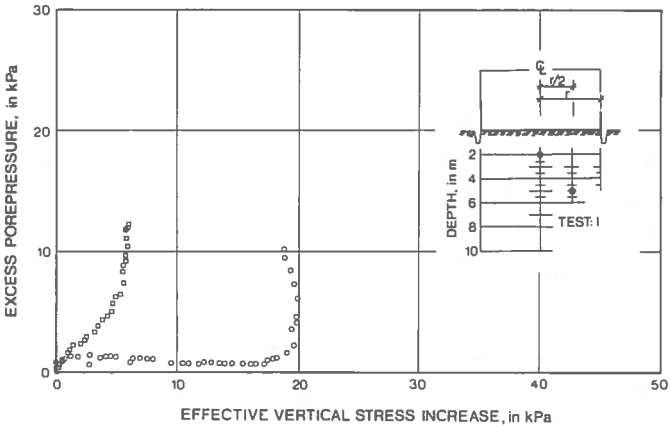

FIG. 119 Variations in excess pore pressure with effectiv vertical stresse increase. Piezometers at depths of 2 and 5 m. Field loading test at Välen.

In FIG. 119 the two pore pressure curves previously discussed a replotted, now in terms of effective vertical stress increase, the stress distribution being taken into account. It can be clearly seen that the effective stress for the 2-m curve does n increase once the preconsolidation pressure is reached, in spit of the increasing total pressure. All additional load is from then on carried by an increase in the pore pressure.

The development of effective stresses at the piezometer at a de of 5 m is quite different. The curve in FIG. 119 is very steep i.e. the largest part of the additional load is already from th beginning of the test carried by an increase in pore pressure. The increase in effective vertical stress is at the most 5 kPa. The clay is therefore believed to be normally consolidated at this level.

The excess pore pressure curves for all piezometers are listed Appendix B.

By using the bend-off ($\Delta\sigma'_k$) in the pore pressure curve as an in dication of the time when the preconsolidation pressure is reac the following values were obtained for the *in situ* preconsolida pressure:

Table 7. Preconsolidation pressures evaluated from field test.

Depth in m	$\sigma_c' = (\sigma_o' + \Delta\sigma_k')$, in kPa
1,5	> 50
2,0	{ 32 34
2,5	26
3,0	22
4,0	17
5,0	27

The test was discontinued at a surface load of 30 kPa, which was allowed to be sustained for 1 month. The pore pressure decreased somewhat at the piezometers at depths of 2, 2,5, and 3 m, but remained constant at the other piezometers.

The tank was then emptied in less than 5 hours, and the following interesting observations were made.

The piezometers at 4 and 5 m gave readings deviating less than 1,5 kPa from the initial value. In other words, the clay was unaffected by the test; the whole additional load had been taken as an increase in pore pressure, and when the load was removed, the pore pressure went down again. The piezometers at 2,0 m gave negative pore pressures of 10 to 15 kPa indicating that a compression had taken place and hence also an increase in effective stresses. The piezometers at 2,5 and 3 m gave readings of -5 and -3 kPa, respectively.

The piezometer at 5 m on the centre line did not show any change in pore pressure at any time. The filter was found to be clogged and the results are therefore not considered.

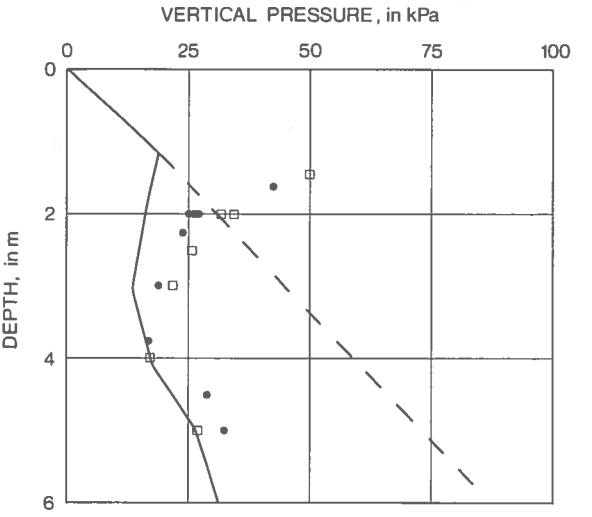

FIG. 120 Comparison of preconsolidation pressures determined from laboratory and field tests.
• σ'_c from CRS tests; □ σ'_c from field tests.

5.3 Comparison of results of laboratory and field tests

As previously pointed out, the determination of the preconsolidat pressure in the field involves, in addition to the load test, also a determination of the pore pressure distribution in the soi profile. This was done twice for the site at Välen and both thes measurements gave relatively high pore pressures, which correspor to the effective overburden pressures shown in FIG. 120.

FIG. 120 gives the preconsolidation pressures determined in the laboratory as well as in the field. The agreement is found to be very good also for this organic clay where the preconsolidation pressures are very low.

6 FULL-SCALE TEST AT KRISTIANSTAD

6.1 Test field

The soil in the test area at Kristianstad is a varved clay with numerous sand and silt layers (very few layers of clay are thicke than 20 mm).

Because of the silt and sand layers, which could be assumed to act as good horizontal drains, the preconsolidation pressure coul hardly be found in a field test by studying the change in pore pressure during a constant rate of loading test, as was done for Bäckebol and Välen. However, if the drainage were efficient, the consolidation settlement would develop fairly quickly, and the preconsolidation pressure could therefore be found from the load/settlement curve.

6.1.1 Geology

The test area is situated in the northern part of the city of Kristianstad, 3 m above the sea level. The uppermost 2,5 m consists of a dry crust followed by a varved clay down to approximat 7 metres, where a clayey silt is found, which in turn rests upon a cohesionless material at 8 to 9 m.

FIG. 121 shows a photograph of a section through the clay. The different layers are clearly visible.

6.1.2 Geotechnical properties

Water content

The water contents are given in FIG. 122. The cone liquid limit and the plasticity limit were determined on a mixture of clay layers trimmed from a sample tube, in order to measure the properties of the clay only. This procedure was followed also when determining the natural water content.

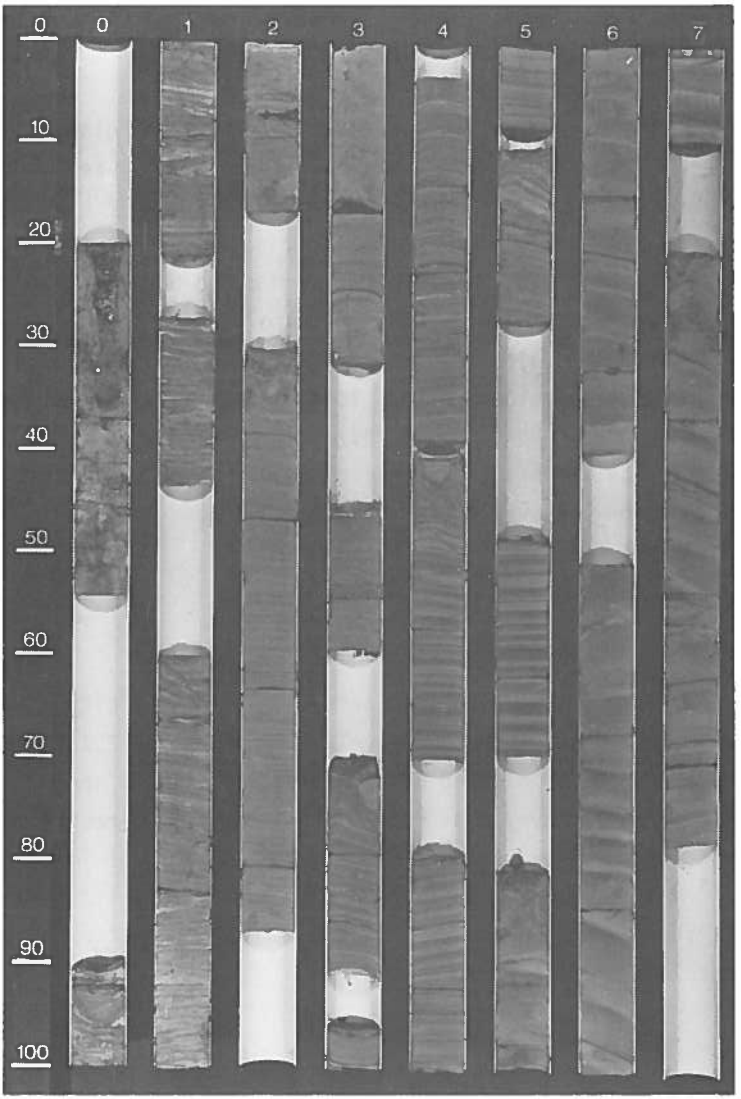

FIG. 121 Photograph showing the stratification of the cla
from Kristianstad. (Torstensson, 1975)

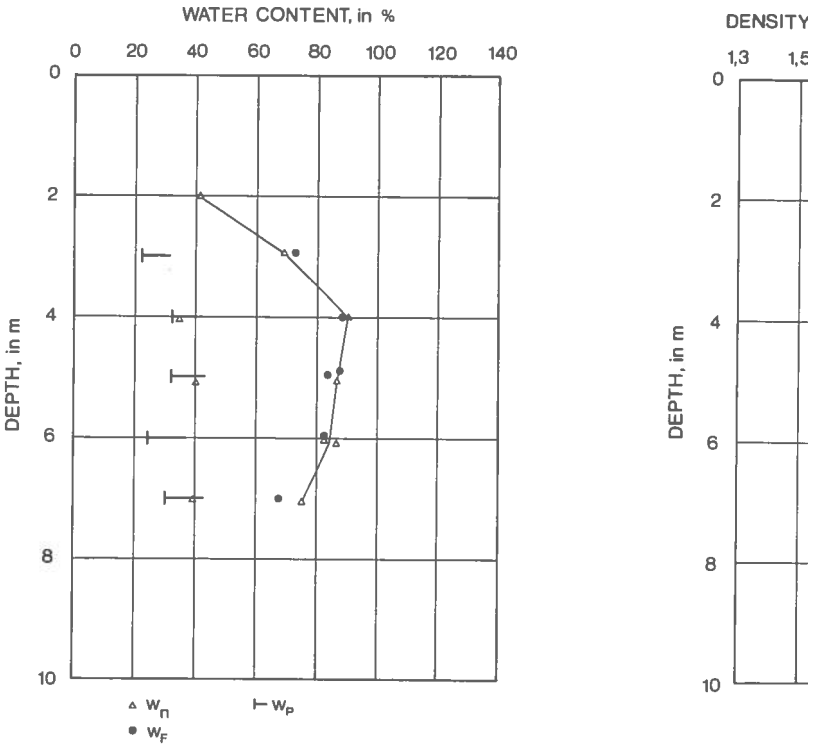

FIG. 122 Water contents for the soil profile in the test area at Kristianstad.

The natural water content in the clay layers is 80 to 90 % and the silt layers 30 to 40 %. The liquid limit, which was determ only for the clay layers, is of the same order of magnitude as the natural water content. The plasticity index for the clay layers is around 50 %.

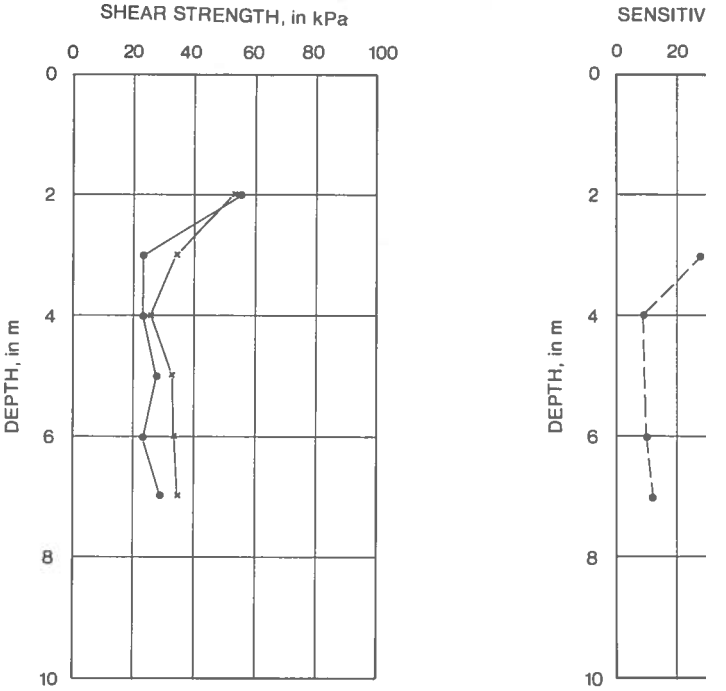

FIG. 123 Variation in shear strength of the soil at Kristianstad. • fall-cone test; × vane boring.

Shear strength

The fall-cone test gives a shear strength of 20 to 25 kPa for the profile, while the vane boring test gives values closer to 30 kPa see FIG. 123. The sensitivity is around 10.

6.1.3 Oedometer tests

A varved clay, like the one just described, is difficult to handle in the laboratory as no negative pore pressures in the sand and silt layers hold the sample together. In order to get good oedometer samples, the following technique was used. The 50-mm oedometer ring described in Section 3.1 was used for the CRS tests. The teflon ring was lubricated with silicone grease and placed on top of the sample extruder. A sample was slowly pushed into the ring so far that 4 to 5 mm of clay was visible

outside the other side of the ring. Both sides were then trimme off with a wire. The sample was rejected if the cut on both sides of the sample was not made through a clay layer. This procedure gave good-quality samples.

Typical results of a CRS test are shown in FIG. 124. The effect of strain rate is clearly illustrated for this test, where the different rates of deformation were used. As a comparison, data are also given on a LIN test where the daily increments all were 20 kPa. The probable interval of the preconsolidation pressure is rather large, see FIG. 125, and the previously suggested construction was used for determining the preconsolidation pressure from the CRS tests. The following values were obtained:

Table 8. Preconsolidation pressures evaluated from CRS tests

Depth in m	σ'_c	rate of deformation
3	81	0,0006 mm/min
	89	0,0012 "
	83	0,0024 "
	90	0,0040 "
4	102	0,0024 "
	105	0,0024 "
	107	0,0024 "
5	110	0,0024 "
	111	0,0024 "
6	133	0,0024 "

The scatter in the results is somewhat larger than at Bäckebol and Välen. This is attributed to the influence of the dry crust and presence of root threads, etc. However, the effect of strai rate seems to be of the same order as for the other two clays studied.

The oedometer curves are given in Appendix C.

It is also interesting to note that the stress path followed by the clay during an oedometer test, see FIG. 126 coincides to a certain degree with the general model suggested in Section 3.2.

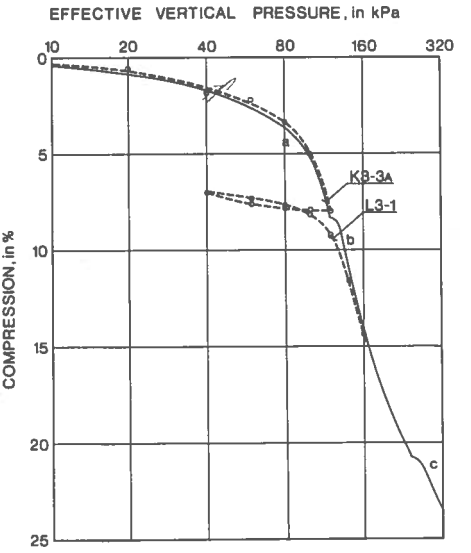

Legend

Test	Depth m	Rate of c mm/min
K3-3A	3	a) 0,0(
		b) 0,0(
		c) 0,0(
L3-1	3	increme

FIG. 124 Pressure/compression curves. Tests K3-3A and L3-1, log scale.

$M_0 = \frac{20}{0,04} = 2\,MPa$

$\approx 3a5\ 6$

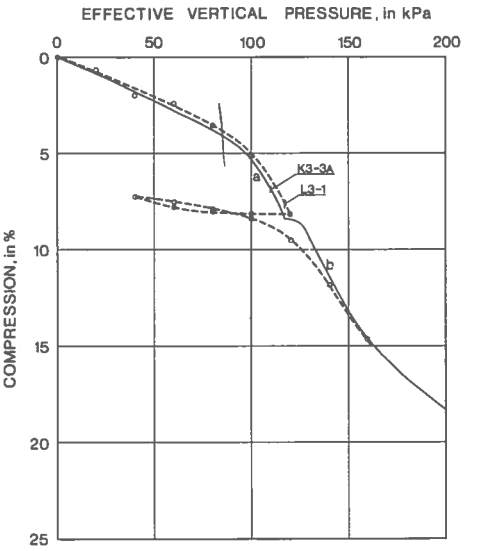

Legend

Test	Depth m	Rate of c mm/min
K3-3A	3	a) 0,0(
		b) 0,0(
L3-1	3	increme

FIG. 125 Pressure/compression curves. Tests K3-3A and L3-1, arithmetic scale.

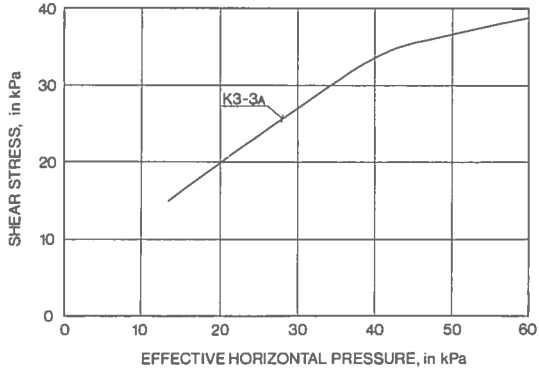

FIG. 126 Stress path. Test K3-3A.

The critical shear stress is not so distinct, probably owing to the presence of silt layers. On the other hand, the pressure/compression curve is very arched and then it is logical that the stress path has the same shape.

6.2 Loading arrangements and results

6.2.1 Loading procedure and instrumentation

The load test was originally made in order to investigate whether the foundation of a two-storey building could be constructed as a raft foundation or if piling was necessary. (In co-operation with AB Jacobson & Widmark)

The test fill was constructed in five steps. First the top soil was scraped off (-5 kPa) and a layer of sand (15 kPa) was placed and compacted so as to provide the future foundation level. One month later the next layer was applied (15 kPa) corresponding to the future load. At this stage the fill measured 23 x 91 m^2. Seven months later the loading was resumed in three increments, 16, 16, and 13 kPa respectively, each with a duration of three weeks, now over an area of 23 x 23 m^2.

The subsoil was instrumented in one section with four bellows hoses of the type described in Section 4.2.3. The pore pressure was measured with one piezometer at a depth of 3,5 m.

In addition, several piezometers and settlement points were installed for measurement of the settlements over the whole area Only the results from the bellows hoses and the piezometer under the centre of the fill will be discussed in this thesis.

6.2.2 Discussion of test results

Stress distribution

As described in Section 6.1, the soil at Kristianstad consists o a 2,5 m thick dry crust overlaying 4 to 5 m of clay. The dry cr has a much higher E-modulus than the clay, and this causes a lar stress distribution with depth. On the other hand, the limited depth, 8 m, as compared with the width of the fill, 23 m, causes a stress concentration towards the centre. A finite element analysis using the theory of elasticity showed that a stress concentration is obtained along the centre.line, the stress ther being equal to 1,1 times the applied surface load, (Wiberg, 1975

Once the preconsolidation pressure and hence the critical shear stress is exceeded, the stress distribution might change somewhat. This is not taken into consideration.

Pore pressures

The pore pressure build-up was followed with one piezometer at a depth of 3,5 m. The readings taken during the fifth increment a given in FIG. 127. It can be seen that once the construction wo is completed, the pore pressure decreases rather rapidly, owing the drainage through the silt layers. The two notches in the cu at A and B represent the breaks in the construction work at brea fast and lunchtime.

No significant differences were found in the build-up of pore pressures during increments giving vertical stresses below or above the preconsolidation pressure.

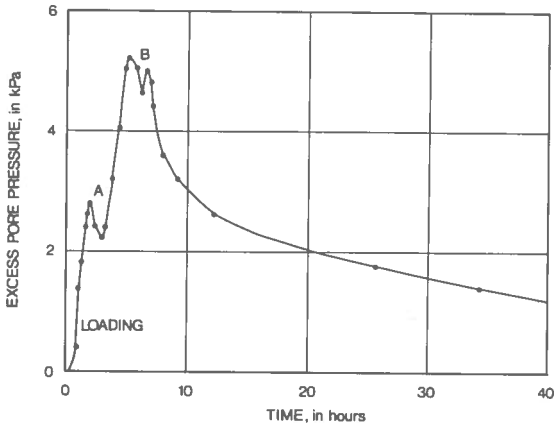

FIG. 127 Pore pressures at 3,5-m depth during load increment No. 5 at Kristianstad.

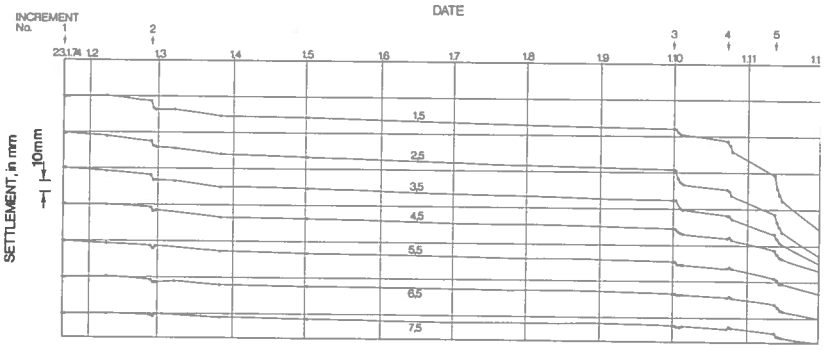

FIG. 128 Settlement record for bellows hose G1. Figures in graph indicate depths of measuring points below ground surface.

Settlements

The distribution of settlements with depth was measured by means bellows hoses. Similar results were obtained, and typical result are given in FIG. 128. The accuracy was about ± 1 mm.

To obtain a load/settlement curve, the following procedure was used. The settlement after three weeks was taken as representing the increment. The settlement at each measuring point was then plotted against surface load as illustrated in FIG. 129.

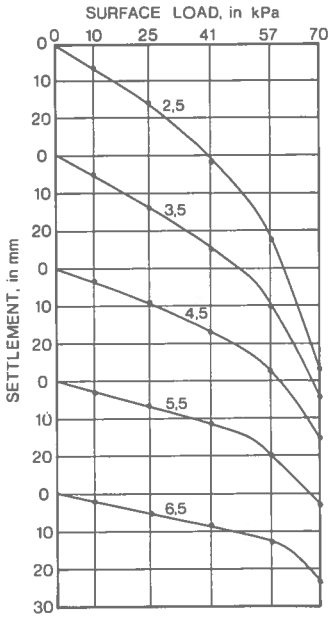

FIG. 129 Load/settlement curves. Bellows hose G1. Figures in graph indicate depths of measuring points below ground surface.

The deformation of one metre of clay was obtained by taking the settlement at one measuring point and subtracting the settlement at the measuring point just below. Thus the compression of the clay between these points was obtained. This method is applicab if the settlements are large in comparison with the accuracy of the measuring system.

The results in FIG. 129 are replotted in FIG. 130 which represen the deformation versus the surface load. The deformation curves tained from another bellows hose are also shown.

The settlement in each layer approximately follows two straight lines as indicated in the figure. The preconsolidation pressure cannot be determined as a unique value but the load increment where it is exceeded can be clearly distinguished.

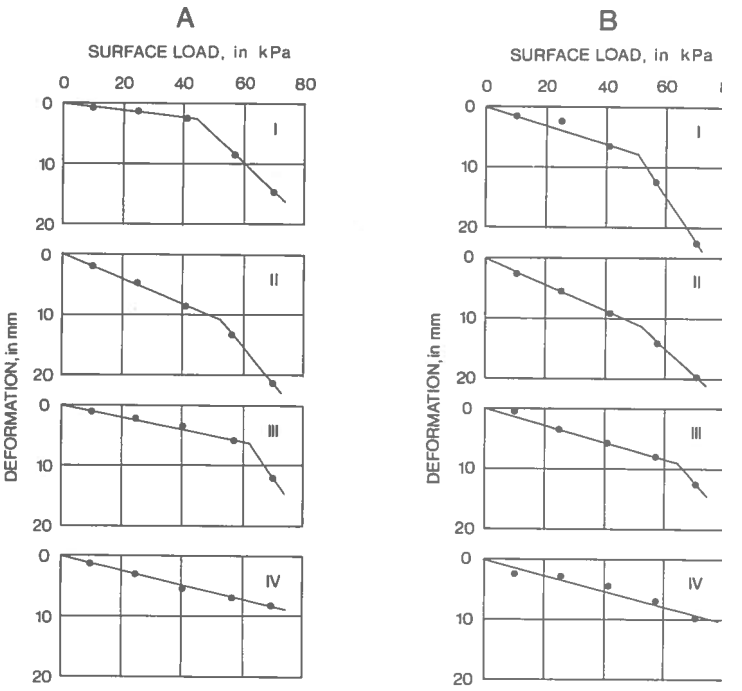

Legend

Depth of clay layer:

I: 2,5 - 3,5 m III: 4,5 - 5,5 m
II: 3,5 - 4,5 m IV: 5,5 - 6,5 m

FIG. 130 Data from FIG. 129 replotted (A) showing deformation of 1 m thick clay-layers.
A bellows hose G1
B bellows hose C2

The following values are obtained, and will be used in the comparison in Section 6.3.

Table 9. $(\sigma_c'-\sigma_0')$ for different layers *in situ*

Depth of layer	Surface load at the time when the preconsolidation pressure is exceeded	
	G1	C2
2,5 to 3,5 m	41 to 57 kPa	41 to 57 kPa
3,5 to 4,5 m	41 to 57 "	41 to 57 "
4,5 to 5,5 m	57 to 70 "	57 to 70 "
5,5 to 6,5 m	> 70 "	>70 (57-70)"

6.3 Comparison of results of laboratory and field tests.

In FIG. 131 the probable intervals of the preconsolidation pressure *in situ* are represented by horizontal full lines together with the values determined in the laboratory from CRS test. The two sets of values agree well. Only for the 4-m level, the laboratory tests result in slightly higher values than those determined *in situ*. The equation suggested by Hansbo (1957) gives values of the preconsolidation pressure that are too low. The reason could be that the clay is somewhat disturbe as the shear strength determined by the fall-cone test only are about 80 % of those determined by the field vane. On the other hand, the higher values of the field vane strength can be due to the silt layers.

It is interesting to note that the oedometer modulus evaluated from the reloading curve in the oedometer is of the same order as that which is obtained from the field test, while the oedometer modulus from the first loading curve is far too small.

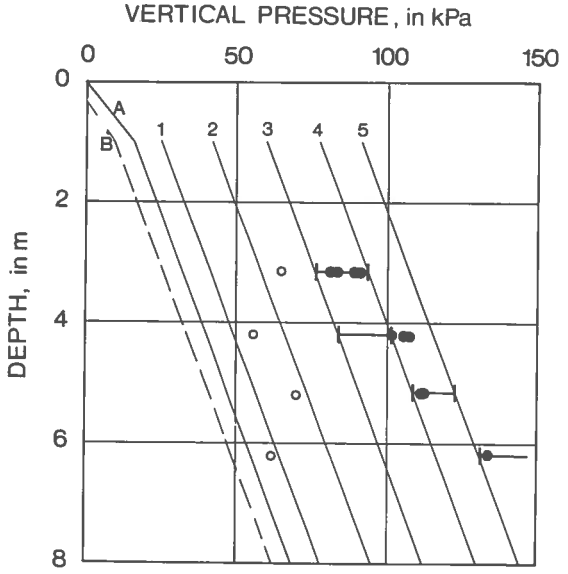

Legend

Effective vertical stress	surface load in kPa
before load test	0
after removal of top soil	-5
1st load increment	10
2st "	25
3rd "	41
4th "	57
5th "	70

FIG. 131 Preconsolidation pressurs determined from laboratory and field tests.

● σ_c' from CRS tests

○ $\sigma_c' = \frac{\tau_{fu}}{0{,}45\ w_F}$

⊢⊣ σ_c' from field loading tests

7 CONCLUSIONS

7.1 General

The experimental part of the present investigation consisted in a detailed study of the oedometer test. Several different loadi routines have been compared. The importance of time effects and shear stresses when determining the preconsolidation pressure wa thoroughly investigated.

Full-scale loading tests were made in order to compare the stress/strain characteristics of the clay *in situ* with those found from laboratory tests.

Three different soft, high-plastic clays with a clay content of 50 to 70 % were studied; one with an organic content of 0,5 to 1 the other with an organic content of 5 to 6 %, and the third bei a varved non-organic clay.

The conclusions that can be drawn from the investigations descri in Chapters 3 to 6 are summarized in the following Sections.

7.2 Oedometer tests

Incremental and continuous loading routines were used. The results obtained by using the different loading routines were compared, and showed that:

- The preconsolidation pressure is time-dependent: the lower th rate of strain, or the longer the duration of each increment, the lower the preconsolidation pressure, see FIG. 59.

- The oedometer modulus increases with increasing rate of strai at loads smaller than the preconsolidation pressure, but is basically independent of strain rate at loads larger than the preconsolidation pressure, see FIG. 50.

- The coefficient of consolidation was found to be independent strain rate at stresses higher than the preconsolidation pres while it was found to increase somewhat with increasing rate strain at stresses lower than the preconsolidation presssure.

- The frictional loss in the oedometer can be rather high (25 to 30 % of the applied load), but can, at least in CRS tests, be reduced to a value of 5 to 8 % if silicon greas used as a lubricant, see FIGs. 36 and 37.

- A constant rate of strain test can be completed in 24 hours, and gives a pressure/compression curve equivalent to that obtained from a standard test. Moreover, the constant rate of strain test can be readily automated, and gives a pressure/compression curve and a pressure/pore pressure curve which are well defined.

7.3 Shear stresses in an oedometer test

An oedometer was constructed which enabled the horizontal stress to be measured. Tests were made on an artificially sedimented clay as well as on clay samples from the different test areas. T results showed that:

- The shear stresses increased rapidly at the beginning of the test up to a critical shear stress, which coincided with the shear stress obtaining at the preconsolidation pressure in the oedometer tes. The critical shear stress is time-dependent, just as the preconsolidation pressure; the lower the strain rate, the lower the critical shear stress, which probably has a lower limit value, see FIG. 68.

- A general stress path model is suggested, and found to be val for the types of clay tested, see FIG. 67.

- The critical shear stress was dependent on the magnitude of t isotropic consolidation pressure, see FIG. 69, in that it decreased with increasing isotropic consolidation pressure, and was equal to zero when the isotropic consolidation pressure reached the horizontal preconsolidation pressure.

- The clay microstructure was discussed, and the generally accepted model, see FIG. 76, can be used to explain the inter action between preconsolidation pressure, shear stresses, and developed pore pressures.

7.4 Determination of preconsolidation pressure

7.4.1 Laboratory tests

A method is suggested for determining the preconsolidation pressu from constant rate of strain tests, see FIG. 74. This method wa found to be objective, and good results were obtained for the artificially sedimented clay as well as for naturally sedimented clays. The preconsolidation pressure determined by means of thi method was little affected by strain rates lower than or equal t 0,0024 mm/min.

7.4.2 Full-scale tests

Two full-scale tests were made on the non-organic clay at Bäckebo and one on the organic clay at Välen. They were carried out as constant rate of loading tests by using a tank, see FIG. 88. The results showed that:

- The excess pore pressures were small during the early stage of the test, but once the preconsolidation pressure was reac a rapid increase was observed, see FIG. 96. This breaking point in the excess pore pressure curve was interpreted as i dicating the preconsolidation pressure.

- If the effective vertical stress increase is plotted against the excess pore pressure, it is found that once the preconso· lidation pressure is reached, no further increase in effecti vertical stresses takes place, see FIG. 101.

- Two different rates of strain were used at Bäckebol (0,8 and 1,3 kPa/day) but no significant time dependence was found, except that higher pore pressures were observed during the more rapid test.

- The varved clay at Kristianstad was loaded in increments, an the settlements at different depths were recorded. The *in s* preconsolidation pressure was interpreted from the compressi of different layers.

7.6 Practical application

From comparisons of laboratory and field results it can be concluded that a very accurate value of the preconsolidation pressu is obtained by applying the suggested construction to the results of a CRS test made at a rate of deformation of 0,0024 mm/m or less. This means that:

- The preconsolidation pressure can be accurately determined i the laboratory by using a constant rate of strain test requiring no more than 24 hours.

- The *in situ* preconsolidation pressure in a homogeneous clay can be determined by taking readings of pore pressures in a constant rate of loading test.

- For a varved clay consisting of closely spaced high-permeabl layers, the preconsolidation pressure can be found by studyi the compression of different layers in a test where the load is applied in increments. The increments should be about on third of the difference between the estimated preconsolidati pressure and the vertical *in situ* stress.

REFERENCES

d'Appolonia, D, Lambe, W & Paulos, H, 1971, Evaluation of Pore Pressures beneath an Embankment. (J.Soil Mech. a. Found. Div., ASCE.) VOL. 97, No. SM6, p.881-897. Ann Arbor, Michigan.

Belotti, R, Formigoni, G & Jamiolkowski, M, B, 1975, Remarks on the Effect of Overconsolidation on the Coefficient of Earth Pressure at Rest. (Proc.Conf.Soil Mech. a. Found. Engng.) VOL.1, p.17-25. Istanbul.

Bergdahl, U & Broms, B, 1967, New Methods of Measuring in situ Settlements. (Sw. Geot. Inst.) Repr. Prel. Reports No.25.Stockho

Berre, T, 1972, Sammenheng mellom tid, deformasjoner og spenning- er for normalkonsoliderte marine leirer. (Proc.Nordic Conf. on Soil Mech.) p.23-26. Trondheim.

Berre, T & Bjerrum, L, 1973, Shear Strength of Normally Consolidated Clays. (Proc. 8th Int. Conf. Soil Mech.a. Found. Engng.) VOL.1, p.39-49. Moscow.

Bjerrum, L, 1967, Seventh Rankine Lecture: Engineering Geology of Norwegian Normally-Consolidated Marine Clays as Related to Settlements of Buildings. (Géotechnique.) VOL.17, No. 2, p.81-11 London.

Bjerrum, L, 1972, Embankments on Soft Ground. (Proc. ASCE, Spec. Conf.) VOL.1, p.885-902. Purdue, Indiana.

Bjerrum, L, 1972, The Effect of Rate of Loading on the p_c-value Observed in Consolidation Tests of Soft Clays. Written contribution to the Discussion in Session III. (Proc. ASCE, Spec. Conf. VOL.3, p.167-168. Purdue, Indiana.

Bjerrum, L, 1973, Problems of Soil Mechanics and Construction on Soft Clays and Structurally Unstable Soils. (Collapsible, Expansive and Others). (Proc.8th Int.Conf.Soil Mech.a.Found.Engng. VOL.3, p.111-159. Moscow.

Brooker, E, W & Ireland, H, O, 1965, Earth Pressure at Rest Related to Stress History. (Can.Geot.J.) VOL.2, No.1. Ottawa.

Burmister, D, M, 1951, The Application of Controlled Test Methoc in Consolidation Testing: Symp.on Consolidation Testing of Soils ASTM. (Spec. Tech. Publ.) No. 126, p. 83. Philadelphia, Pennsylvania.

Casagrande, A, 1936, The Determination of the Preconsolidation Load and its Practical Significance. (Proc.1st Int. Conf. Soil Mech. a. Found. Engng.) VOL.3, p.60. Cambridge.

Crawford, C, B, 1964, Interpretation of the Consolidation Test. (J.Soil Mech. a. Found.Div.,ASCE.) VOL.90, No. SM5, p.87-109. Ann Arbor, Michigan.

Crawford, C, B, 1965, The Resistance of Soil Structure to Consolidation. (Can.Geot.J.) VOL.2, No.2, p.90-97. Ottawa.

Dascal, O & Tournier,J-P, 1975, Embankments on Soft and Sensitiv Clay Foundation. (J.Geot.Div.,ASCE.)VOL.101,No.GT3,p.297-314. New York.

Frimann-Claussen,C-J, 1970, Resultater av et belastningsforsøk på Mastemyr i Oslo. (Nor.Geot.Inst.) Publ.84,p.29-40. Oslo.

Hamilton, J & Crawford,C, B, 1959, Improved Determination of Pre consolidation Pressure of a Sensitive Clay. ASTM. (Spec. Tech. Publ.) No. 254, p.254-271. Philadelphia, Pennsylvania.

Hansbo, S, 1957, A New Approach to the Determination of the Shea Strength of Clay by the Fall-cone Test. (Sw.Geot.Inst.) Proc. No. 14. Stockholm.

Hansbo, S, 1960, Consolidation of Clay, with Special Reference t Influence of Vertical Sand Drains. (Sw.Geot.Inst.) Proc. No. 18. Stockholm.

Hansbo, S, 1966, Kompendium i geoteknik, allmän kurs. (Inst. f. geot.m.grundläggn., CTH.) Göteborg.

Hansbo, S, 1975, Jordmateriallära. (AWE/Gebers, AB Jacobson & Widmark.) Stockholm.

Harr, M, 1966, Foundations of Theoretical Soil Mechanics. (McGra Hill.) New York.

Heiberg, S & Wissa, A, E, 1969, One-Dimensional Consolidation Test. (MIT Dept. of Civ. Engng. Res. 69-9,Soils Publ.) No. 229. Cambridge, Massachussets.

Höeg,K, Andersland,O & Rolfsen,E, 1969, Undrained Behaviour of Quick Clay under Load Test at Asrum. (Géotechnique.) VOL.19, No.1, p.101-115. London.

Jamiolkowski,M & Marchetti,S, 1969, The Determination of Pre-consolidation Load from a Controlled Gradient Consolidometer Device. (Proc. 7th Int. Conf. Soil Mech. a. Found.Engng.) VOL.3, p.523. Mexico City.

Jamiolkowski,M & Marchetti,S, 1971, Alcuni risultati sperimental ottenuti mediante un apparecchio di consolidazione edometrica a gradiente idraulico controllato. (Rivista Italiana di Geotechnic VOL.45, No.4. Napoli.

Janbu,N, 1963, Soil Compressibility as Determined by Oedometer and Triaxial Tests. (Proc.3rd Europ.Conf. Soil Mech. a. Found. Engng.) VOL.1, p. 19-25. Wiesbaden.

Janbu,N, 1965, Consolidation of Clay Layers Based on Non-Linear Stress-Strain. (Proc.6th Int.Conf.Soil Mech. a. Found.Engng.) VOL.2, p.83-87. Montreal.

Janbu,N, 1969, The Resistance Concept Applied to Deformations of Soils. (Proc.7th Int.Conf.Soil Mech. a. Found. Engng.) VOL.1, p. 191-196. Mexico City.

Janbu,N, 1973,NGF Foredraget 1973: Shear Strength and Stability of Soils. (Nor. Geot.Inst. & Nor.Geot.Soc.) Oslo

Kallstenius,T, 1963, Studies on Clay Samples Taken with Standar Piston Sampler. (Sw.Geot.Inst.) Proc. No. 21. Stockholm.

Karlsson,R & Wiberg,L, 1967, Ratio c/p' in Relation to Liquid Limit and Plasticity Index, with Special Reference to Swedish Clays.(Proc. 4th Europ. Conf. Soil Mech.a.Found. Engng.) VOL.I, p.43-47. Oslo.

Larsson,R, 1975*a*, Spänningar och deformationer i jord vid på- o avlastning med förhindrad sidodeformation (ödometerfallet). (Inst.f.geot.m.grunläggn.,CTH.) Göteborg.

Larsson,R, 1975*b*, Measurement and Calculation of Horizontal Stresses in Clay and their Importance for Strength- and Deformation Parameters. (Geot.Dept., Chalmers Univ. of Technology.) Göteborg.

Larsson,R, 1975*c*, The Effect of Rate of Loading on the Shear Strength Parameters of a High-Plastic Marine Clay. (Geot.Dept., Chalmers Univ. of Technology.) Göteborg.

Leonards,G,A & Ramiah,B,K, 1959, Time Effects in the Consolidati of Clay. ASTM.(Spec.Tech. Publ.) No.254, p. 116-130. Philadelphi Pennsylvania.

Leonards,G,A & Girault,P, 1961, A Study of the One Dimensional Consolidation Test. (Proc.5th Int.Conf.Soil Mech.a.Found.Engng.) VOL.1, p.213. Paris.

Leonards,G,A, 1962, Engineering Properties of Soils, Chapter 2 o Foundation Engineering. (McGraw-Hill.) New York.

Leonards,G,A & Altschaeffl,A,G, 1964, Compressibility of Clay. (J.Soil Mech.a. Found.Div.,ASCE.) VOL.90, No. SM5, p.133-155. Ann Arbor, Michigan.

Leonards,G,A, 1972, Written Contribution to the Discussion in Session III.(Proc. ASCE, Spec.Conf.) VOL.3,p.169-173, Purdue,Ind

Lowe III,J & Obrician,V, 1969, Controlled Gradient Consolidation Test. (J.Soil Mech. a. Found.Div., ASCE.)VOL.95, No. SM1,p.77-97 Ann Arbor, Michigan.

Lowe III,J, 1974, New Concepts in Consolidation and Settlement Analysis. (J.Geot.Engng.Div.,ASCE.) VOL.100, GT6, p. 571-613. Ann Arbor, Michigan.

Massarsch,R, 1975, New Method for Measurement of Lateral Earth Pressure in Cohesive Soils. (Can.Geot.J.) VOL.12, No.1.Ottawa.

Pusch,R, 1970, Clay Microstructure, Document D8:1970. (Statens institut för byggnadsforskning.) Stockholm.

Pusch,R, 1973, Influence of Organic Matter on the Geotechnical Properties of Clays, Document D11:1973. (Statens institut för byggnadsforskning.) Stockholm.

Roscoe,K & Schofield,A, 1963, Mechanical Behaviour of an Idealized "Wet-Clay". (Proc.3rd Europ.Conf.Soil Mech.a.Found.Engng.) VOL.1, p.47-54. Wiesbaden.

Schmertmann,J.M. 1953, Estimating the True Consolidation Behaviour of Clay from Laboratory Test Results. (J.Soil Mech.a. Found.Div., ASCE.) VOL.79, Separate No.311,p.26. New York.

Schmidt,B, 1967, Lateral Stresses in Uniaxial Strain. (Dan.Geot Inst.) Bull.No. 23. Copenhagen.

Schofield,A & Wroth,P, 1968, Critical State Soil Mechanics. (McGraw-Hill.) London.

Simons,N,E & Som,N,N,1969, The Influence of Lateral Stresses on the Stress Deformation Characteristics of London Clay.(Proc.7th Int.Conf.Soil Mech.a.Found.Engng.) VOL.1,p.369-377.Mexico City.

Skempton,A,W, 1954, Discussion of the Structure of Inorganic Soi (J.Soil Mech.a.Found.Div., ASCE.) VOL.80, Separate, No.478, p. 19-22. New York.

Smith,R,E & Wahls,H,E, 1969, Consolidation Under Constant Rate o Strain. (J.Soil Mech.a.Found.Div.,ASCE.) VOL.95, No. SM2, p. 519-539. Ann Arbor, Michigan.

Som,N,N, 1970, Lateral Stresses During One Dimensional Consolida tion of an Over-Consolidated Clay. (Proc.2nd S.E.Asian Conf.Soil Mech.) p.295-307. Singapore.

Statens Järnvägar, 1922, Geotekniska kommissionen, 1914-1922, Slutbetänkande. (Statens Järnvägar.) Geotekniska Meddelanden, Nr 2. Stockholm.

Sällfors,G, 1973*a*, Utvärdering av förkonsolideringstryck hos ler Redovisning av enkätsvar. (Inst.f.geot.m.grundläggn., CTH.) Göte borg.

Sällfors,G, 1973*b*, Konsolideringssättning i lera. Delrapport 1. (Inst.f.geot.m.grundläggn., CTH.) Göteborg.

Sällfors,G, 1974*a*, Konsolideringssättning i lera. Delrapport 2. (Inst.f.geot.m.grundläggn., CTH.) Göteborg.

Sällfors,G, 1974*b*, The Nature of the Preconsolidation Pressure i Soft, High-Plastic Clays.(Proc.Conf.Settlement of Structures.) p.696-698. Cambridge.

Sällfors,G, 1974*c*, Datorbearbetning av ödometer- och triaxial- försök. (Inst.f.geot.m.grundläggn., CTH.) Göteborg.

Sällfors,G, 1975*a*, New Oedometer Routines-Advantages in Engineeri Practice. (Proc.Conf.Soil Mech.a.Found.Engng.)VOL.1,p.129-136. Istanbul.

Sällfors,G, 1975*b*, The Preconsolidation Pressure of a High Plasti Clay – A Comparison between Field and Laboratory Testing. (Proc. Nordic Conf.Soil Mech.)p.143-154. Copenhagen.

Tavenas,F, Chapeau,C, LaRochelle,P & Roy,M, 1974, Immediate Settlements of Three Test Embankments on Champlain Clay. (Can. Geot.J.) VOL.11, No.1,p.109-141. Ottawa.

Taylor,D,W, 1942, Research on the Consolidation of Clays. (Mass. Inst.Techn.Publ.Dept.Civ.a.Sanit.Engng.) Ser.82. Boston.

Terzaghi,K & Frölich,O, 1936, Theorie der Setzung von Tonschicht (F.Deutike.) Wien.

Terzaghi,K, 1941, Undisturbed Clay Samples and Undisturbed Clays (J.Boston Soc. Civ. Engng.) VOL.28. Boston.

Terzaghi,K, 1943, Theoretical Soil Mechanics. (John Wiley & Sons Inc.) New York.

Torstensson,B-A, 1973, Kohesionspålar i lös lera. En fältstudie. Thesis. Rapport R38:1973. (Statens inst.f.byggnadsforskn.) Stockholm.

Wager,O, 1972, Bälgsättningsmätare för mätning av vertikal-rörelser i jord. (Proc.Nordic Conf.on Soil Mech.)p.95-98. Trondheim.

Virgin,Å, 1918, Markytans höjdförändringar hos lösa jordlager. (Tekn.Tidskr., VoV.) VOL.48, H.6. Stockholm.

Wissa,A, 1969, A New One-Dimensional Consolidation Test. (Proc. 8th Int.Conf.Soil Mech.a.Found.Engng.) VOL.3, p.524. Mexico City

Personal Communication:
Bengtsson, P-E, 1975
Leonards, G, A, 1975
Torstensson, B-A, 1975
Wiberg, N-E, 1975

CONTENTS

RESULTS FROM TEST FIELD AT BÄCKEBOL

Oedometer tests, incremental loading

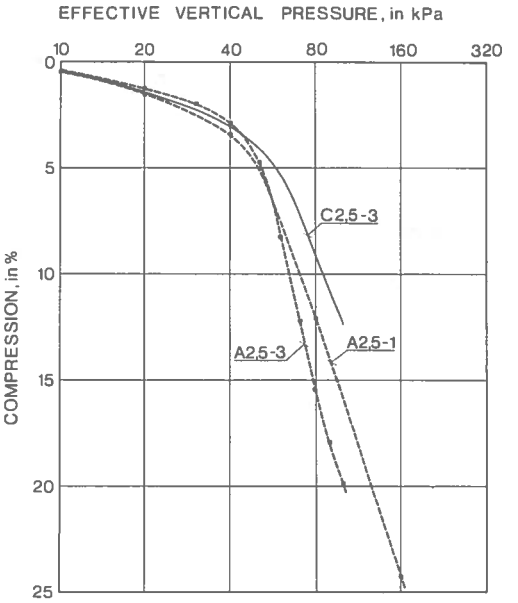

Legend
Bäckebol, 2,5 m

Test	Type of te
A2,5-1	STD
A2,5-3	LIN
C2,5-3	CRS 0,0024 mm/

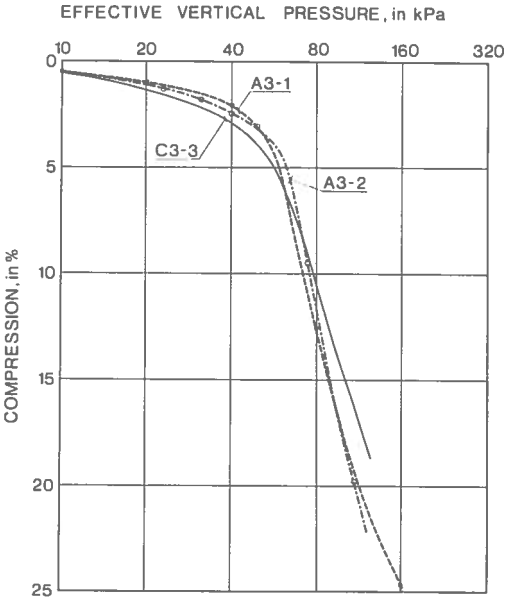

Legend
Bäckebol, 3 m

Test	Type of tes
A3-1	STD
A3-2	NGI
C3-3	CRS 0,0024 mm/m

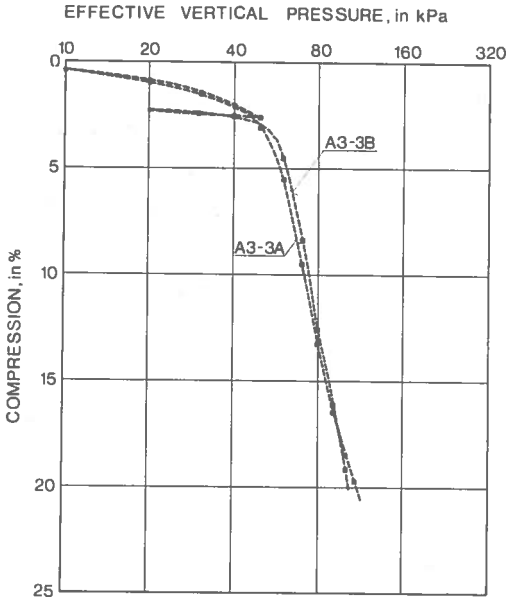

Legend
Bäckebol, 3 m

Test	Type of tes
A3-3A	LIN
A3-3B	LIN

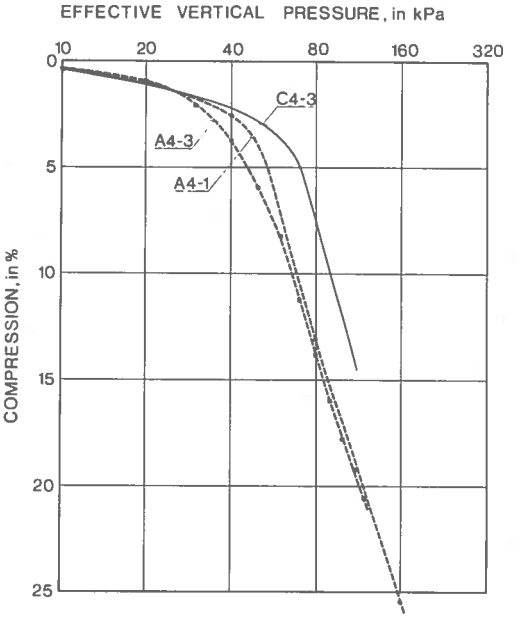

Legend
Bäckebol, 4 m

Test	Type of tes
A4-1	STD
A4-3	LIN
C4-3	CRS 0,0024 mm/m

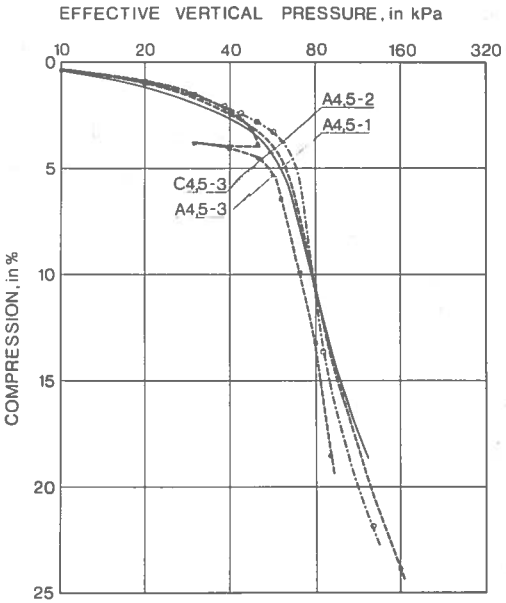

Legend
Bäckebol, 4,5 m

Test	Type of tes
A4,5-1	STD
A4,5-2	NGI
A4,5-3	LIN
C4,5-3	CRS 0,0024 mm/m

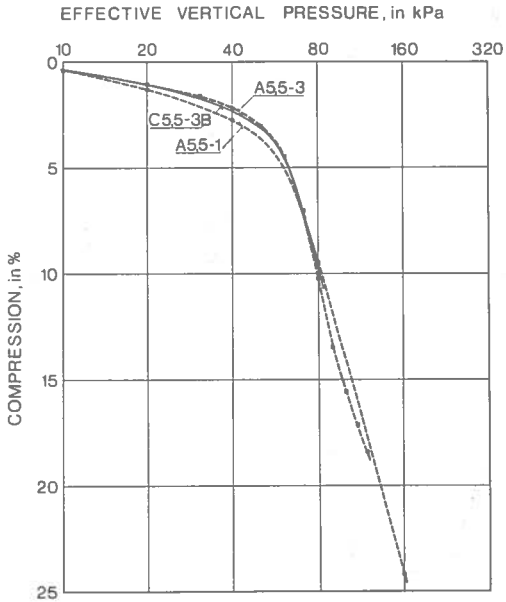

Legend
Bäckebol, 5,5 m

Test	Type of te
A5,5-1	STD
A5,5-3	LIN
C5,5-3B	CRS 0,0024 mm/

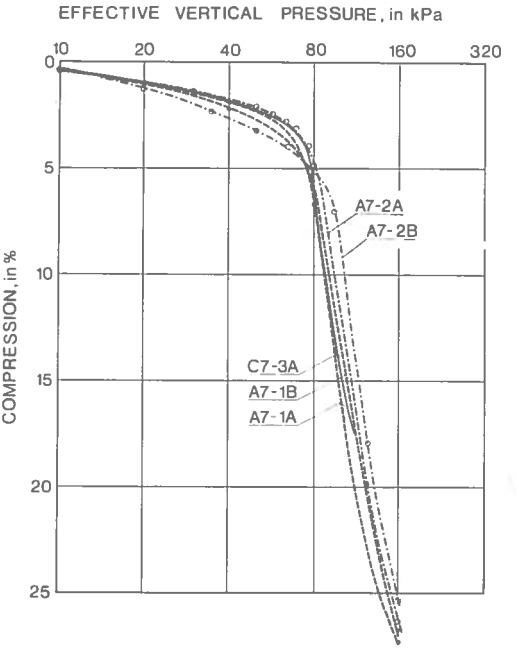

Legend
Bäckebol, 7 m

Test	Type of tes
A7-1A	STD
A7-1B	STD
A7-2A	NGI
A7-2B	NGI
C7-3A	CRS 0,0024 mm/m

Oedometer tests, constant rate of strain

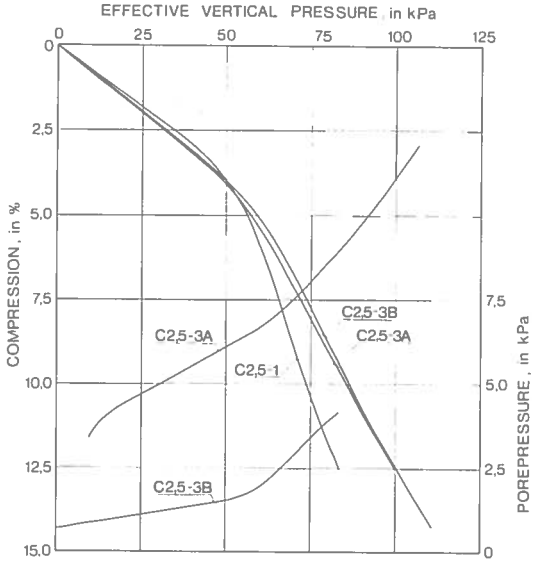

Legend
Bäckebol, 2,5 m

Test	Rate of de mm/min
C2,5-1	0,0006
C2,5-3A	0,0024
C2,5-3B	0,0024

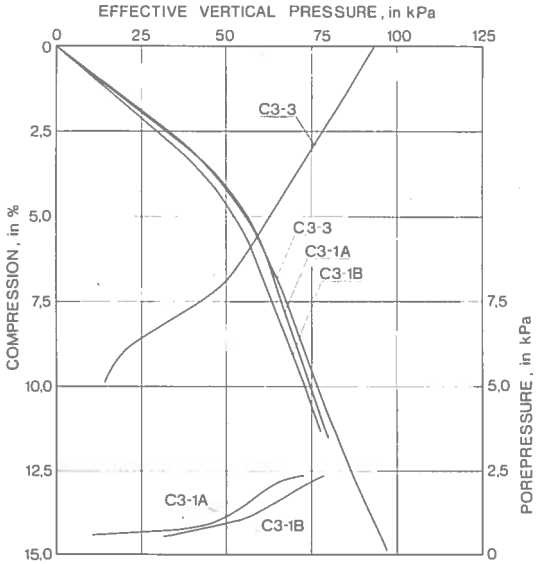

Legend
Bäckebol, 3 m

Test	Rate of de mm/min
C3-1A	0,0006
C3-1B	0,0006
C3-3	0,0024

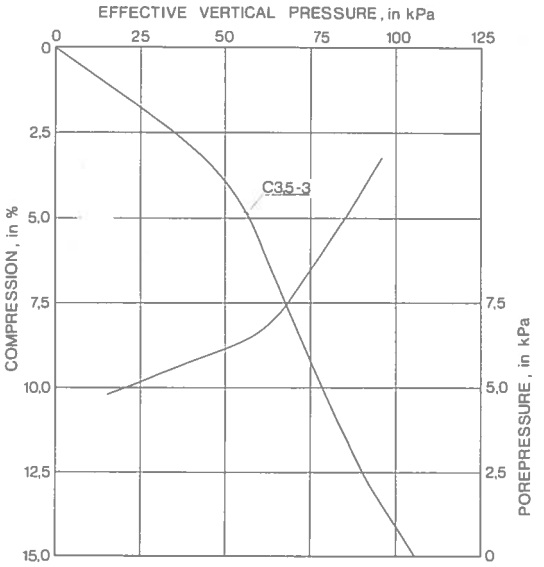

Legend
Bäckebol, 3,5 m

Test	Rate of de mm/min
C3,5-3	0,0024

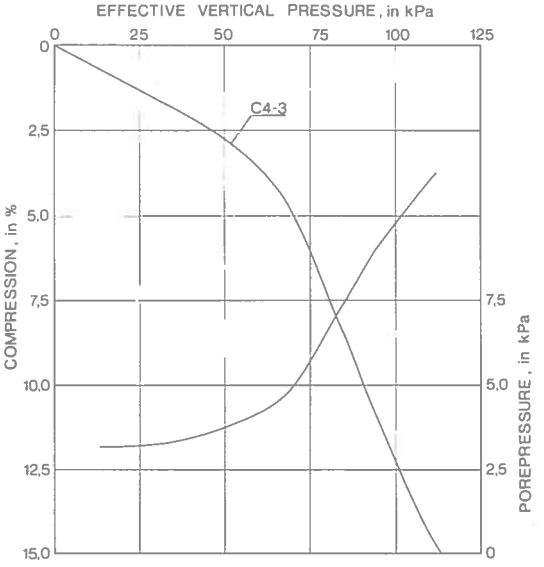

Legend
Bäckebol, 4 m

Test	Rate of def mm/min
C4-3	0,0024

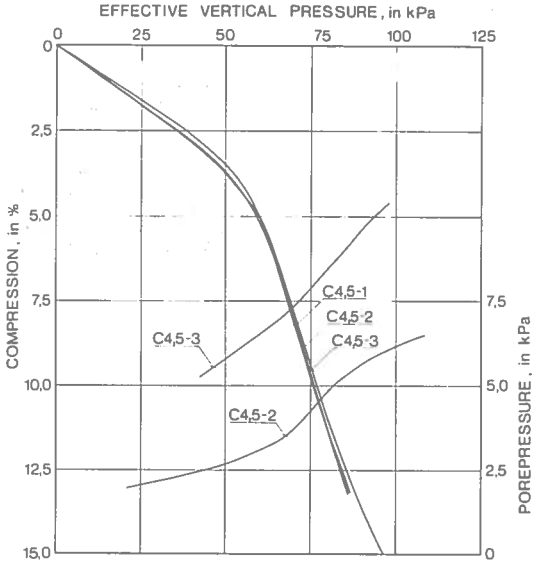

Legend
Bäckebol, 4,5 m

Test	Rate of de mm/min
C4,5-1	0,0006
C4,5-2	0,0012
C4,5-3	0,0024

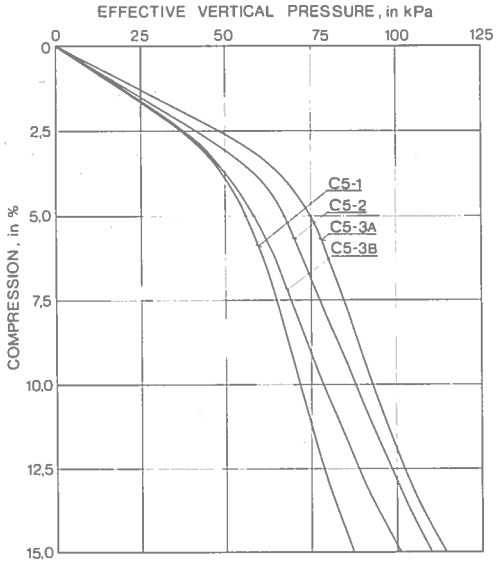

Legend
Bäckebol, 5 m

Test	Rate of def mm/min
C5-1	0,0006
C5-2	0,0012
C5-3A	0,0024
C5-3B	0,0024

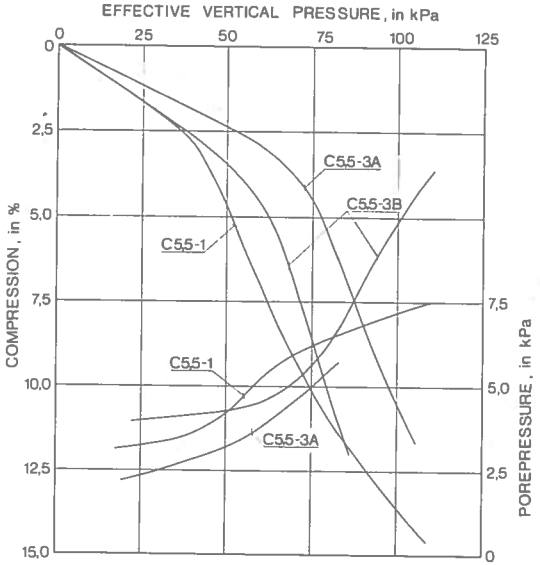

Legend
Bäckebol, 5,5 m

Test	Rate of de mm/min
C5,5-1	0,0006
C5,5-3A	0,0024
C5,5-3B	0,0024

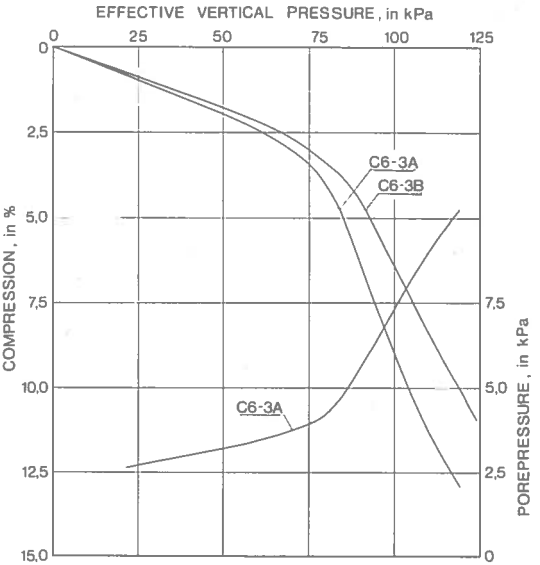

Legend
Bäckebol, 6 m

Test	Rate of def mm/min
C6-3A	0,0024
C6-3B	0,0024

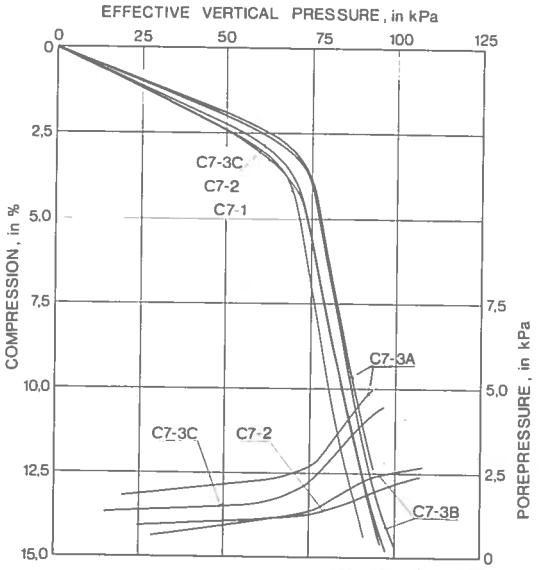

Legend
Bäckebol, 7 m

Test	Rate of de mm/min
C7-1	0,0006
C7-2	0,0012
C7-3A	0,0024
C7-3B	0,0024
C7-3C	0,0024

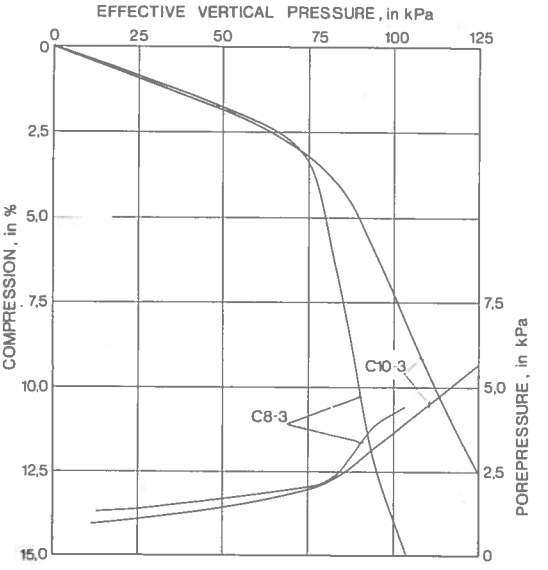

Legend
Bäckebol

Test	Depth in m	Rate mm/
C8 -3	8	0,0
C10-3	10	0,0

Excess pore pressure curves, field test I,

Rate of loading: 1,3 kPa/day

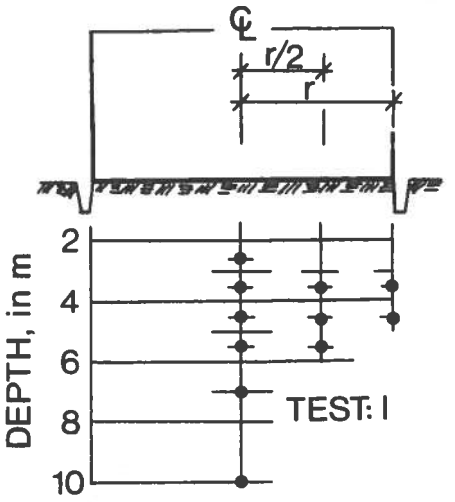

Location of piezometer given individually in each figure.

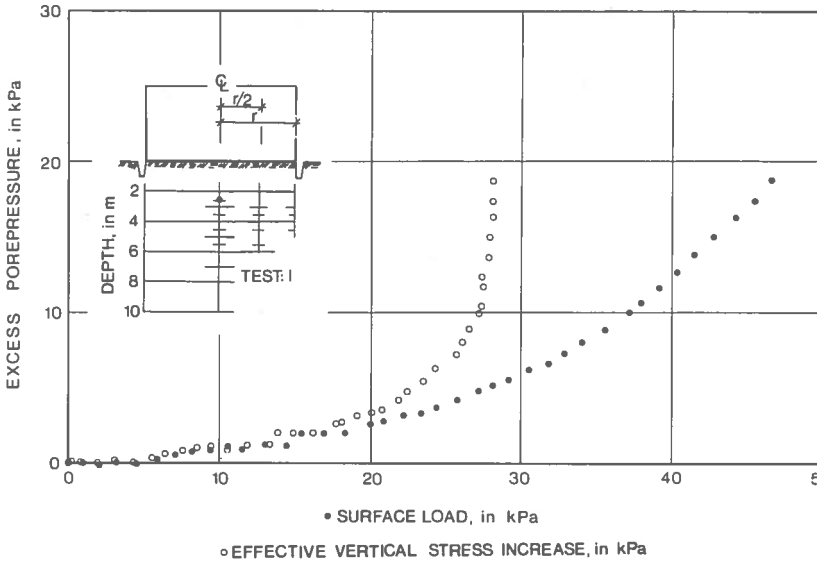
EXCESS POREPRESSURE, in kPa
30
20
10
0
0
10
20
30
40
DEPTH, in m
2
4
6
8
10
TEST: I
r/2
r
• SURFACE LOAD, in kPa
○ EFFECTIVE VERTICAL STRESS INCREASE, in kPa

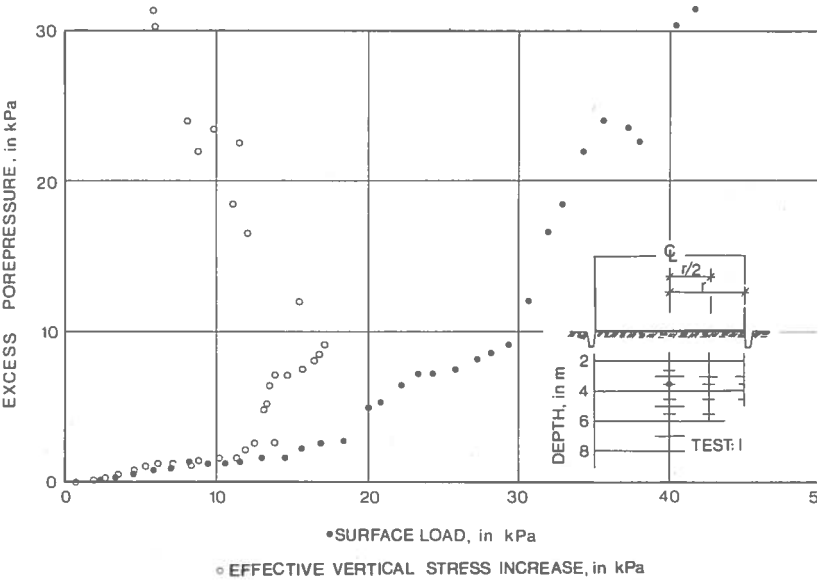
EXCESS POREPRESSURE, in kPa
30
20
10
0
0
10
20
30
40
DEPTH, in m
2
4
6
8
TEST: I
r/2
r
• SURFACE LOAD, in kPa
○ EFFECTIVE VERTICAL STRESS INCREASE, in kPa

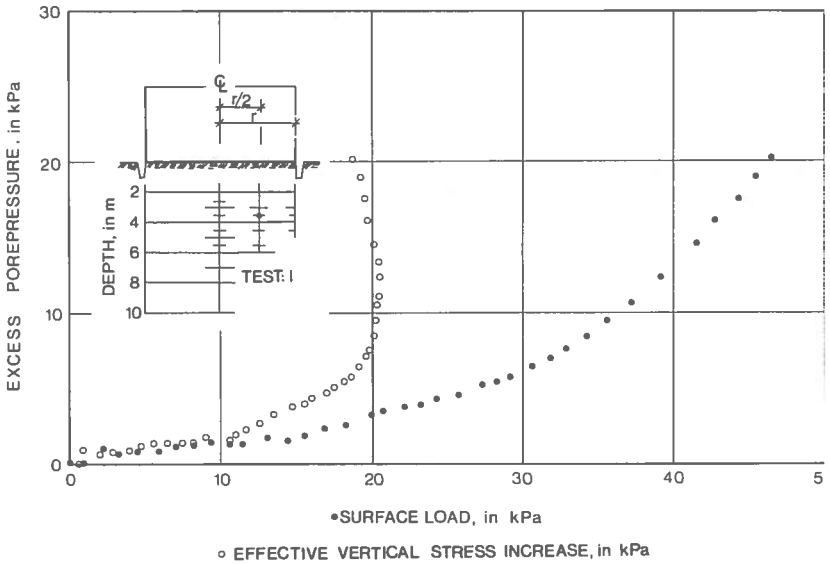
EXCESS POREPRESSURE, in kPa
30
20
10
0
0
10
20
30
40
5
℄
r/2
r
DEPTH, in m
2
4
6
8
10
TEST: I
•SURFACE LOAD, in kPa
○ EFFECTIVE VERTICAL STRESS INCREASE, in kPa

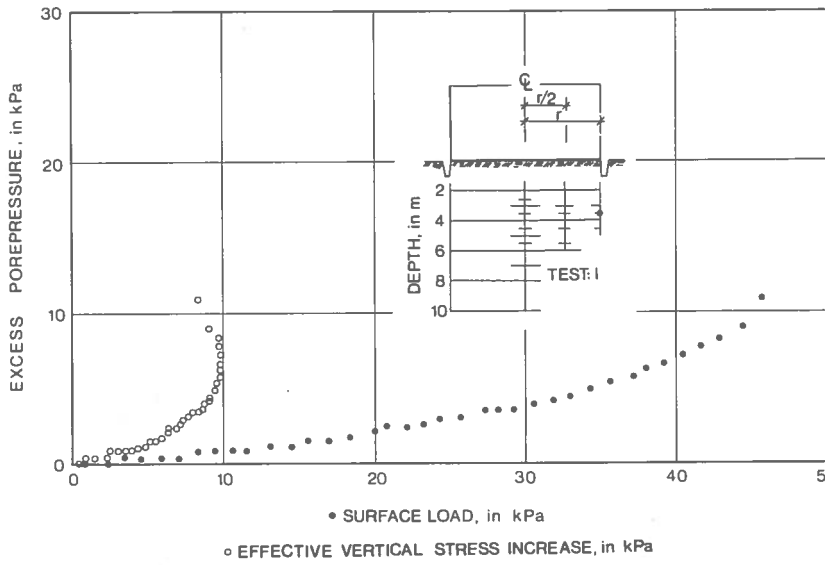
EXCESS POREPRESSURE, in kPa
30
20
10
0
0
10
20
30
40
5
℄
r/2
r
DEPTH, in m
2
4
6
8
10
TEST: I
• SURFACE LOAD, in kPa
○ EFFECTIVE VERTICAL STRESS INCREASE, in kPa

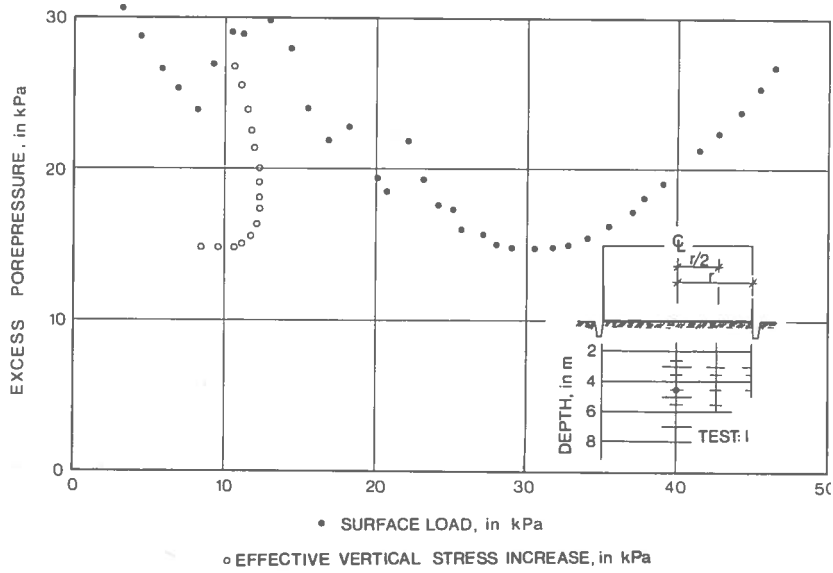
EXCESS POREPRESSURE, in kPa
30
20
10
0
0
10
20
30
40
50
DEPTH, in m
2
4
6
8
TEST: I
r/2
r
• SURFACE LOAD, in kPa
o EFFECTIVE VERTICAL STRESS INCREASE, in kPa

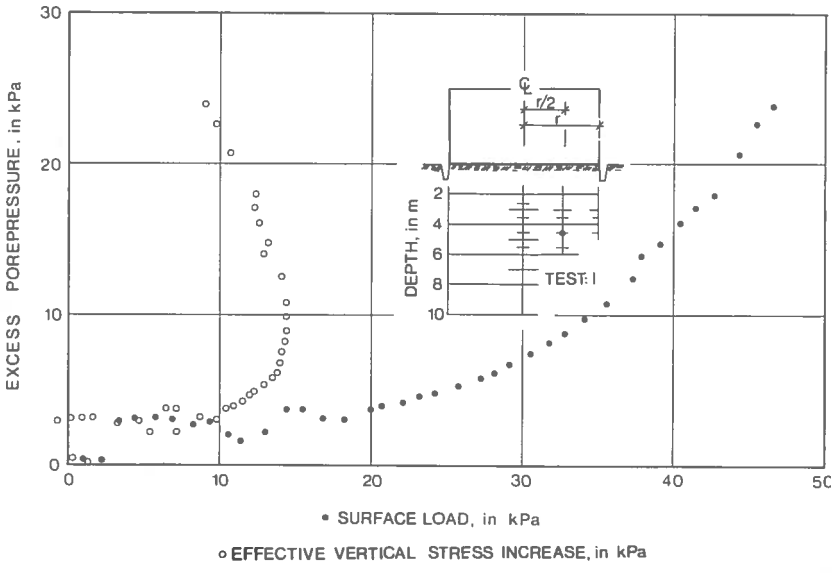
EXCESS POREPRESSURE, in kPa
30
20
10
0
0
10
20
30
40
50
DEPTH, in m
2
4
6
8
10
TEST: I
r/2
r
• SURFACE LOAD, in kPa
o EFFECTIVE VERTICAL STRESS INCREASE, in kPa

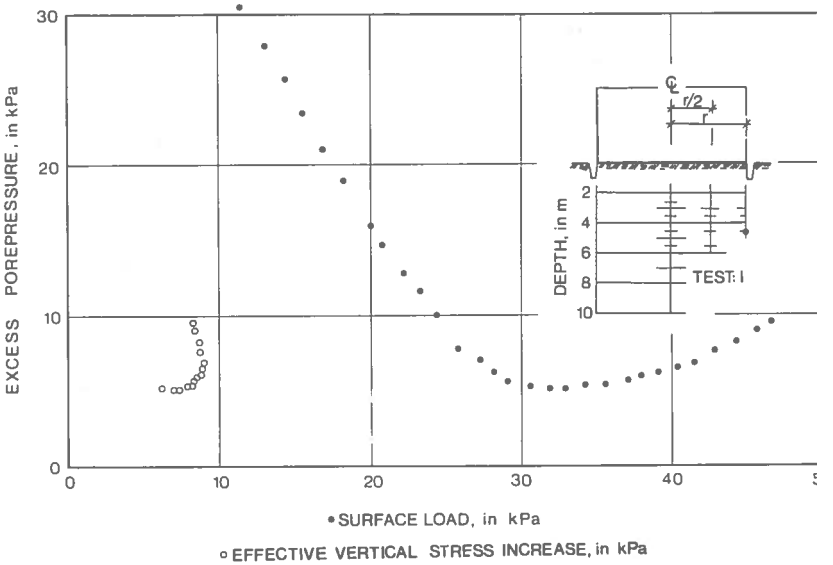
EXCESS POREPRESSURE, in kPa
30
20
10
0
0
10
20
30
40
℄
r/2
r
DEPTH, in m
2
4
6
8
10
TEST: I
• SURFACE LOAD, in kPa
○ EFFECTIVE VERTICAL STRESS INCREASE, in kPa

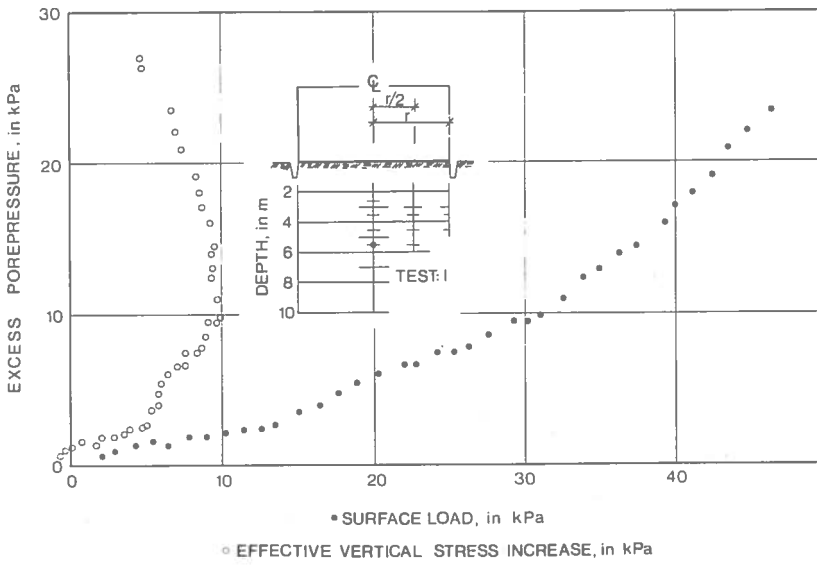
EXCESS POREPRESSURE, in kPa
30
20
10
0
0
10
20
30
40
℄
r/2
r
DEPTH, in m
2
4
6
8
10
TEST: I
• SURFACE LOAD, in kPa
○ EFFECTIVE VERTICAL STRESS INCREASE, in kPa

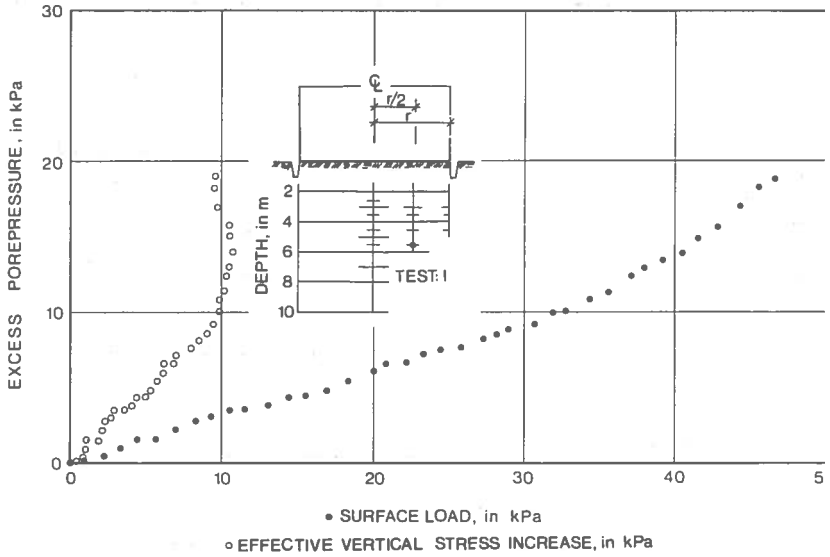
EXCESS POREPRESSURE, in kPa
30
20
10
0
0
10
20
30
40
5
DEPTH, in m
2
4
6
8
10
TEST: I
℄
r/2
r
• SURFACE LOAD, in kPa
○ EFFECTIVE VERTICAL STRESS INCREASE, in kPa

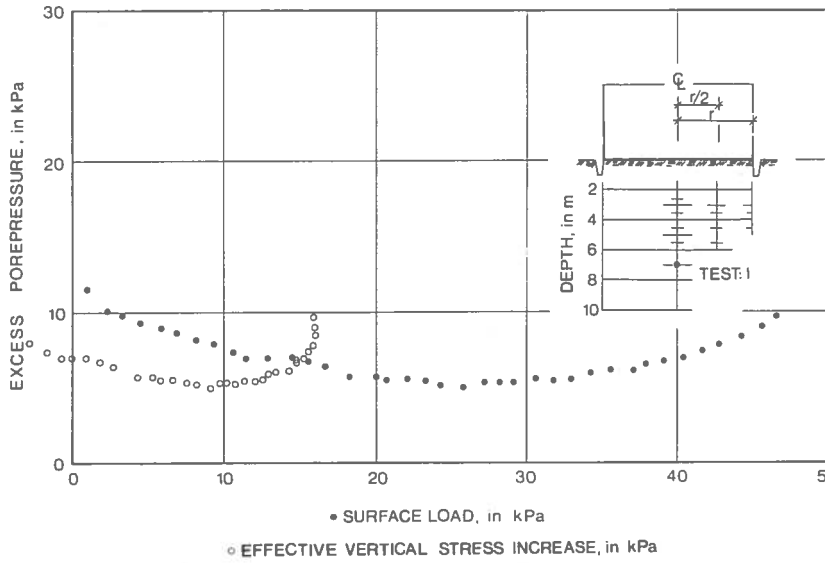
EXCESS POREPRESSURE, in kPa
30
20
10
0
0
10
20
30
40
5
DEPTH, in m
2
4
6
8
10
TEST: I
℄
r/2
r
• SURFACE LOAD, in kPa
○ EFFECTIVE VERTICAL STRESS INCREASE, in kPa

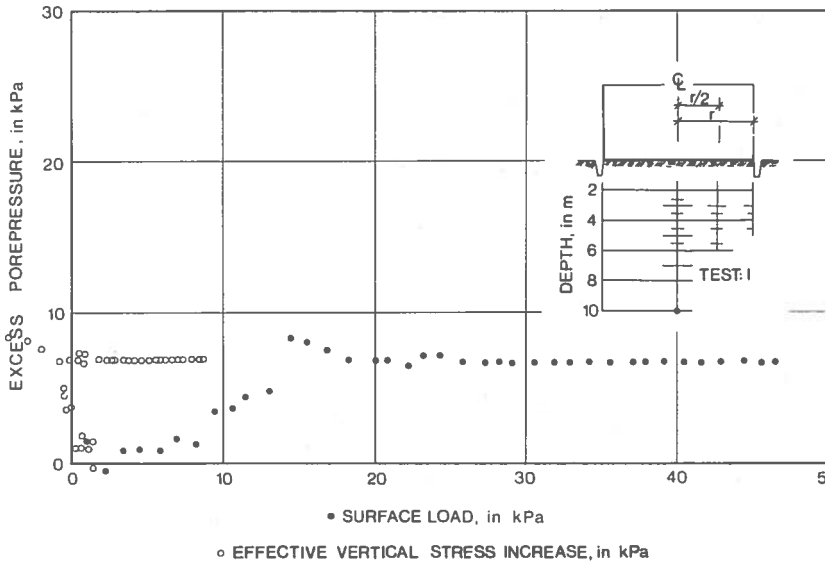
EXCESS POREPRESSURE, in kPa
30
20
10
0
0
10
20
30
40
DEPTH, in m
2
4
6
8
10
TEST: I
r/2
r
• SURFACE LOAD, in kPa
o EFFECTIVE VERTICAL STRESS INCREASE, in kPa

Excess pore pressure curves, field test II,

Rate of loading: 0,8 kPa/day

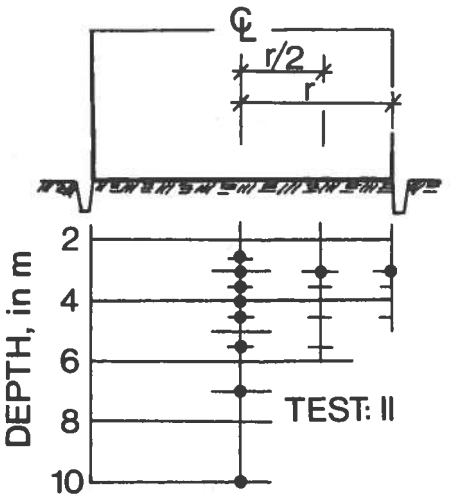

Location of piezometer given individually in each figure.

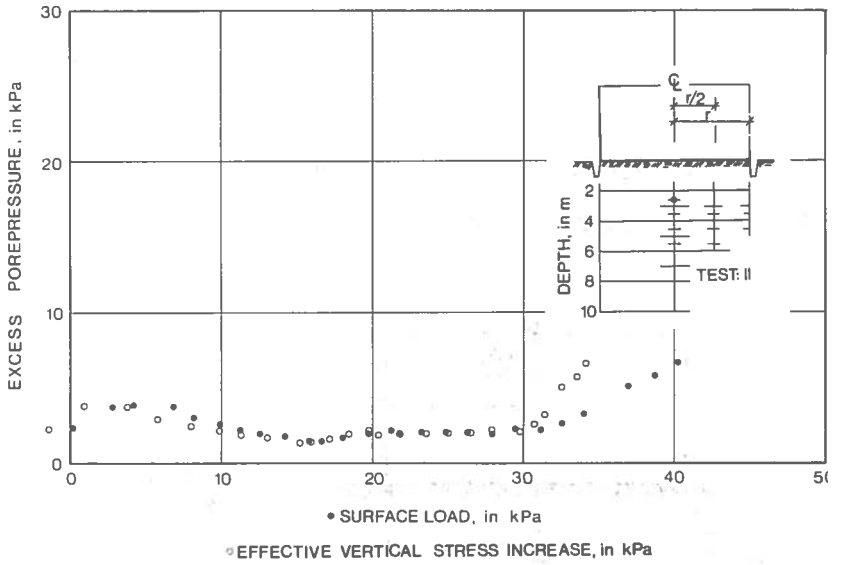
EXCESS POREPRESSURE, in kPa
30
20
10
0
0
10
20
30
40
℄
r/2
r
DEPTH, in m
2
4
6
8
10
TEST: II
• SURFACE LOAD, in kPa
◦ EFFECTIVE VERTICAL STRESS INCREASE, in kPa

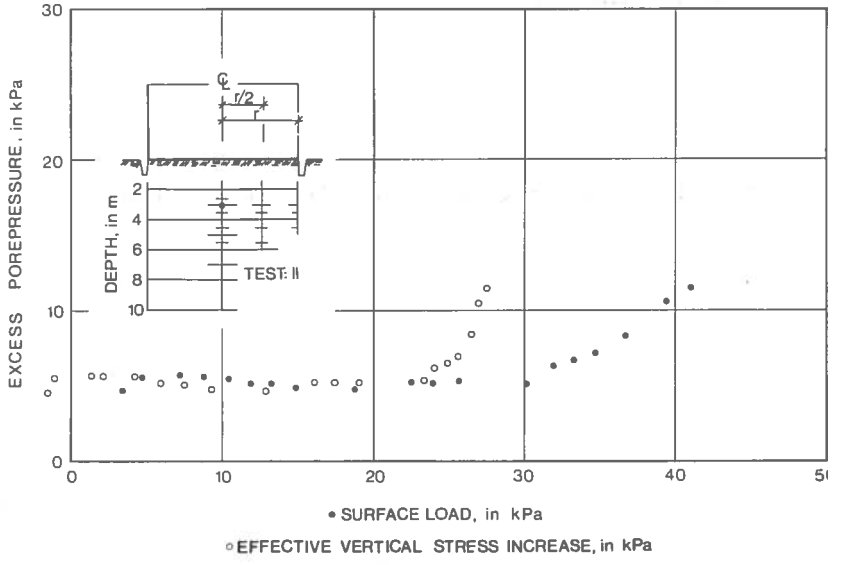
EXCESS POREPRESSURE, in kPa
30
20
10
0
0
10
20
30
40
℄
r/2
r
DEPTH, in m
2
4
6
8
10
TEST: II
• SURFACE LOAD, in kPa
◦ EFFECTIVE VERTICAL STRESS INCREASE, in kPa

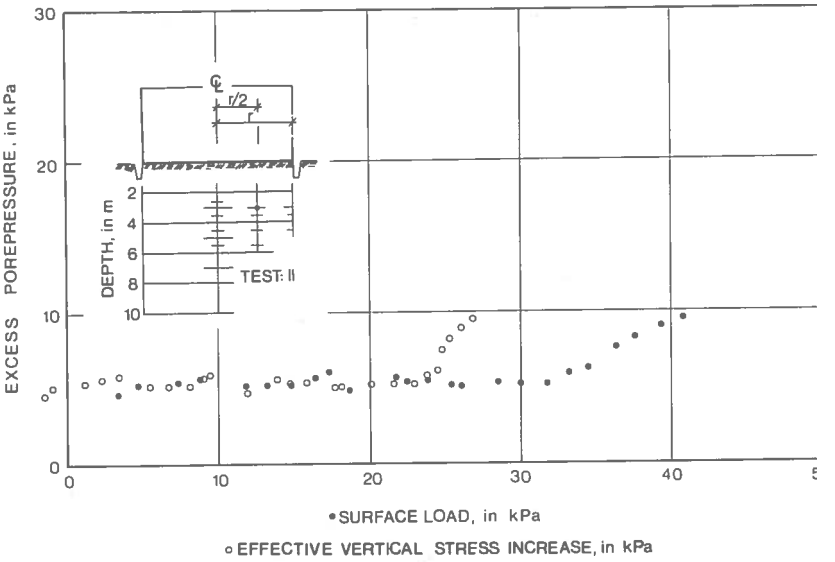
EXCESS POREPRESSURE, in kPa
30
20
10
0
0
10
20
30
40
℄
r/2
r
DEPTH, in m
2
4
6
8
10
TEST: II
• SURFACE LOAD, in kPa
○ EFFECTIVE VERTICAL STRESS INCREASE, in kPa

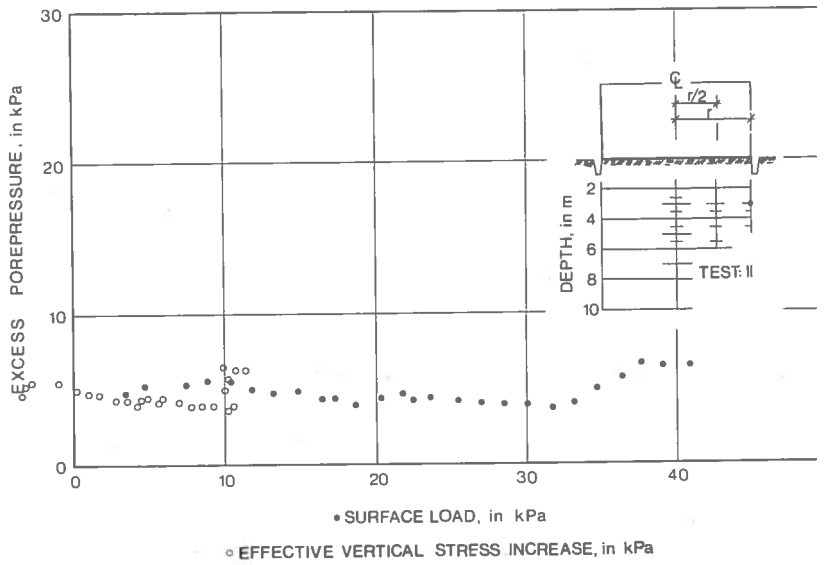
EXCESS POREPRESSURE, in kPa
30
20
10
0
0
10
20
30
40
℄
r/2
r
DEPTH, in m
2
4
6
8
10
TEST: II
• SURFACE LOAD, in kPa
○ EFFECTIVE VERTICAL STRESS INCREASE, in kPa

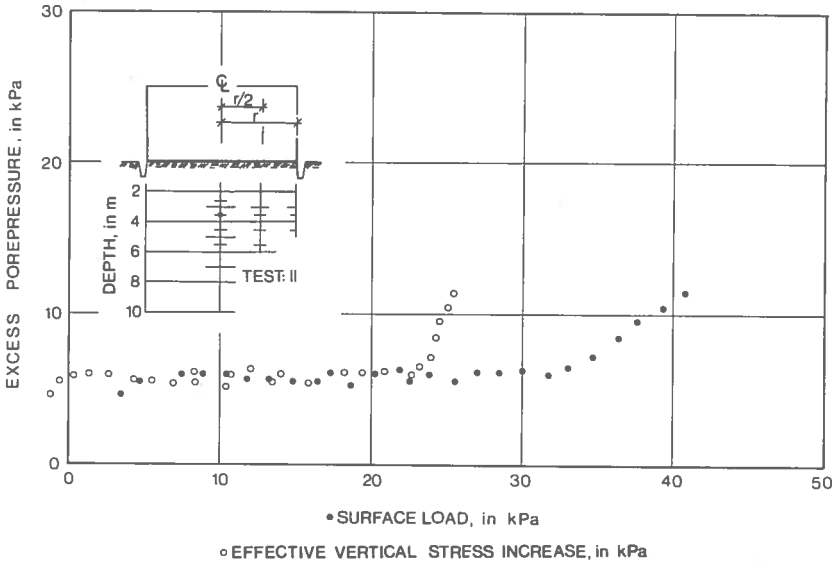
EXCESS POREPRESSURE, in kPa
30
20
10
0
0
10
20
30
40
50
℄
r/2
r
DEPTH, in m
2
4
6
8
10
TEST: II
• SURFACE LOAD, in kPa
○ EFFECTIVE VERTICAL STRESS INCREASE, in kPa

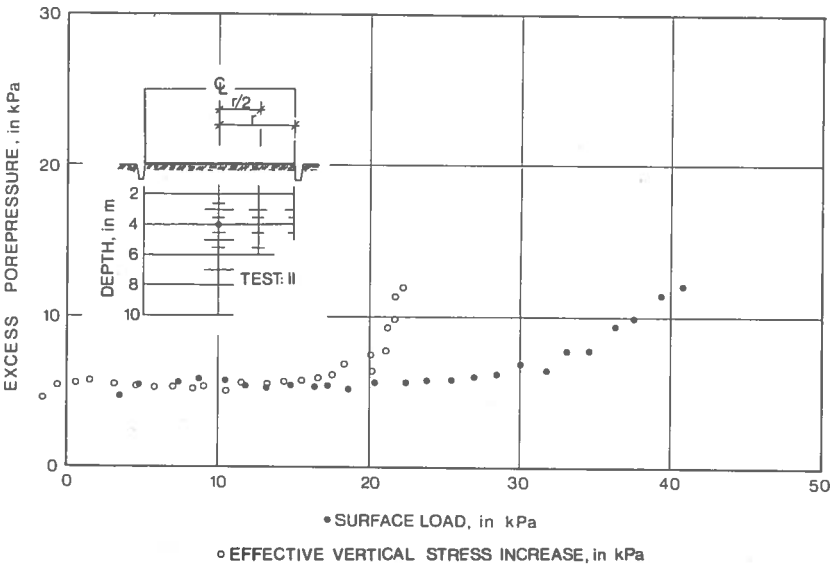
EXCESS POREPRESSURE, in kPa
30
20
10
0
0
10
20
30
40
50
℄
r/2
r
DEPTH, in m
2
4
6
8
10
TEST: II
• SURFACE LOAD, in kPa
○ EFFECTIVE VERTICAL STRESS INCREASE, in kPa

Oedometer tests

RESULTS FROM TEST FIELD AT VÄLEN

Appendix B.1 Oedometer tests

Appendix B.2 Excess pore pressure curves, field test rate of loading: 0,5 kPa/day

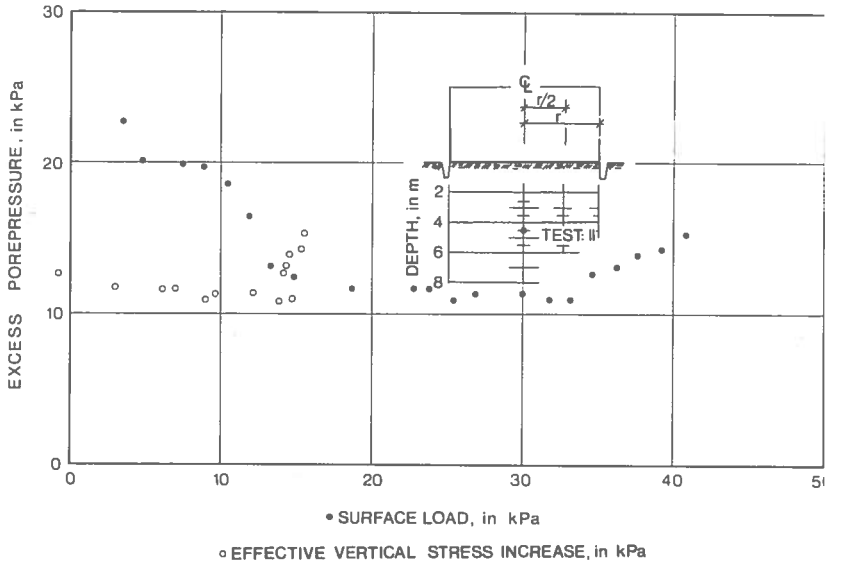
EXCESS POREPRESSURE, in kPa
30
20
10
0
0
10
20
30
40
DEPTH, in m
2
4
6
8
TEST: II
r/2
r
• SURFACE LOAD, in kPa
o EFFECTIVE VERTICAL STRESS INCREASE, in kPa

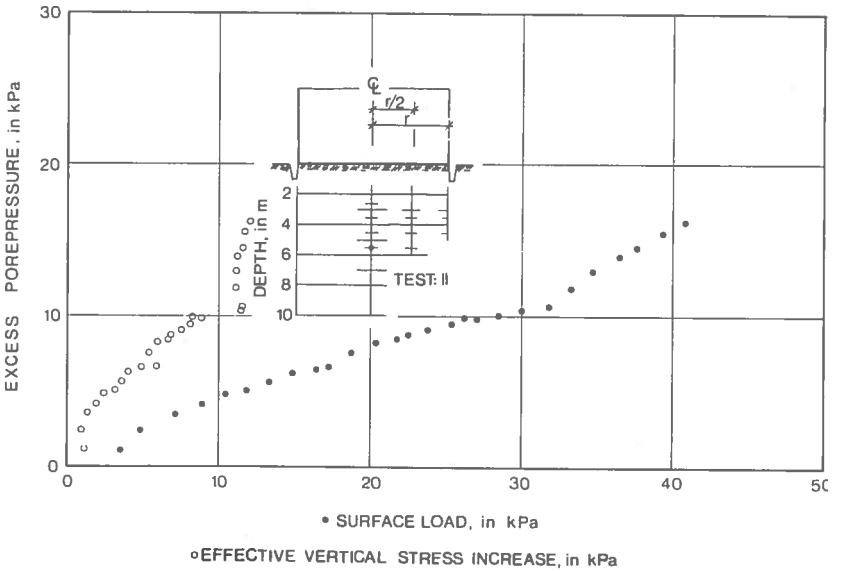
EXCESS POREPRESSURE, in kPa
30
20
10
0
0
10
20
30
40
DEPTH, in m
2
4
6
8
10
TEST: II
r/2
r
• SURFACE LOAD, in kPa
o EFFECTIVE VERTICAL STRESS INCREASE, in kPa

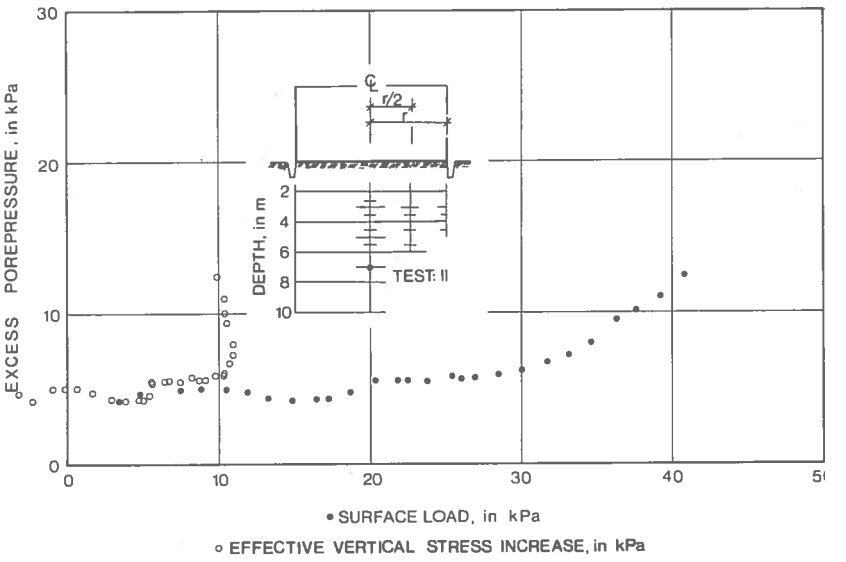
EXCESS POREPRESSURE, in kPa
30
20
10
0
0
10
20
30
40
℄
r/2
r
DEPTH, in m
2
4
6
8
10
TEST: II
• SURFACE LOAD, in kPa
○ EFFECTIVE VERTICAL STRESS INCREASE, in kPa

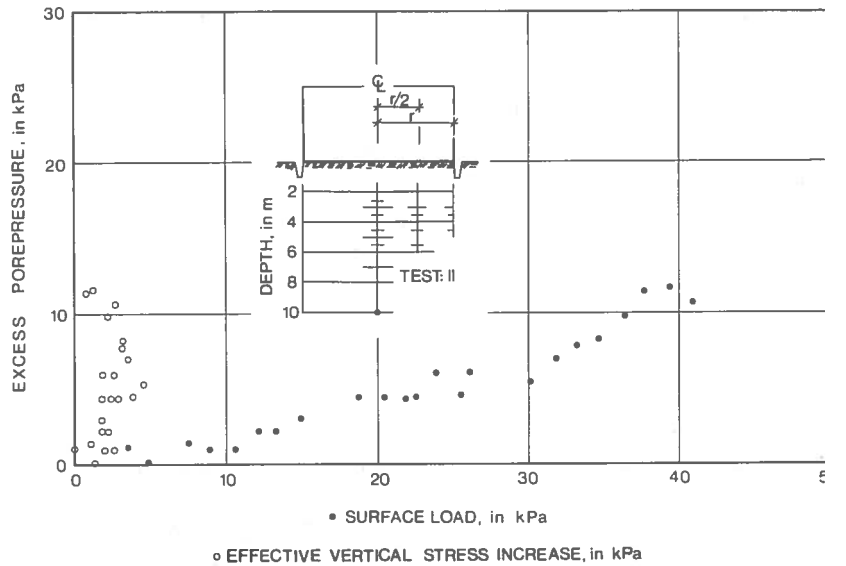
EXCESS POREPRESSURE, in kPa
30
20
10
0
0
10
20
30
40
℄
r/2
r
DEPTH, in m
2
4
6
8
10
TEST: II
• SURFACE LOAD, in kPa
○ EFFECTIVE VERTICAL STRESS INCREASE, in kPa

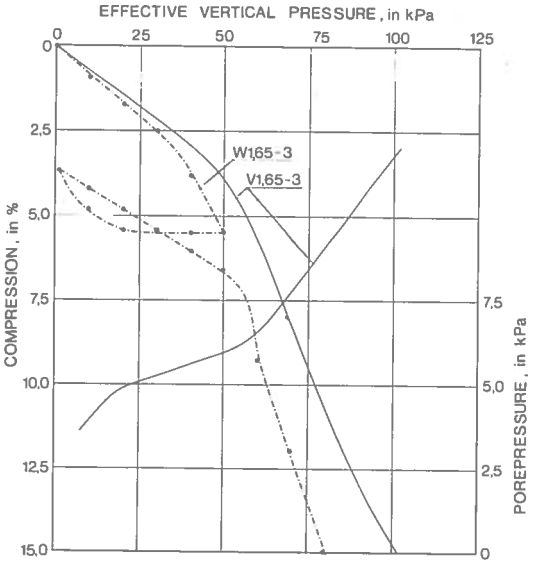

Legend
Välen, 1,65 m

Test	Type of te
W1,65-3	LIN
V1,65-3	CRS
	0,0024

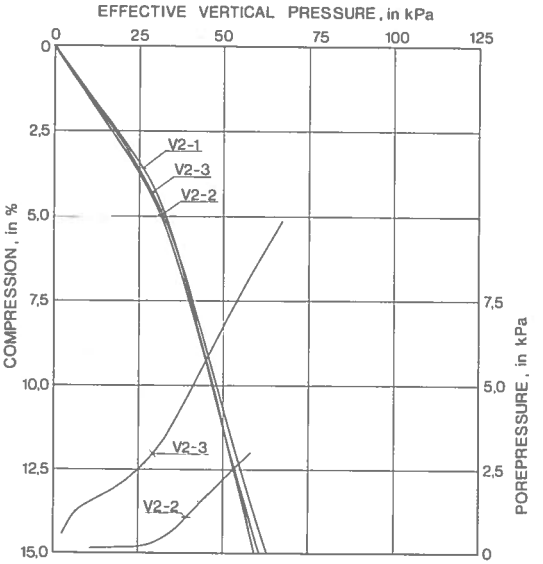

Legend
Välen, 2 m

Test	Rate of de
	mm/min
V2-1	0,0006
V2-2	0,0012
V2-3	0,0024

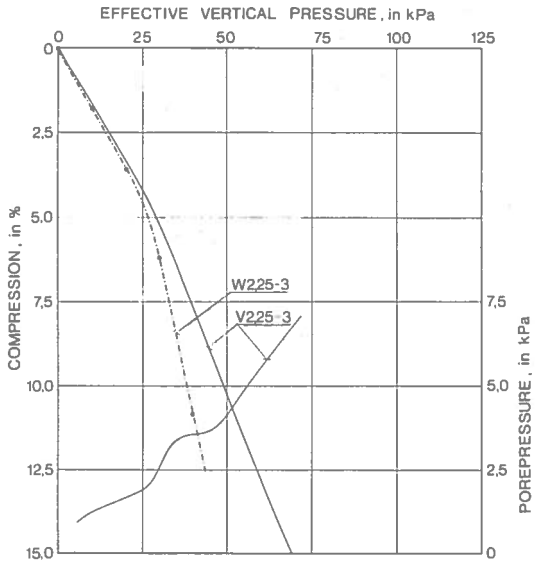

Legend
Välen, 2,25 m

Test	Type of t
W2,25-3	LIN
V2,25-3	CRS
	0,0024

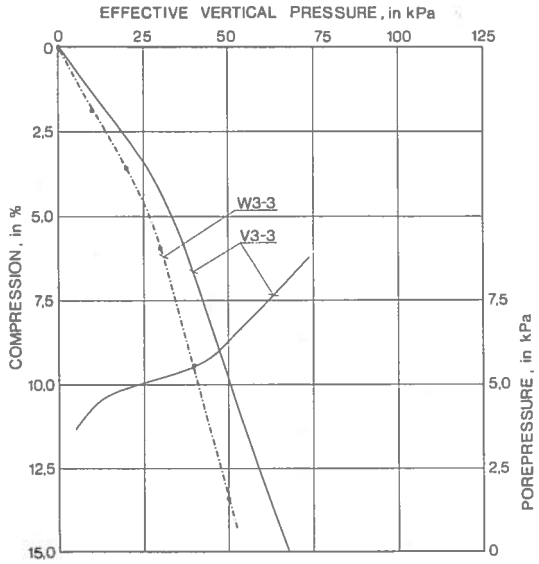

Legend
Välen, 3 m

Test	Type of t
W3-3	LIN
V3-3	CRS
	0,0024

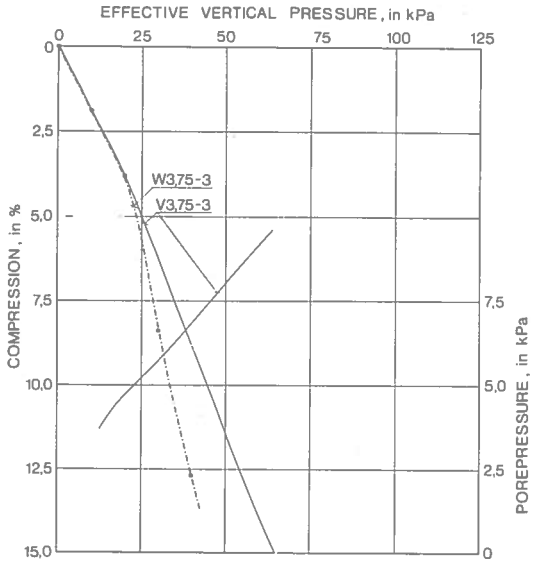

Legend
Välen, 3,75

Test	Type of te
W3,75-3	LIN
V3,75-3	CRS
	0,0024 m

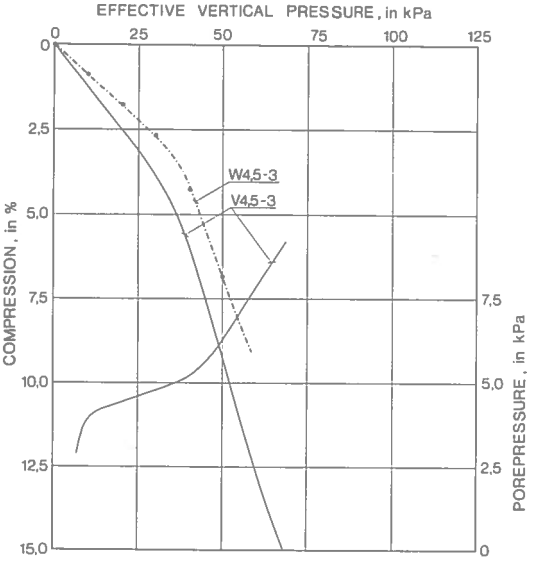

Legend
Välen, 4,5 m

Test	Type of te
W4,5-3	LIN
V4,5-3	CRS
	0,0024 m

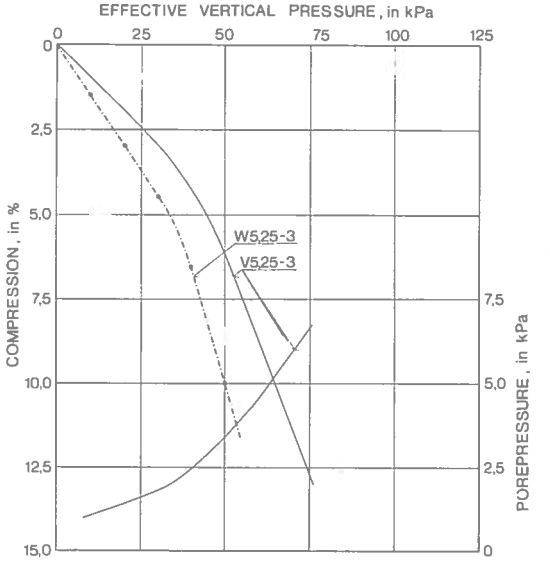

Legend
Välen, 5,25 m

Test	Type of te
W5,25-3	LIN
V5,25-3	CRS
	0,0024

Excess pore pressure curves, field test,

Rate of loading: 0,5 kPa/day

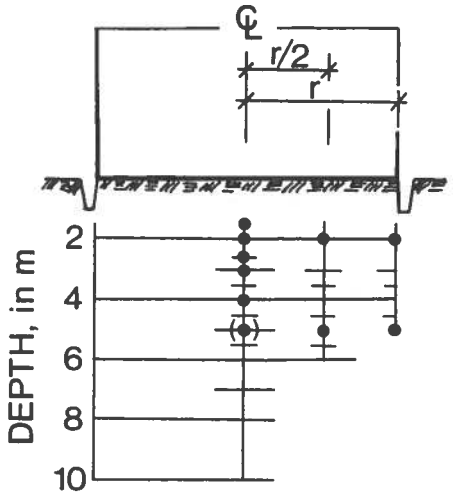

Location of piezometer given individually in each figure.

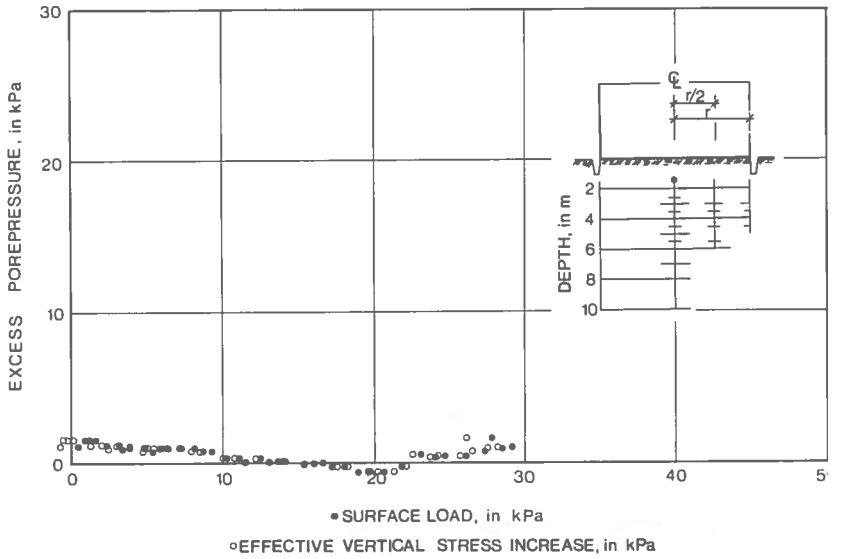
EXCESS POREPRESSURE, in kPa
30
20
10
0
0
10
20
30
40
DEPTH, in m
2
4
6
8
10
r/2
r
• SURFACE LOAD, in kPa
○ EFFECTIVE VERTICAL STRESS INCREASE, in kPa

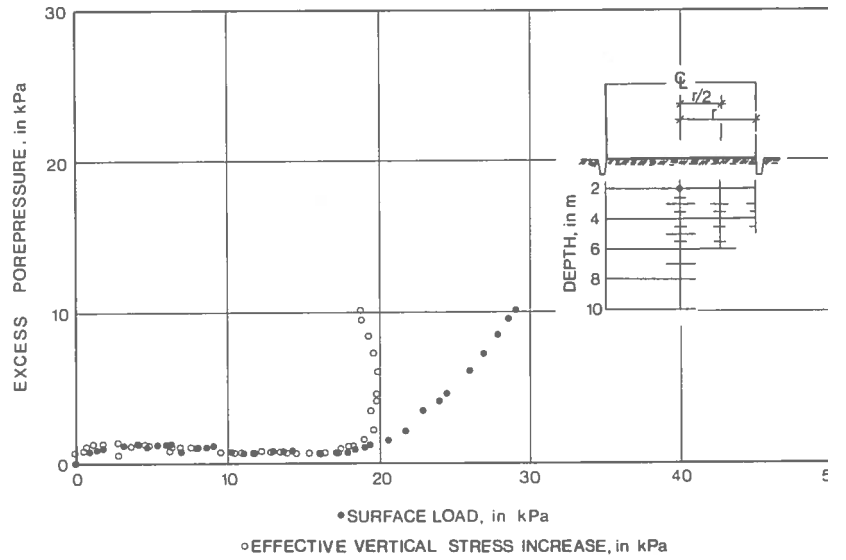
EXCESS POREPRESSURE, in kPa
30
20
10
0
0
10
20
30
40
DEPTH, in m
2
4
6
8
10
r/2
r
• SURFACE LOAD, in kPa
○ EFFECTIVE VERTICAL STRESS INCREASE, in kPa

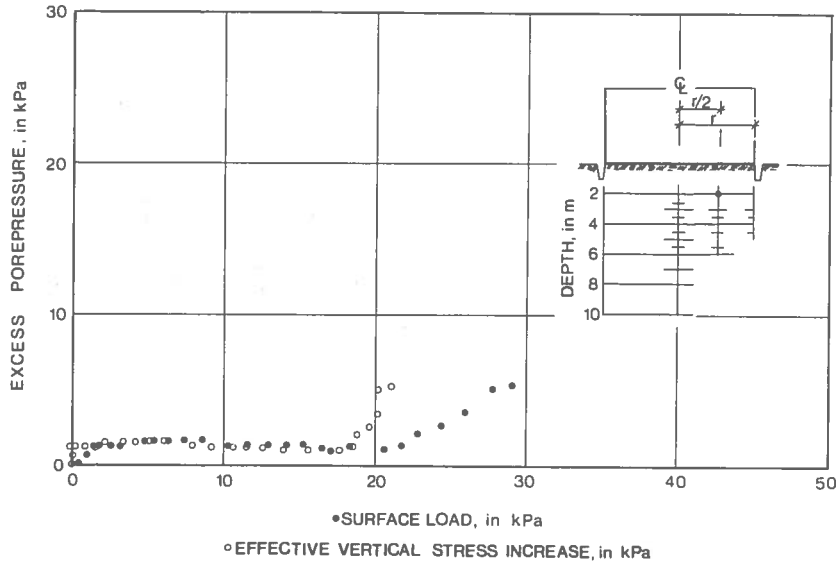
EXCESS POREPRESSURE, in kPa
30
20
10
0
0
10
20
30
40
50
DEPTH, in m
2
4
6
8
10
r/2
•SURFACE LOAD, in kPa
○EFFECTIVE VERTICAL STRESS INCREASE, in kPa

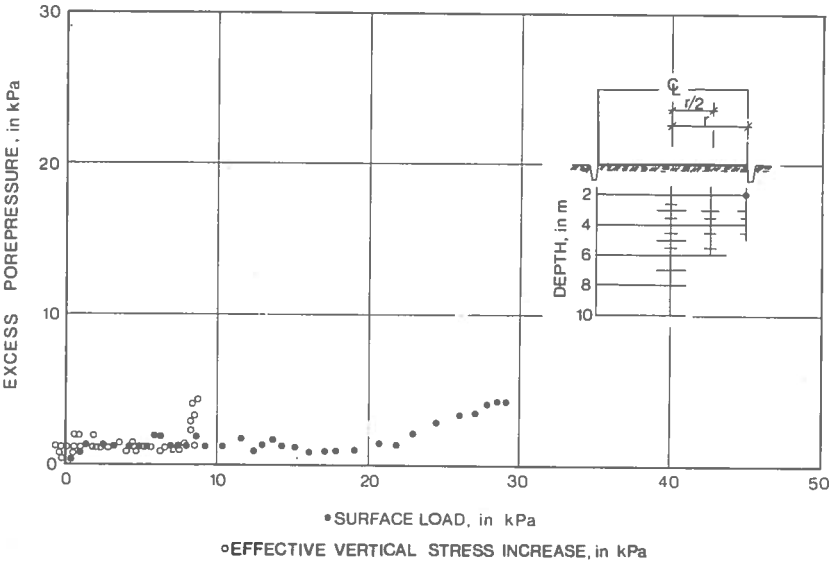
EXCESS POREPRESSURE, in kPa
30
20
10
0
0
10
20
30
40
50
DEPTH, in m
2
4
6
8
10
r/2
•SURFACE LOAD, in kPa
○EFFECTIVE VERTICAL STRESS INCREASE, in kPa

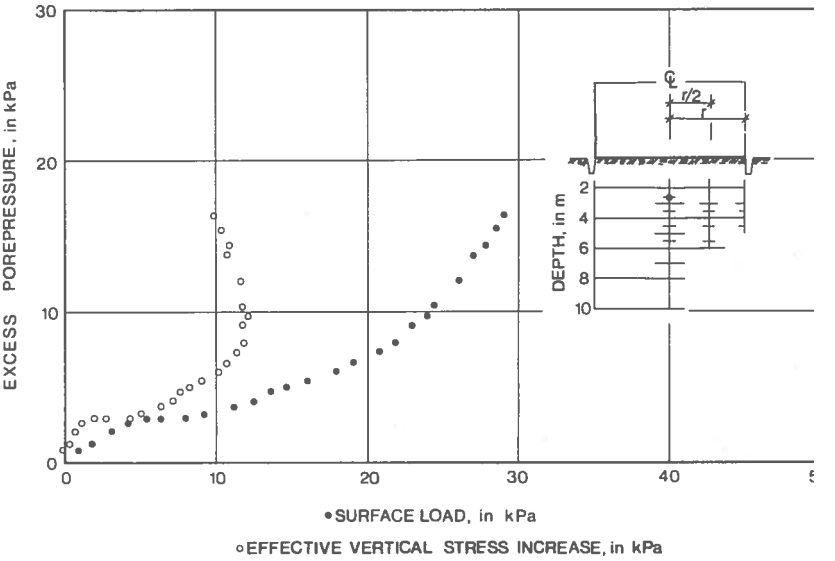
EXCESS POREPRESSURE, in kPa
30
20
10
0
0
10
20
30
40
DEPTH, in m
2
4
6
8
10
r/2
r
•SURFACE LOAD, in kPa
○EFFECTIVE VERTICAL STRESS INCREASE, in kPa

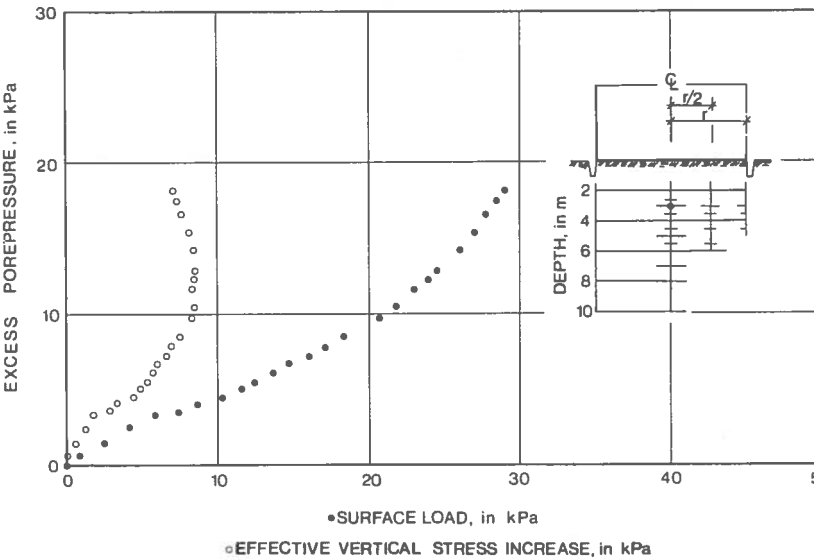
EXCESS POREPRESSURE, in kPa
30
20
10
0
0
10
20
30
40
DEPTH, in m
2
4
6
8
10
r/2
r
•SURFACE LOAD, in kPa
○EFFECTIVE VERTICAL STRESS INCREASE, in kPa

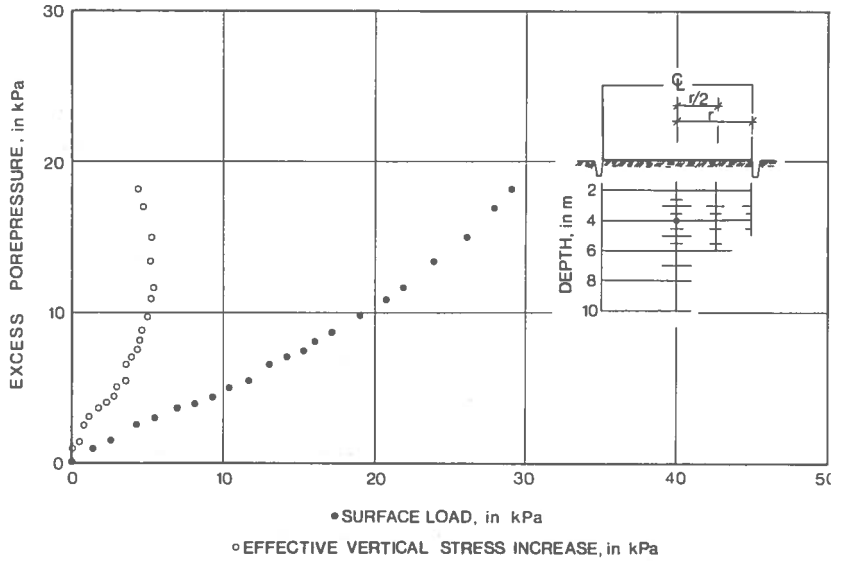
EXCESS POREPRESSURE, in kPa
30
20
10
0
0
10
20
30
40
50
DEPTH, in m
2
4
6
8
10
r/2
r
℄
• SURFACE LOAD, in kPa
○ EFFECTIVE VERTICAL STRESS INCREASE, in kPa

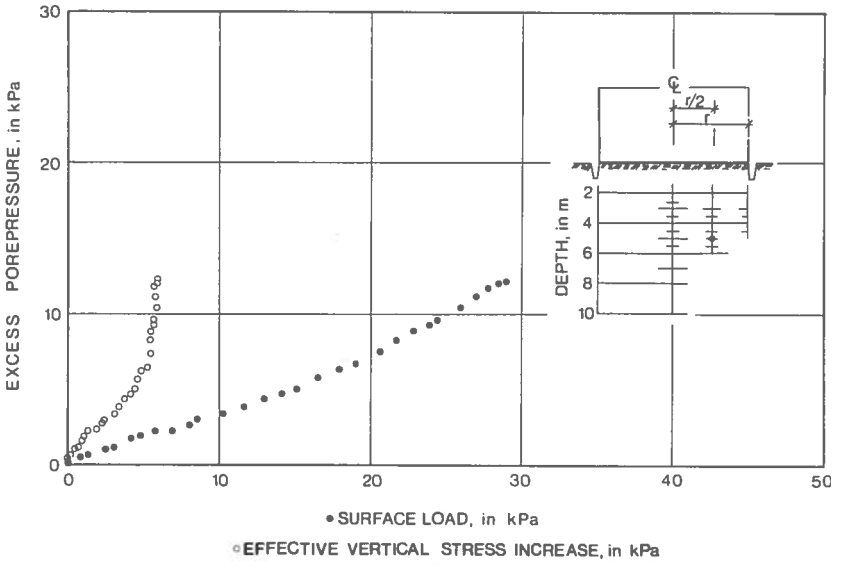
EXCESS POREPRESSURE, in kPa
30
20
10
0
0
10
20
30
40
50
DEPTH, in m
2
4
6
8
10
r/2
r
℄
• SURFACE LOAD, in kPa
○ EFFECTIVE VERTICAL STRESS INCREASE, in kPa

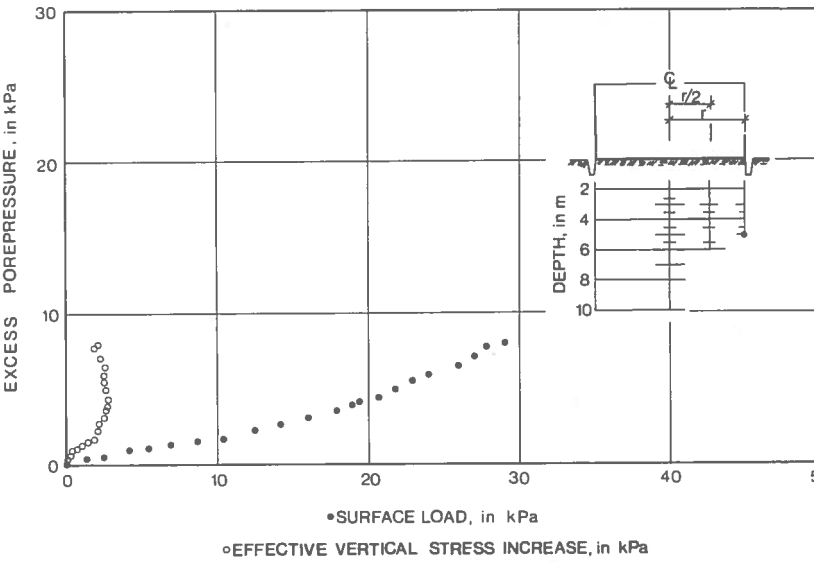
EXCESS POREPRESSURE, in kPa
30
20
10
0
0
10
20
30
40
DEPTH, in m
2
4
6
8
10
r/2
r
•SURFACE LOAD, in kPa
○EFFECTIVE VERTICAL STRESS INCREASE, in kPa

RESULTS FROM TEST FIELD AT KRISTIANSTAD

Oedometer tests

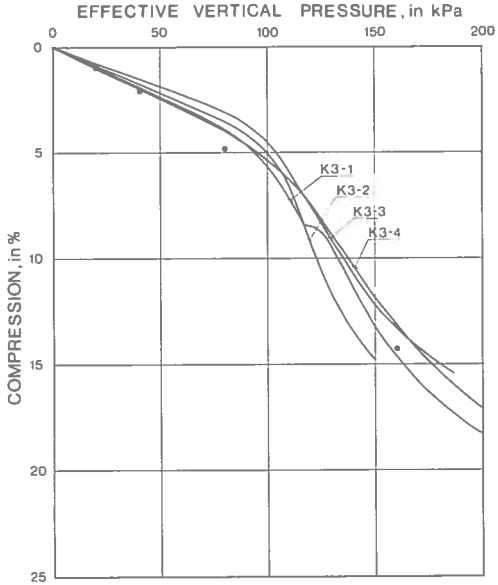

Legend
Kristianstad, 3 m

Test	Rate of def mm/min
K3-1	0,0006
	0,0024
K3-2	0,0012
K3-3	0,0024
K3-4	0,0040
•L3-1	STD test

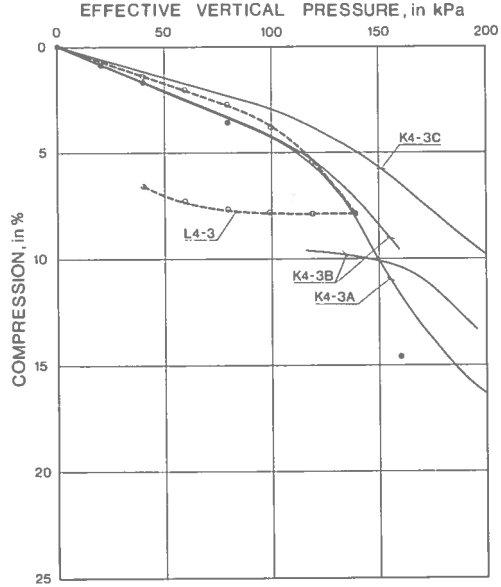

Legend
Kristianstad, 4 m

Test	Rate of def mm/min
K4-3A	0,0024
K4-3B	0,0024
K4-3C	0,0024
•L4-1	STD test
L4-3	LIN test

100 kPa / 0,03 = 3

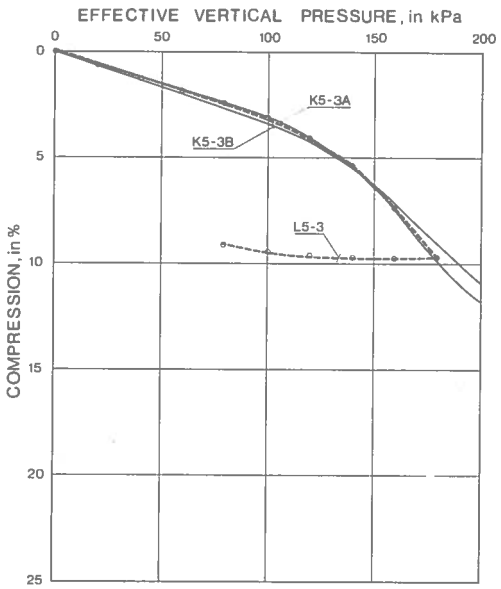

Legend
Kristianstad,5 m

Test	Rate of def mm/min
K5-3A	0,0024
K5-3B	0,0024
L5-3	LIN test

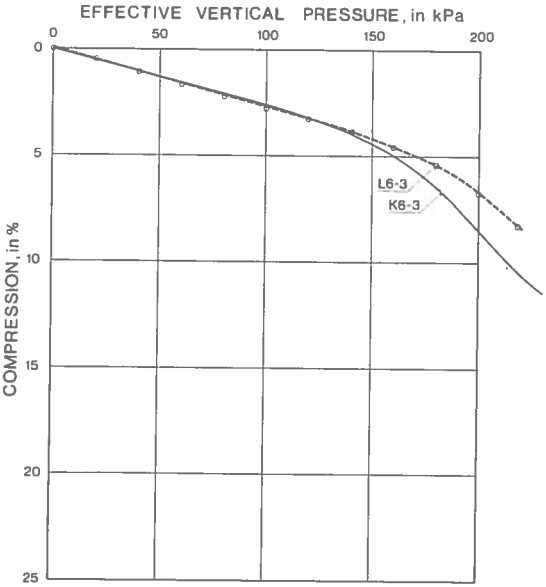

Legend
Kristianstad, 6 m

Test	Rate of def. mm/min
K6-3	0,0024
L6-3	LIN test